USDA
United States Department of Agriculture

Climate Scenarios and Projections

A Technical Document Supporting the USDA Forest Service 2020 RPA Assessment

Linda A. Joyce and David Coulson

Forest Service Gen. Tech. Rep. RMRS-GTR-413 May 2020

Citation

Citation: Joyce, Linda A.; Coulson, David. 2020. Climate Scenarios and Projections: A technical document supporting the USDA Forest Service 2020 RPA Assessment. Gen. Tech. Rep. RMRS-GTR-413. Fort Collins, CO: U.S. Department of Agriculture, Forest Service, Rocky Mountain Research Station. 85 p. https://doi.org/10.2737/RMRS-GTR-413

Abstract

The 2020 RPA Assessment includes climate change as a driver affecting natural resources on forests and rangelands in the United States. This publication describes the process used to select the scenarios, climate models, and climate projections that will be used to project renewable resource conditions 50 years into the future. Downscaled climate data selected are the MACAv2-METDATA developed by Abatzoglou and others at the University of Idaho. The dataset covers the conterminous United States at a grid size of approximately 4 km (1/24 degree) on a side. The two selected scenarios are the Representative Concentration Pathways (RCPs) 4.5 and 8.5. Three criteria were used to select the climate models: (1) identification and elimination of poor performing models based on historical climate projections, (2) restriction of selection to only one model from a modeling institution, and (3) selection of a climate model that could provide projections for both the RCP 4.5 and RCP 8.5 scenarios. Climate models and projections were selected to capture a range of future climates at the conterminous scale: least warm projection, hottest projection, driest projection, and wettest projection, and one projection that reflected the middle of these ranges. The core model projections to be used in the 2020 RPA Assessment under RCP 4.5 and RCP 8.5 are: Least Warm—MRI-CGCM3; Hot—HadGEM2-ES; Dry—IPSL-CM5A-MR; Wet—CNRM-CM5; Middle—NorESM1-M. Future climates at mid-century (2041–2070) are summarized for the conterminous United States. The data are available at the USDA Forest Service Research and Development Data Archive.

Keywords: selection process, climate model evaluation, mid-century, RCP 4.5, RCP 8.5

Authors

LINDA A. JOYCE is an Emeritus Scientist with the USDA Forest Service, Rocky Mountain Research Station in Fort Collins, Colorado.

DAVID COULSON is a retired Statistician with the USDA Forest Service, Rocky Mountain Research Station in Fort Collins, Colorado.

Acknowledgments

We wish to acknowledge the team of RPA scientists who convened to identify climate information needed and to vet the available climate datasets: Tom Brown, Curt Flather, Matt Reeves, Linda Langner, Jeff Prestemon, and David Wear, all with the USDA Forest Service; and Jen Costanza, North Carolina State University. We wish to acknowledge John Abatzoglou and Katherine Hegewisch for their advice and consultation on the use of the MACA climate data. We appreciate the comments from reviewers: John Gross, National Park Service; Brice Hanberry, Forest Service, Rocky Mountain Research Station; and Imtiaz Rangwala, University of Colorado. The dataset MACAv2-METDATA was produced with funding from the Regional Approaches to Climate Change (REACCH) project, the Climate Impacts Research Consortium (CIRC), and the Northwest and Southeast Climate Science Centers. Developers acknowledge the World Climate Research Programme's Working Group on Coupled Modeling, which is responsible for the Coupled Model Intercomparison Project (CMIP), and thanks to the climate modeling groups for producing and making available their model output. For CMIP, the U.S. Department of Energy's Program for Climate Model Diagnosis and Intercomparison provided coordinating support and led development of software infrastructure in partnership with the Global Organization for Earth System Science Portals. We thank Laurie Porth, Archivist, Forest Service, for her assistance in archiving the climate data. We thank Cynthia Moser, Contract Editor, whose careful review significantly improved the manuscript, and Frances Smith, Visual Information Specialist, for her efforts to craft a visually pleasing read. The Forest Service, Rocky Mountain Research Station and the Inventory, Monitoring and Assessment Research unit of Research and Development helped fund the collection of these data and supported the analysis of these data for the 2020 RPA Assessment.

CONTENTS

INTRODUCTION 1

SCENARIO AND MODEL SELECTION 3

Climate Information Needed in the RPA Assessment Resource Analyses 3

Scenarios, Climate Models, and Projections—An Overview 4

Criteria and Selection Process for Scenarios 6

Criteria and Selection Process for Core Climate Models and Projections 6

IDENTIFICATION OF CORE MODELS 11

Temperature and Precipitation Change at Mid-Century for the Conterminous United States 11

Model Performance 13

Selecting Projections that Characterize Climate Change at Mid-Century 16

Mid-Century Core Models 27

TEMPORAL INFLUENCE ON CORE MODEL SELECTION: END OF CENTURY 38

Selecting Projections that Characterize Climate Change at End of Century 38

End-of-Century Core Models 47

MODEL AND PROJECTION SELECTION FOR NATIONAL FOREST REGIONS 51

Use of the Selection Process by National Forest System Region 52

Use of the National Core Model Projections in Individual National Forest Regions 58

Climate Model and Projection Selection in the National Forest Regions 61

AVAILABILITY OF RPA CLIMATE DATA 63
Downscaled Modeled Historical and Projected Data 63
Training Data—Historical Observed Gridded Data 63
SUMMARY AND CONCLUSIONS 65
REFERENCES 67
APPENDIX A 72
APPENDIX B 77

INTRODUCTION

The Forest Service, U.S. Department of Agriculture (hereafter, Forest Service) is mandated to examine potential climate change effects on forests and rangelands in its decadal report, the Resources Planning Act (RPA) Assessment. The legislation, Forest and Rangeland Renewable Resources Planning Act of 1974 (P.L. 93-378, 88 Stat. 475), as amended in 1990, specifically requires "an analysis of the potential effects of global climate change on the condition of renewable resources on the forests and rangelands of the United States" (USDA FS 2001a, p. 4-4). Since 1990, climate change has been a component of the RPA Assessment and the analysis has expanded from a focus on timber to include multiple renewable resources (USDA FS 1993, 2001b, 2007, 2012a, 2016).

Explorations of the potential effect of climate change on natural resources in the RPA Assessment have ranged from a qualitative review (Joyce and Birdsey 2000; Joyce et al. 1990) to the development of climate scenarios and data for use in resource models (Joyce et al. 2014). Climate scenarios are plausible future climates, where each scenario is a time-series of climate variables such as temperature and precipitation specifically developed to investigate the potential consequences of anthropogenic climate change (IPCC 2013a). The development of these potential climate futures involves assumptions about changes in the atmosphere and the modeling of those atmospheric changes using global climate models. Output from these global models is used to create climate datasets for use in natural resource models to examine the potential effects of climate change (for example, see Reeves et al. 2017).

The RPA Assessment must also look at the potential effects of socioeconomic changes on forests and rangelands in the United States. Consequently, potential futures of population growth, economic growth, and land use change must be integrated with climate futures. The scenario approach used in the third and fourth Intergovernmental Panel on Climate Change (IPCC) reports effectively integrated socioeconomic and climate futures (IPCC 2001, 2007). This approach was adopted in the 2010 RPA Assessment (USDA FS 2012a,b). For the IPCC's Fifth Assessment, a new process was used to generate climate and socioeconomic scenarios (IPCC 2013b; Moss et al. 2008, 2010). Given these changes in scenarios and improvements in climate models, the challenge for the 2020 RPA Assessment was to select a set of integrated scenarios that could be used to explore the potential effects of climate and socioeconomic drivers on renewable resource production from forests and rangelands. A scoping process was begun in early 2016 to determine the level of detail in climate and socioeconomic information

that would be needed in the analyses of natural resources (see Wear and Prestemon 2019 and Langner et al. 2020).

This report describes the selection process that was used to identify scenarios, climate models, and climate projections that could be applied at the scale of the conterminous United States. Scenarios, models, and projections selected at the conterminous scale were then evaluated as to their utility at the scale of a national forest region. The timeframe for selection was 50 years into the future and the scenarios, models, and projections were similarly evaluated as to their utility if the timeframe were extended to 2100. Descriptions of future climates at mid-century are included.

SCENARIO AND MODEL SELECTION

Climate Information Needed in the RPA Assessment Resource Analyses

Climate information for the 2020 RPA Assessment must meet the needs of multiple resource analyses—wildlife, rangeland and forest condition, water, urban forests, forest products, and recreation (USDA FS 2012a; see also individual resource publications at the RPA website: https://www.fs.fed.us./research/rpa). A team of scientists who conduct the resource analyses was convened to identify the climate information needed, and to select the specific future scenarios, climate models, and projections (see Acknowledgments). Initial discussions focused on identifying the climate variables needed in different resource analyses (table 1). This list of climate variables and their temporal and spatial extent was used by the team to evaluate the suitability of available downscaled climate datasets for use in the 2020 RPA Assessment.

Table 1—Climate information needs identified for natural resource analyses in the 2020 RPA Assessment.

Climate information	Description
Spatial scale of climate data	Extent: conterminous United States Grain: as fine-scale as possible up to U.S. county level
Time period of historical climate data	As many years as possible
Time period for future climate data	Present to 2070 (RPA 50-year projection) Present to 2099 (timescale available for climate data)
Temperature data	Mean monthly temperature (°C) Minimum and maximum monthly temperature (°C) Mean daily temperature (°C)
Precipitation data	Monthly total precipitation (mm) Annual total precipitation (mm) Daily precipitation (mm)
Other climate data	Potential and actual evapotranspiration Solar radiation Minimum and maximum relative humidity, or vapor pressure deficit or specific humidity Wind speed

As with most natural resource analyses, temperature and precipitation variables were requested; however, scientists were also interested in additional climate data that could be used for drought calculations, such as potential and actual evapotranspiration, solar radiation, relative humidity, and wind speed (table 1). The temporal extent required historical data as well as projections for future periods to 2100. The spatial extent for the RPA Assessment is the United States; however, few resource models were available that link climate with resource production in Alaska, Hawaii and Pacific Island territories, the U.S. Virgin Islands, and Puerto Rico. In addition, fine-scale projections for islands were limited. Consequently, the spatial extent for resource analyses was the conterminous United States.

Scenarios, Climate Models, and Projections—An Overview

Identifying which scenarios and climate models, and how many climate projections to use in an analysis of climate change effects, can be challenging (Hayhoe et al. 2017; Vano et al. 2018). The development of scenarios associated with climate change has been influenced by scientists working with global climate models, economic models, and the assessments conducted by the IPCC. We briefly describe terms used in this community to aid in understanding the climate scenarios, models, and projections used in the 2020 RPA Assessment (table 2).

Scenarios are constructed descriptions of how a future may develop over a period of years. These descriptions can pertain to biological, physical, or socioeconomic futures. With respect to climate, these descriptions include factors that influence atmospheric processes in the global climate—global emissions of greenhouse gases and aerosols, and changes in land use and land cover. These emissions and changes in land use and land cover are influenced by global population growth, economic growth, and changes in technology. Plausible futures are constructed using models that quantify the interactions among the biological, physical, and socioeconomic systems globally.

For the IPCC's Third and Fourth Assessments, scenarios were developed by first drawing out potential futures of population dynamics, economic growth, and other technical and social characteristics (Nakićenović et al. 2000). Using plausible time-series of this information, integrated assessment models analyzed interactions of the physical climate system and associated biological, socioeconomic, and policy processes to produce a time-series of emissions and concentrations of greenhouse gases. This time-series of emissions and concentrations of greenhouse gases, and the associated land use changes, were then used as input to global climate models to quantify potential changes in climate. These scenarios are referred to as the SRES scenarios, based on the Special Report on Emission Scenarios by Nakićenović et al. (2000). The 2010 RPA Assessment used three of these scenarios (A1B, A2, B1) (Joyce et al. 2014; USDA FS 2012a).

Table 2—Definitions of climate-related terms used in this report. Unless noted, all definitions are from IPCC (2013a).

Term	Definition
Climate projection	The simulated response of the climate system to a scenario of future emission or concentration of greenhouse gases and aerosols, generally derived using climate models.
Climate scenario	A plausible and often simplified representation of the future climate, based on an internally consistent set of climatological relationships that has been constructed for explicit use in investigating the potential consequences of anthropogenic climate change, often serving as input to impact models.
Emission scenario	A plausible representation of the future development of emissions of substances that are potentially radiatively active (e.g., greenhouse gases, aerosols) based on a coherent and internally consistent set of assumptions about driving forces (such as demographic and socioeconomic development and technological change) and their key relationships.
Integrated assessment	A method of analysis that combines results and models from the physical, biological, economic, and social sciences, and the interactions among these components, in a consistent framework to evaluate the status and the consequences of environmental change and the policy responses to it (IPCC 2014).
Radiative forcing	The change in the net, downward minus upward, radiative flux (expressed in W m^{-2}; Watts per square meter) at the tropopause or top of atmosphere due to a change in an external driver of climate change, such as a change in the concentration of carbon dioxide or the output of the Sun.
Representative Concentration Pathways (RCPs)	Scenarios that include time-series of emissions and concentrations of the full suite of greenhouse gases and aerosols and chemically active gases, as well as land use and land cover (Moss et al. 2008). The word representative signifies that each RCP provides only one of many possible scenarios that would lead to the specific radiative forcing characteristics.
Scenario	A plausible description of how the future may develop based on a coherent and internally consistent set of assumptions about key driving forces (e.g., rate of technological change, prices) and relationships. Note that scenarios are neither predictions nor forecasts, but are useful to provide a view of the implications of developments and actions.
Special Report on Emission Scenarios (SRES) scenarios	Emission scenarios developed by Nakićenović et al. (2000) and used, among others, as a basis for some of the climate projections shown in IPCC (2007) and IPCC (2011).

For the IPCC's Fifth Assessment, a new process was used to generate climate and socioeconomic scenarios (IPCC 2013b; Moss et al. 2008, 2010). In contrast to the SRES scenarios, these scenarios start with a physical characteristic of the climate system, radiative forcing (table 2). Atmospheric scientists were interested in exploring the potential consequences of specific changes in the radiative forcing since preindustrial times: 2.6, 4.5, 6, and 8.5 W m^{-2} (Watts per square meter). These scenarios are called Representative Concentration Pathways (RCPs). Increases in radiative forcing can occur with fluctuations in the solar energy received, contributions of greenhouse gases to the atmosphere, and changes in land use and land cover. The four RCPs differ by the amount of radiative forcing that is added to the atmosphere by 2100 (IPCC 2013a). RCP 2.6 represents the addition of a low forcing by 2100 and assumes constant emissions thereafter, whereas RCP 8.5 reflects a very high radiative forcing increase by 2100. The greater the radiative forcing added, the greater are the changes in climate likely to occur. To develop the information needed for climate models, integrated assessment models were used to generate a time-series of emissions and concentrations of the full suite of greenhouse gases and aerosols and chemically active gases, as well as land use and land cover (Moss et al. 2010). This information was then used in climate models to investigate the potential consequences

of anthropogenic climate change. Over 20 climate research institutions have used RCPs to explore the potential global changes in temperature and precipitation.

Criteria and Selection Process for Scenarios

The objective of the RPA team was to select all or a subset of the RCPs that could be coupled with socioeconomic scenarios, resulting in a manageable number of scenarios for use in the 2020 RPA Assessment. In discussions among members of the RPA team, the desired number of RCPs and associated climate models and projections varied by resource area. Where the analysis focused only on the ecological or physical dynamics of the resource, more RCPs, climate models, and climate projections were desired to capture a broad range of future climates as well as variation in model responses. However, when socioeconomic scenarios were added, the complexity of analysis increased. Consequently, the team decided to follow the approach used in the Fourth National Climate Assessment, where RCP 4.5 and RCP 8.5 were used as bounding scenarios (USGCRP 2017). These scenarios are the ones used most often by the climate modeling community. The team further determined that for each RCP, the number of climate model and projection combinations would be limited to five.

Criteria and Selection Process for Core Climate Models and Projections

Determining which climate models and associated projections to use was dependent on the availability of downscaled climate projections. Global climate models use a large global grid, and cell sizes can range from 30 miles (48 km) to 200 miles (322 km) on a side (Hayhoe et al. 2017). Climate projections used in the most recent IPCC reports draw on climate model output archived in the web portal of the fifth phase of the Coupled Model Intercomparison Project, known as CMIP5 (https://esgf-node.llnl.gov/projects/cmip5/). Though this archive allows other researchers to access and analyze global climate projections (Hayhoe et al. 2017), the spatial scale of the climate data is too coarse for natural resource analyses. Consequently, a number of downscaling methods have been developed to take global model output and develop climate projections at scales close to the scale of historical weather observations and the scale needed for resource management and planning.

We chose several downscaled climate datasets to review: The National Aeronautics and Space Administration (NASA) Earth Exchange-Global Daily Downscaled Projections (NEX-GDDP) (Thrasher et al. 2012), NASA Earth Exchange-Downscaled Climate Projections (NEX-DCP30) (Thrasher et al. 2013), Bias-Correction Constructed Analogs version 2 CMIP5 Daily Projections (BCCAv2-CMIP5) (Maurer et al. 2002), Multivariate Adaptive Constructed Analogs (MACAv2) (Abatzoglou 2013; Abatzoglou and Brown 2012), and Localized Constructed Analogs (LOCA) (Pierce et al. 2014,

2015). The number of climate models run under both the RCP 4.5 and RCP 8.5 scenarios in each dataset varied from 20 models in MACAv2 to 33 in NEX-DCP30. Spatial and temporal extent also varied across the datasets. At the time all except the LOCA data were available. Because of unavailability, the LOCA data were dropped from further consideration.

Using the criteria established in table 1, we reviewed these downscaled datasets for their ability to provide the needed climate information. The need for fine-scale data was not met by the NEX-GDDP dataset, where the grain of analysis was approximately 25 km. The need for additional variables such as solar radiation, relative humidity, or wind speed was not met by the BCCAv2-CMIP5 Daily Projections dataset. The need for daily data was not met by the NEX-DCP30 dataset.

The downscaled dataset selected was MACAv2-METDATA (Abatzoglou 2013; Abatzoglou and Brown 2012). Downscaled climate projections from 20 climate models were available under the RCP 4.5 and RCP 8.5 scenarios (table 3). The spatial scale for this downscaled dataset (approximately a 4-km grid) met the fine-scale requirement (table 1). Both daily and monthly downscaled projections were provided, as well as the historical observed climate that was used in the MACA downscaling process (University of Idaho n.d.). Other climate variables, such as solar radiation, were also available. Further, this dataset was used in analyzing climate change effects on vegetation with the MC2 model (Bachelet et al. 2016), providing a link with other analyses in the 2020 RPA Assessment. This downscaled climate dataset has been used in several climate assessments (Loehman et al. 2018; Sheehan et al. 2019; Yazzie and Chang 2017).

The combination of 20 climate models and 2 RCP scenarios resulted in 40 climate model projections in the MACAv2-METDATA dataset. The literature often recommends using as many climate models and projections as feasible, or using an ensemble (average) of several climate models (Mote et al. 2011). Where the MACAv2-METDATA dataset has been used in climate change analyses, various reasons are given for the number of climate models selected. For example, Yazzie and Chang (2017) selected 10 of the 20 models from the MACAv2-METDATA dataset based on the models' ability to capture the region's historical climate. Sheehan et al. (2019) used only one model (CCSM4) and one scenario (RCP 8.5) in a study focused on teasing out the effects of fire, carbon dioxide, and climate using the MC2 dynamic vegetation model. Luce used all 20 models for an analysis of snow and water on national forest lands (USDA FS n.d.). All 20 models downscaled using MACAv2-Livneh data (slightly different from the dataset used here) were used by Lute et al. (2015) in a study on projected changes in snowfall extremes in the western United States.

Table 3—The 20 climate models available in the downscaled climate dataset, MACAv2-METDATA (University of Idaho n.d.), selected for use in the 2020 RPA Assessment (Abatzoglou 2013; Abatzoglou and Brown 2012), with modeling institution and projection resolution. Historical modeled data cover the 1950–2005 period; projections cover the 2006–2099 period.

Model name	Modeling institution and location	Resolution (longitude × latitude)[a]
bcc-csm1-1	Beijing Climate Center, China Meteorological Administration (China)	2.8 deg × 2.8 deg
bcc-csm1-1-m	Beijing Climate Center, China Meteorological Administration (China)	1.12 deg × 1.12 deg
BNU-ESM	Beijing Normal University (China)	2.8 deg × 2.8 deg
CanESM2	Canadian Centre for Climate Modelling and Analysis (Canada)	2.8 deg × 2.8 deg
CCSM4	National Center of Atmospheric Research (United States)	1.25 deg × 0.94 deg
CNRM-CM5	National Centre of Meteorological Research and European Centre for Advanced Research and Training (France)	1.4 deg × 1.4 deg
CSIRO-Mk3-6-0	Queensland Climate Change Centre of Excellence and Commonwealth Scientific and Industrial Research Organization (Australia)	1.8 deg × 1.8 deg
GFDL-ESM2M	National Oceanic and Atmospheric Administration [NOAA], Geophysical Fluid Dynamics Laboratory (United States)	2.5 deg × 2.0 deg
GFDL-ESM2G	NOAA Geophysical Fluid Dynamics Laboratory (United States)	2.5 deg × 2.0 deg
HadGEM2-ES[b]	Met Office Hadley Centre (United Kingdom)	1.88 deg × 1.25 deg
HadGEM2-CC[b]	Met Office Hadley Centre (United Kingdom)	1.88 deg × 1.25 deg
inmcm4	Institute for Numerical Mathematics (Russia)	2.0 deg × 1.5 deg
IPSL-CM5A-LR	Institut Pierre Simon Laplace (France)	3.75 deg × 1.8 deg
IPSL-CM5A-MR	Institut Pierre Simon Laplace (France)	2.5 deg × 1.25 deg
IPSL-CM5B-LR	Institut Pierre Simon Laplace (France)	2.75 deg × 1.8 deg
MIROC5	University of Tokyo, National Institute for Environmental Studies, and Japan Agency for Marine-Earth Science and Technology	1.4 deg × 1.4 deg
MIROC-ESM	University of Tokyo, National Institute for Environmental Studies, and Japan Agency for Marine-Earth Science and Technology	2.8 deg × 2.8 deg
MIROC-ESM-CHEM	University of Tokyo, National Institute for Environmental Studies, and Japan Agency for Marine-Earth Science and Technology	2.8 deg × 2.8 deg
MRI-CGCM3	Meteorological Research Institute (Japan)	1.1 deg × 1.1 deg
NorESM1-M	Norwegian Climate Center (Norway)	2.5 deg × 1.9 deg

[a] deg = degree

[b] HadGEM2-ES and HadGEM2-CC are both 360-day models, but 365-day outputs are needed for most impact analyses. Consequently, the MACA developers interpolated these data to 365 days before downscaling them to create the models HadGEM2-ES365 and HadGEM2-CC365 (University of Idaho n.d.). For economy of space, we have dropped the 365 in this text.

The projected changes in precipitation and temperature can differ widely across models within a single scenario. For example, Byun and Hamlet (2018) plotted the projected changes in precipitation against the projected changes in temperature under RCP 8.5 by the 2080s. The projected changes across the 31 models covered a space that ranged from temperature increases of 3 °C to 9 °C and precipitation increases of near 0 percent to 25 percent (see figure 5 in Byun and Hamlet 2018). Researchers have used a variety of approaches to select a subset of projections that characterize this range of changes in temperature and precipitation. The CREAT tool developed by the U.S. Environmental Protection Agency (USEPA 2016) identifies scenarios and projections based on combinations of changes in temperature and precipitation. Byun and Hamlet (2018) used a series of circles in the precipitation versus temperature graph to identify 10 representative models out of the original 31 models. Climate projections might be selected without reference to RCPs; here the hottest projection across all RCP scenarios could be chosen to focus on what happens without regard to economic or land use changes. Information in the socioeconomic scenarios was linked to a particular RCP scenario; consequently, selection of projections for the RPA Assessment was based within a scenario (RCP 4.5, RCP 8.5).

Given the objective of identifying five model-projection combinations for each RCP, a process was developed to scrutinize both the climate models and the projections (fig. 1). Selection of climate models was based on three criteria. The first criterion evaluated the ability of each model to capture historical model projections. Based on this criterion, models that were consistently rated as poor performers were dropped from further consideration. The second criterion restricted selection to only one model from a modeling institution; climate scientists emphasize the importance of using models from different modeling institutions (Knutti 2010; Knutti et al. 2013). The third criterion considered whether the same climate model could be used for RCP 4.5 and RCP 8.5 to reduce model variation across scenarios. Selection of individual projections was based on identifying a set of projections that would characterize the temperature and precipitation changes of the 20 models: least warm, hot, dry, and wet at mid-century as well as a future that could characterize the middle of the temperature and precipitation ranges.

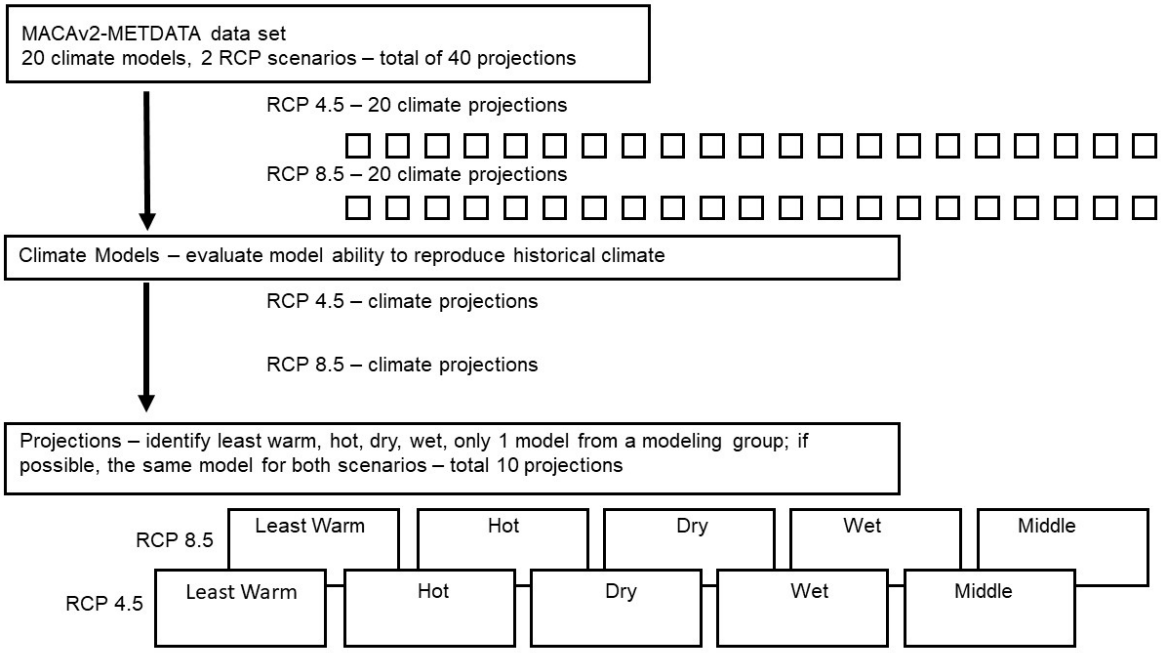

Figure 1—Process used to identify five climate projections from the MACAv2-METDATA climate dataset to be used under RCP 4.5 and RCP 8.5 in the 2020 RPA Assessment.

IDENTIFICATION OF CORE MODELS

Temperature and Precipitation Change at Mid-Century for the Conterminous United States

To determine the range in projected mean temperature and annual precipitation change across all projections, we computed the grid-cell area-weighted change in temperature and precipitation from the historical (1971–2000) to the mid-century (2041–2070) period for the conterminous United States. The 1971–2000 period was chosen as the historical basis for determining future changes to avoid mixing historical modeled projections ending in 2005 with future projections starting in 2006. The 2041–2070 period was chosen for the mid-century basis as this 30-year period would reflect the normal climate on which management decisions would be based in 2070. Temperature and precipitation change in each grid cell was computed as the difference in temperature and percent change in precipitation. Models were ranked within each climate variable on the basis of these changes at the conterminous scale.

Mean temperature was projected to increase across all model projections and under both scenarios by mid-century (figs. 2a, b). Increases ranged from 1.17 °C to 3.40 °C under RCP 4.5 and from 1.84 °C to 4.26 °C under RCP 8.5. By individual model, projected increases under RCP 8.5 were greater than under RCP 4.5. However, projected change in temperature for some models under RCP 4.5 was greater than projected change in temperature for other models under RCP 8.5. For example, 8 of the 20 models under RCP 4.5 projected greater increases in mean temperature than 4 models under RCP 8.5—MRI-CGCM3, inmcm4, GFDL-ESM2M, and GFDL-ESM2G (figs. 2a,b). An overlap of projected temperature changes under the RCP 4.5 and RCP 8.5 scenarios was also reported by Hayhoe et al. (2017).

Changes in annual precipitation ranged from a 4.76-percent decrease to a 10.00-percent increase under RCP 4.5 and from a 6.47-percent decrease to a 9.14-percent increase under RCP 8.5 (figs. 2c, d). Most models projected precipitation increases. Decreases in precipitation were greater under RCP 8.5 than RCP 4.5. Only one model, IPSL-CM5A-MR, projected decreases under both scenarios. Individual model projections varied between scenarios. For example, models bcc-csm1-1 and bcc-csm1-1-m projected decreases in precipitation under RCP 4.5 and increases under RCP 8.5.

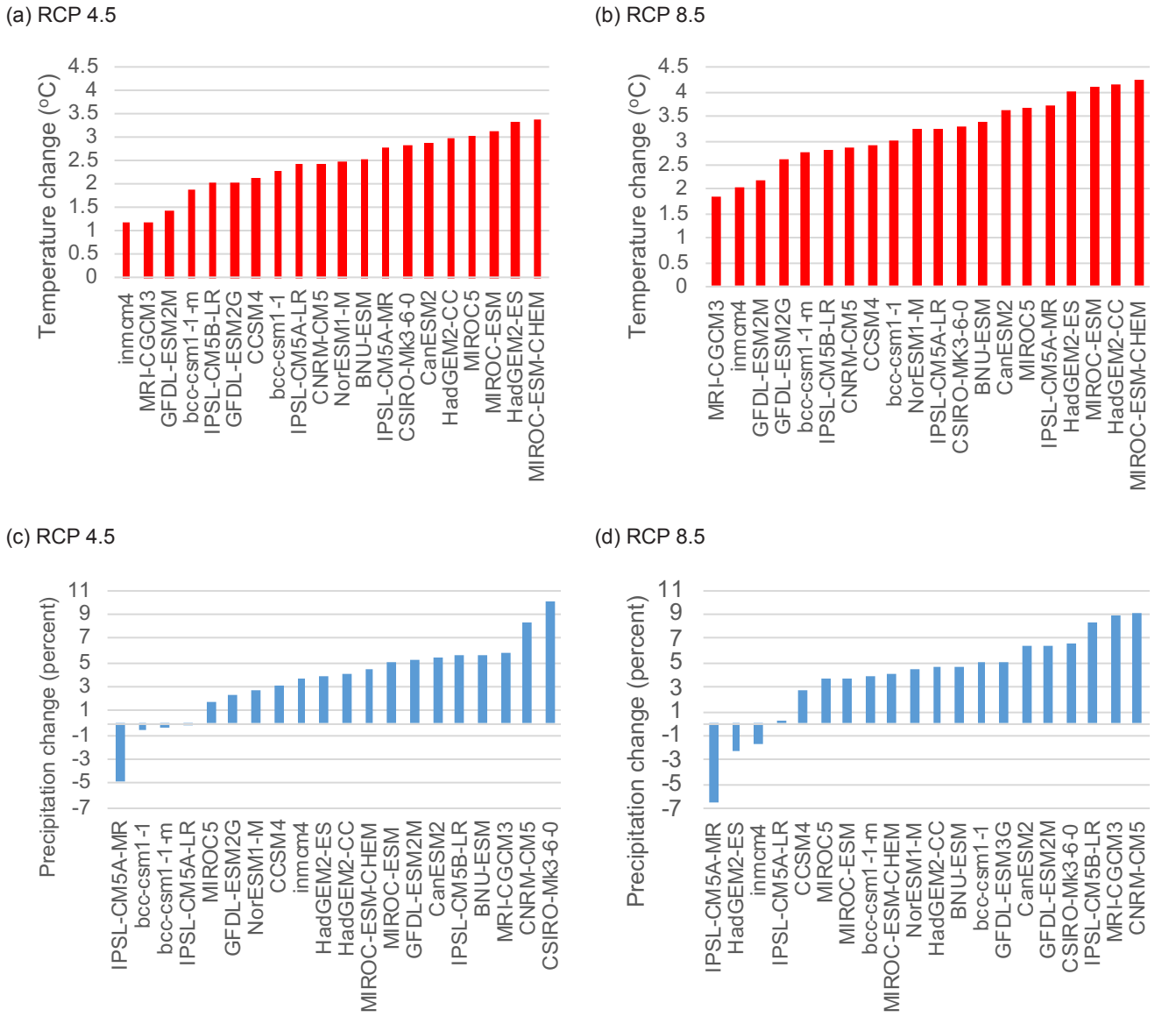

Figure 2—Area-weighted change in mean temperature (°C) and annual precipitation (percent) at mid-century (2041–2070) from the historical period (1971–2000) under RCP 4.5 (a, b) and RCP 8.5 (c, d) for all 20 models at the conterminous U.S. scale.

By this initial ranking, the smallest change in temperature (least warm) varied by scenario, with the inmcm4 model projecting the smallest change under RCP 4.5 and the MRI-CGCM3 model projecting the smallest change under RCP 8.5. The hottest projection for both scenarios by the 2041–2070 period was the MIROC-ESM-CHEM model projection (figs. 2a,b). The driest projection for both scenarios was the IPSL-CM5A-MR projection (figs. 2c,d). The wettest projection varied by scenario; CSIRO-Mk3-6-0 projected the greatest increase in precipitation under RCP 4.5 and CNRM-CM5 projected the greatest precipitation increase under RCP 8.5.

Model Performance

Historical model performance rankings developed by Rupp et al. (2013) and Rupp (2016a,b) were used to identify models that poorly capture the 20th-century observed climate. A wide variety of temporal and spatial metrics have been used to compare historical model projections with observed climate at the global and conterminous U.S. scales (Flato et al. 2013; Sanderson and Wehner 2017; Sheffield et al. 2013). Model performance at one scale may differ from model performance at a different scale (global versus regional) (Flato et al. 2013). In studies by Rupp et al. (2013) and Rupp (2016a,b), a consistent methodology is used for three regions in the United States: Pacific Northwest, Southwest, and Southeast. Their evaluation focuses in particular on temperature and precipitation, important variables in the RPA analysis. The spatial extent for the climate change analysis for the RPA Assessment was the conterminous United States, with consideration for large subregions within the United States (USDA FS 2012a, 2016).

In the studies by Rupp and others, the Pacific Northwest encompasses the States of Washington, Oregon, and Idaho, and the western part of Montana (Rupp et al. 2013). The Southeast study area encompasses the eastern parts of Nebraska, Oklahoma, and Texas; all of Louisiana, Georgia, Alabama, Florida, North Carolina, South Carolina, Virginia, West Virginia, Kentucky, Maryland, Delaware, and New Jersey; nearly all of Missouri; the southern parts of Illinois, Indiana, and Ohio; and a small fraction of Pennsylvania (Rupp 2016a). The Southwest study encompasses nearly all of California, Nevada, and Utah; the entire State of Arizona; and the western parts of Colorado and New Mexico (Rupp 2016b).

Across these studies, Rupp and others use 41 models for the Pacific Northwest and the Southeast, and 43 models for the Southwest. For our study, we dropped the 2 models from the Southwest analysis that were not included in the Pacific Northwest and Southeast analyses so that all sets included the same 41 models. We then reranked the Southwest model results as 1 to 41. Given that the downscaled climate dataset had 20 models, we explored the consequences of reranking model performance to a range of 1 to 20. As this reranking did not change the relative ranking, particularly where the standard errors were high, we retained the individual model ranking based on all 41 models for this analysis. Hence, ranking values across the models ranged from 1 to 41.

Rupp et al. (2013) use a suite of 42 climate metrics to evaluate historical model performance. Individual metrics include correlation between modeled and observed values and variance for mean seasonal spatial patterns, amplitude of seasonal cycle, diurnal temperature range, and other temperature or precipitation variables. In all 3 studies, climate models are ranked using 2 methods: (1) all 42 metrics treated equally, and (2) a subset of 18 metrics that considered (a) redundancy of information (dependence) among metrics, and (b) confidence in the reliability of an individual metric

for accurately ranking models (Rupp et al. 2013). Using the rankings from Rupp and others' studies, we developed for each model a subconterminous U.S. model ranking. This ranking was computed as the mean of the 3 regional rankings using the 42-metric ranking and as the mean of the 18-metric rankings.

The historical model performance of each model, based on the 42- and the 18-variable metric, is shown as the mean across all regions (fig. 3a); also shown is the individual model ranking for each region: Pacific Northwest (Rupp et al. 2013), Southeast (Rupp 2016a), and Southwest (Rupp 2016b) (fig. 3b). A lower rank indicated a better model performance in capturing the historical climate. The ranking order using 42 metrics was fairly similar to the ranking order using 18 metrics. Based on the 3-region mean rank using either the 42- or 18-variable method, the same models were in the top 9 ranks, albeit in a different order. Based on the mean rank in either method, the CNRM-CM5 model had the lowest rank. This model was also among the top 10 ranked models within each region, based on either the 42- or 18-metric method.

With respect to performance, the objective was to drop models that appeared to perform poorly in capturing the historical observed climate. Using the 18-metric ranking averaged across all regions, the 4 models that performed poorly were IPSL-CM5B-LR, MIROC-ESM-CHEM, MIROC-ESM, and bcc-csm1-1 (fig. 3a). These models were consistently in the worst performing ranks of both the 42-metric rankings and the 18-metric rankings, with the order of the 4 models shifting between the 2 analyses. These four models were dropped from further consideration. The range of mid-century changes in temperature and precipitation were influenced by removing these models from consideration; for example, MIROC-ESM-CHEM was the hottest projection of all 20 models under RCP 4.5 and RCP 8.5 and MIROC-ESM was the 3rd-hottest model (figs. 2a, b). Similarly, bcc-csm1-1 was the second driest projection under RCP 4.5 and IPSL-CM5B-LR was the third wettest projection under RCP 8.5 (figs. 2c, d).

These three studies did not include the northern Great Plains, the northern Midwest, or the northeastern United States. Byun and Hamlet (2018) evaluated the historical performance for the Midwest and Great Lakes region for 31 models and projections that were downscaled using a method they developed. Recognizing that there are several differences in climate dataset and downscaling method, they removed from their analysis, on the basis of historical performance, the four models dropped in this study (see figure 3 in Byun and Hamlet 2018). In addition, the recent National Climate Assessment evaluated the skill of 41 climate models used in that assessment (Sanderson and Wehner 2017). The geographic extent of that analysis was the conterminous United States and Canada. The models dropped from our study were ranked close to or at the bottom of the 41 models: IPSL-CM5B-LR at 33, bcc-csm1-1 at 34, MIROC-ESM at 40, and MIROC-ESM-CHEM at 41 (Sanderson and Wehner 2017). These results support our decision to remove those models from our study as well.

(a) Three-region mean performance results for each model

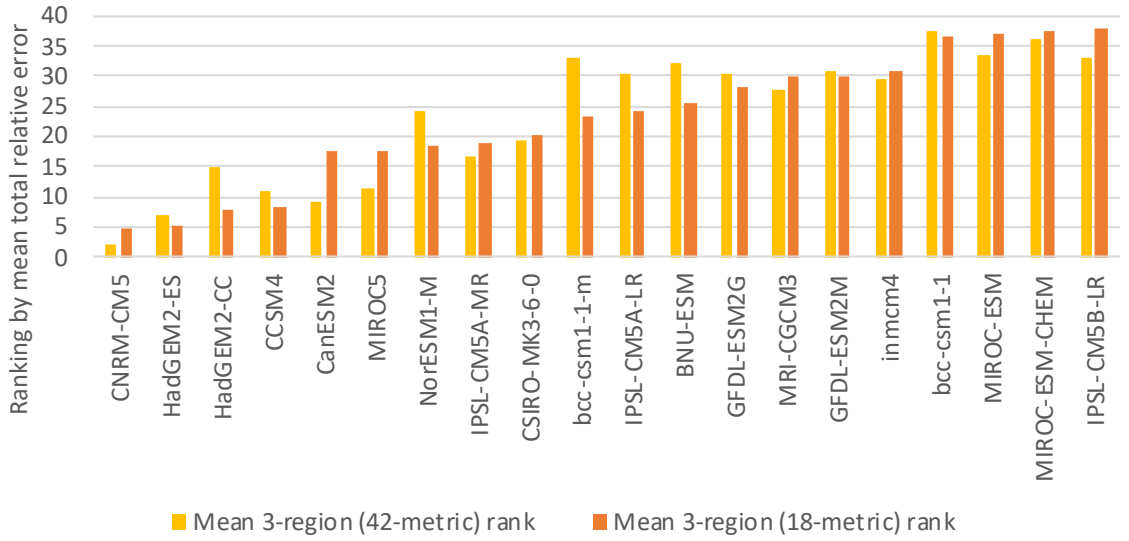

(b) Performance results for each model within each region

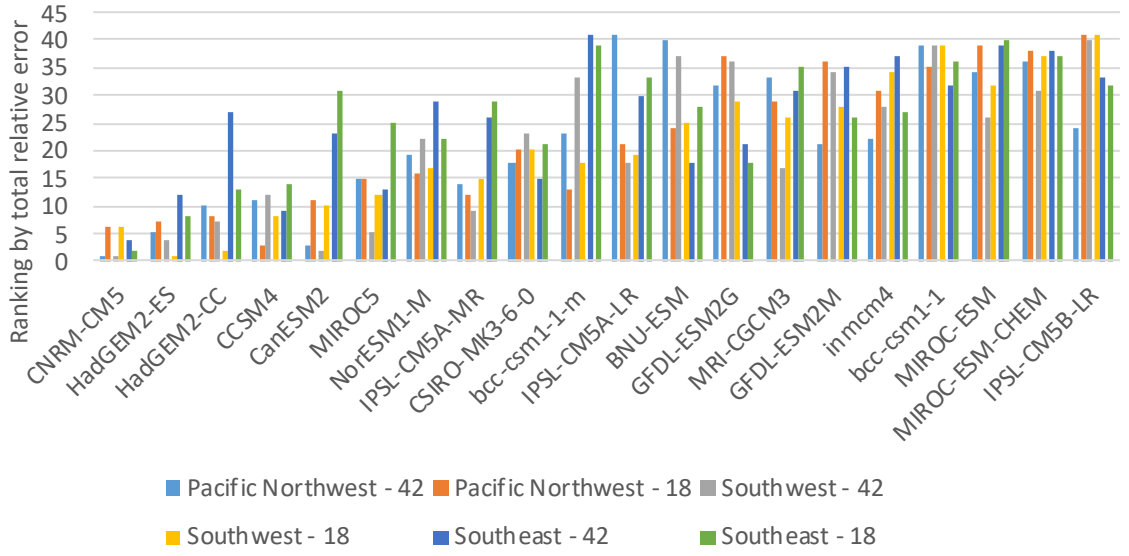

Figure 3—Model performance results for 20 models from Rupp et al. (2013) and Rupp (2016a,b) for the 3-region mean results (a), and model results within each of the 3 regions (Pacific Northwest, Southwest, Southeast) (b). Results shown for both methods (42 variable, 18 variable). The lower the performance metric, the better the projection reproduced the 20th-century observed climate. The order of the performance results in each graph was based on the rankings of the 3-region mean results for the 18-metric analysis.

Selecting Projections that Characterize Climate Change at Mid-Century

Using the change in temperature and precipitation between 2041–2070 and 1971–2000, we selected three projections for the lower and the upper range of changes in temperature and precipitation under each scenario (table 4). Our objective was to select a projection that (1) met the criterion of a distinct change in the one climate variable and (2) was close to the ensemble mean for the other climate variable. We required that only one model from a modeling institution be represented within these five projections (least warm, hot, dry, wet, middle) and if possible, that the same model represent the core model for each climate range under both scenarios (RCP 4.5, RCP 8.5).

Table 4—Top three ranked projections in terms of temperature (least warm, hot) and precipitation (dry, wet) change at mid-century (2041–2070) under scenarios (RCP 4.5, RCP 8.5) at the conterminous U.S. scale, with poor performers excluded. Temperature and precipitation change was computed relative to the historical period (1971–2000) as shown in figure 2.

Scenario	Rank	Least Warm	Hot	Dry	Wet
RCP 4.5	1	inmcm4	HadGEM2-ES	IPSL-CM5A-MR	CSIRO-Mk3-6-0
	2	MRI-CGCM3	MIROC5	bcc-csm1-1-m	CNRM-CM5
	3	GFDL-ESM2M	HadGEM2-CC	IPSL-CM5A-LR	MRI-CGCM3
RCP 8.5	1	MRI-CGCM3	HadGEM2-CC	IPSL-CM5A-MR	CNRM-CM5
	2	inmcm4	HadGEM2-ES	HadGEM2-ES	MRI-CGCM3
	3	GFDL-ESM2M	PSL-CM5A-MR	inmcm4	CSIRO-Mk3-6-0

Generally, the two scenarios had similar models in the top three ranks under the RCP 4.5 and the RCP 8.5 scenario (table 4). For the least warm and wet categories, the same three models appeared under both scenarios but in different rank orders. For the hot category, two models appeared under both scenarios. For the dry category, only one model appeared under both scenarios, IPSL-CM5A-MR. More than one model from a modeling institution appeared in the hot (Hadley models) and dry categories (IPSL models).

Least Warm

The same three models fell into the top three ranks under RCP 4.5 and RCP 8.5, although the ranking differed between the scenarios (table 4). Under RCP 4.5, the inmcm4 model and the MRI-CGCM3 model projected nearly the same mid-century increase in temperature, 1.17 °C and 1.20 °C, respectively (fig. 2a). Under RCP 8.5, both models again projected nearly the same increase in temperature but with greater separation, 1.84 °C for MRI-CGCM3 and 2.02 °C for inmcm4. The projection for GFDL-ESM2M was warmer than both inmcm4 and MRI-CGCM3 (fig. 2b). Though inmcm4 could be chosen as the Least Warm core model for RCP 4.5, and MRI-CGCM3 for RCP 8.5, we explored the projections from these two models to determine whether one model could be used for both scenarios as the Least Warm core model.

We ranked temperature change from the historical period to mid-century for each grid cell across all 16 projections, where the smallest change for an individual grid cell projected by 1 of the 16 climate models was rank 1 and the largest change for that grid cell projected by 1 of the climate models, rank 16. Ideally, the Least Warm core model would have nearly all grid cells ranked 1, 2, or 3, the smallest change in temperature of all 16 models. Under RCP 4.5, all grid cells in the projection by MRI-CGCM3 and inmcm4 had temperature differences ranked as 1, 2, or 3. Under RCP 8.5, most grid cells projected by MRI-CGCM3 and inmcm4 were ranked as the least temperature change (ranks 1–3). However, for different areas of the United States, some grid-cell projections were ranked at 4 or greater (figs. 4c, d).

The spatial patterns of temperature change varied more between models than between scenarios (fig. 4). The smallest temperature changes under RCP 4.5 occurred in the western through southern parts of the United States for inmcm4 but along the West Coast and across the Central Plains to the southern United States for MRI-CGCM3 (figs. 4a, b). Under RCP 8.5, the smallest temperature changes for inmcm4 retreated to the coastal areas, whereas the areas with the smallest change for MRI-CGCM3 remained geographically similar to the patterns for this model under RCP 4.5 (figs. 4c, d).

The second criterion was to explore whether the case could be made to use one model as the core model for both scenarios. Differences in temperature change between the inmcm4 projection and the MRI-CGCM3 projection under RCP 4.5 were less than 0.05 °C (fig. 2). The MRI-CGCM3 projection showed the smaller change of these two models at mid-century under RCP 8.5. The spatial patterns were more similar within a model than across scenarios (fig. 4), potentially resulting in a more consistent comparison for the least warm projection if the same model were chosen as the core model for least warm under both scenarios. We selected MRI-CGCM3 as the Least Warm core model.

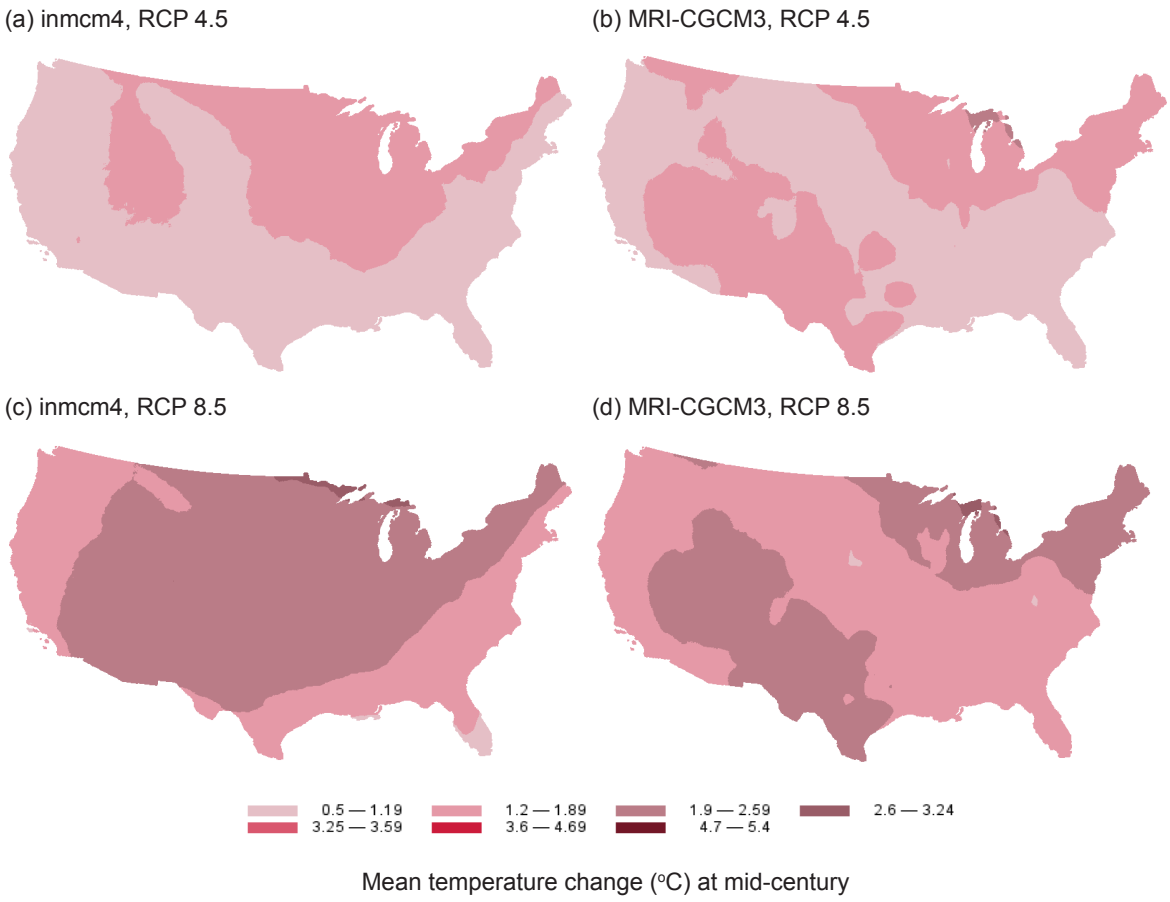

Figure 4—Mean temperature change (°C) at mid-century (2041–2070) from the historical period (1971–2000) as projected by the inmcm4 model under RCP 4.5 (a) and RCP 8.5 (c) and the MRI-CGCM3 model under RCP 4.5 (b) and RCP 8.5 (d).

Hot

The three hottest projections under both scenarios had two models in common: HadGEM2-ES, the hottest projection for RCP 4.5 and second under RCP 8.5, and HadGEM2-CC, the hottest projection for RCP 8.5 and third under RCP 4.5 (table 4). Two additional models filled out the top three projections: MIROC5 and IPSL-CM5A-MR. Under RCP 4.5, the projected increases for the top three models were small, within 0.35 °C: an increase of 3.34 °C for HadGEM2-ES, 3.03 °C for MIROC5, and 2.99 °C for HadGEM2-CC (fig. 2a). Under RCP 8.5, the top three projections differed by 0.44 °C, with increases of 4.14 °C for HadGEM2-CC, 4.01 °C for HadGEM2-ES, and 3.70 °C for IPSL-CM5A-MR.

The models with the hottest projections under each scenario were from the same modeling institution (table 4). Given that one criterion was to avoid selecting more than one model from a modeling institution, one of the Hadley models had to be dropped or another model chosen for RCP 4.5 or RCP 8.5. The IPSL-CM5A-MR projection was not among the three

hottest projections under RCP 4.5, and it was a distant third under RCP 8.5. Similarly, the MIROC5 projection was not ranked in the top three under RCP 8.5. A third criterion for model selection was, if possible, to select the same model for both RCPs. We evaluated the tradeoffs between HadGEM2-ES and HadGEM2-CC in the selection of the Hot core model for both scenarios.

As with the least warm model comparison, we ranked the temperature changes of the Hadley projections; ideally, most of the grid cells would fall into the hottest ranks. To map, we grouped rankings where the least change was defined as ranks 1 through 3, middle as ranks 4 through 13, and greatest change as ranks 14 through 16. Under RCP 4.5, most grid-cell projections by HadGEM2-ES fell into the hottest category (ranks 14–16), whereas a greater proportion of the grid-cell projections of HadGEM2-CC fell into the middle category (ranks 4–13) for the western United States and the eastern coastline (figs. 5a,b). The ranking pattern reversed for the RCP 8.5 projections (figs. 5c,d). Here, grid cells for the HadGEM2-CC projection were in the hottest

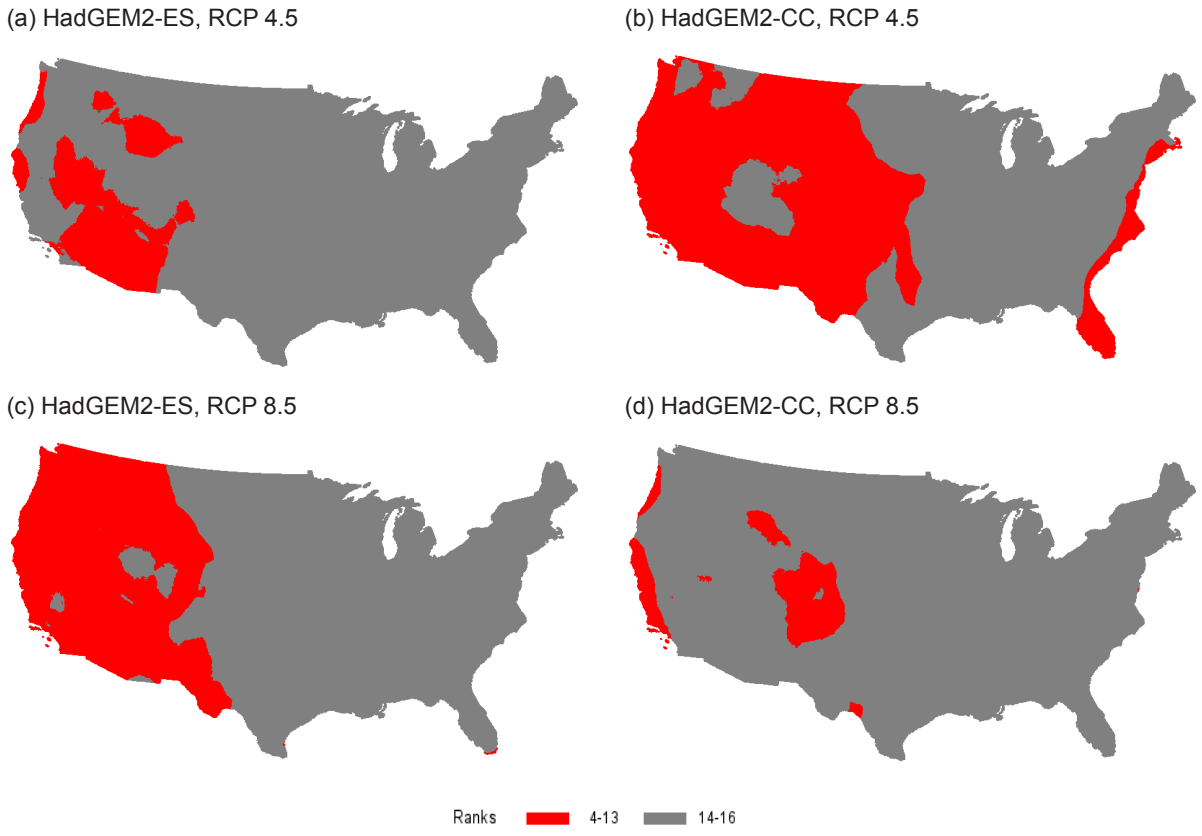

Figure 5—Ranking of grid-cell projected temperature change at mid-century (2041–2070), where ranks 1 through 3 reflect the least change, ranks 4 through 13 the mid-range change, and ranks 14 through 16 the greatest change: HadGEM2-ES under RCP 4.5 (a); HadGEM2-CC under RCP 4.5 (b); HadGEM2-ES under RCP 8.5 (c); HadGEM2-CC under RCP 8.5 (d). All grid cells were rank 4 or higher; hence no grid cell results were in the least change category (ranks 1–3).

category (ranks 14–16) throughout the conterminous United States; grid cells for the HadGEM2-ES projection were in the hottest category for the eastern and midwestern portions of the Nation.

We explored the frequency distribution of individual grid-cell rankings by HadGEM2-CC and HadGEM2-ES at the conterminous scale (fig. 6). The HadGEM2-ES model projected the hottest temperatures (rank 16) for nearly 60 percent of the grid cells under RCP 4.5, whereas, not unexpectedly, HadGEM2-CC had few grid cells in rank 16 (fig. 6a). Under RCP 8.5, HadGEM2-CC projected the greatest change (rank 16) for 45 percent of the grid cells, whereas HadGEM2-ES projected the greatest change for fewer than 25 percent of the grid cells (fig. 6b). Combining the top two ranks, HadGEM2-ES was the hottest or second hottest projection for 61 percent of the conterminous United States, in contrast to the 74 percent that HadGEM2-CC captured.

(a) Frequency distribution of grid-cell ranks for change in mean temperature under RCP 4.5

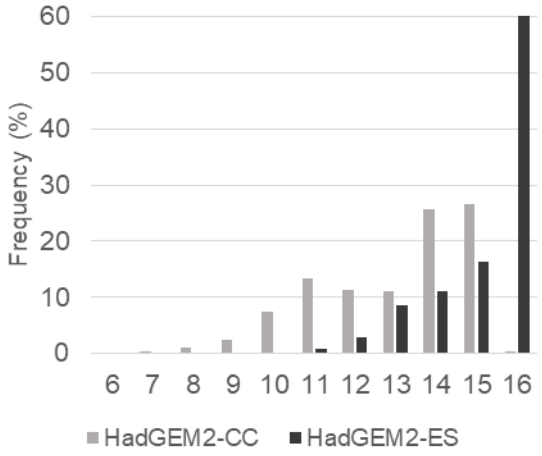

(b) Frequency distribution of grid-cell ranks for change in mean temperature under RCP 8.5

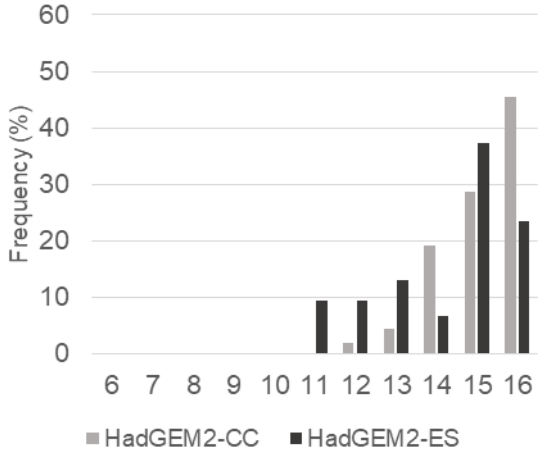

Figure 6—Frequency distribution (percent) of grid-cell ranks from the HadGEM2-CC and HadGEM2-ES projections relative to all 16 models under RCP 4.5 (a) and RCP 8.5 (b). If a model had the largest change in temperature of all models, the grid cell rank was 16. If the model had the lowest change, the grid cell rank was 1. For both models, all grid cells were rank 6 or higher in terms of temperature change under RCP 4.5 and rank 11 or higher under RCP 8.5.

The spatial patterns of the projected differences in both Hadley models were similar within a scenario (figs. 7a, b; 7c, d) and across scenarios (figs. 7a, c; 7b, d). In all maps, the greatest temperature change occurred in the north-central area of the conterminous United States, radiating out to areas of least change along the coastal areas and the southern part of the United States. Given that HadGEM2-ES was the hottest model for RCP 4.5, and the tradeoffs were small for selecting HadGEM2-ES for RCP 8.5, we selected HadGEM2-ES as the Hot core model representative of the upper end of the temperature change for RCP 4.5 and RCP 8.5.

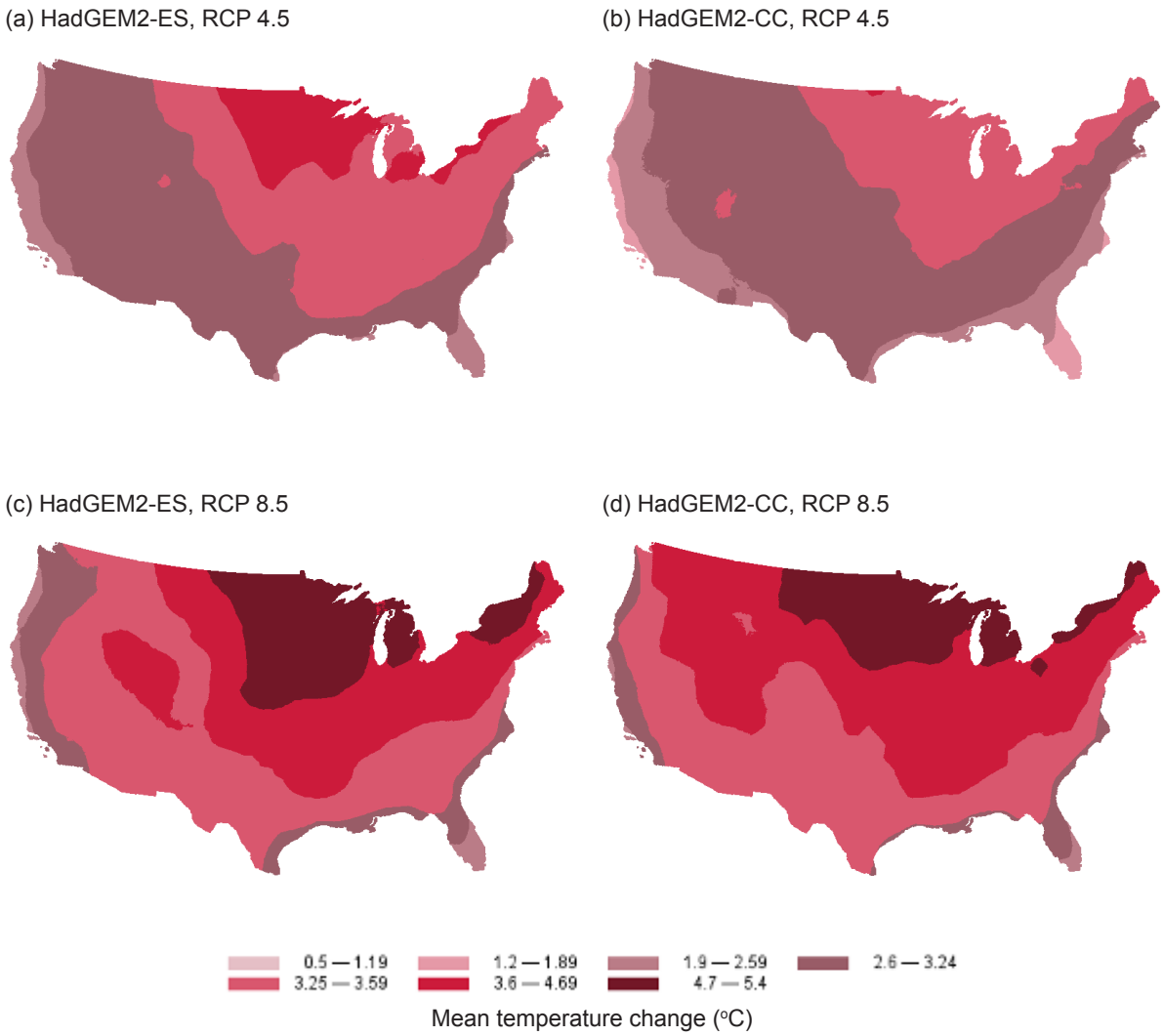

Figure 7—Mean temperature change (°C) at mid-century (2041–2070) from the historical period (1971–2000) as projected by HadGEM2-ES and HadGEM2-CC under RCP 4.5 (a,b) and RCP 8.5 (c,d).

Dry

In contrast to the commonality of models under each scenario for the temperature ranges, only one model was common to the three driest projections for both scenarios: IPSL-CM5A-MR (table 4). Models projecting the second and third driest futures differed between the scenarios. This total of five different models in the top three ranks of both scenarios contrasted with the least warm range (three different models) or the hottest range (four different models) (table 4). These differences suggest greater variation across precipitation projections.

Not only was IPSL-CM5A-MR common to the top-ranked projections in both scenarios, this model was also the driest projection under both scenarios. Of the 16 projections, only 3 under RCP 4.5 and only 3 under RCP 8.5 showed decreases in annual precipitation at the conterminous scale at mid-century (fig. 2). Under RCP 4.5, precipitation was projected to decrease more than 4.76 percent by IPSL-CM5A-MR, whereas the next ranking models projected less than a 1-percent decrease in precipitation. Under RCP 8.5, precipitation was projected to decrease 6.47 percent by IPSL-CM5A-MR, with the next ranking model projecting a 2.16-percent decrease.

Given that the projection for IPSL-CM5A-MR was the driest projection under both RCP 4.5 and RCP 8.5, the IPSL-CM5A-MR model was selected as the Dry core model representing the lower end of the change in precipitation for both scenarios.

Wet

The same three models were ranked as the three wettest futures at mid-century under both RCP 4.5 and RCP 8.5, with order varying by scenario: CSIRO-Mk3-6-0, CNRM-CM5, and MRI-CGCM3 (fig. 2, table 4). The CSIRO-Mk3-6-0 model produced the wettest projection at a 10.00-percent increase under RCP 4.5 but was the distant third under RCP 8.5 (table 4), projecting an increase of 6.63 percent. The CNRM-CM5 model had the wettest projection under RCP 8.5 at a 9.14-percent increase and was ranked second under RCP 4.5 with an 8.31-percent increase.

Percent change in annual precipitation at mid-century varied spatially across the United States (fig. 8). The CSIRO-Mk3-6-0 projections under both scenarios showed the largest increases in precipitation in the southwestern United States, with precipitation projected to double at mid-century. The projections by CNRM-CM5 and MRI-CGCM3 suggested a more uniform increase in precipitation across the conterminous United States, with small areas seeing increases or decreases.

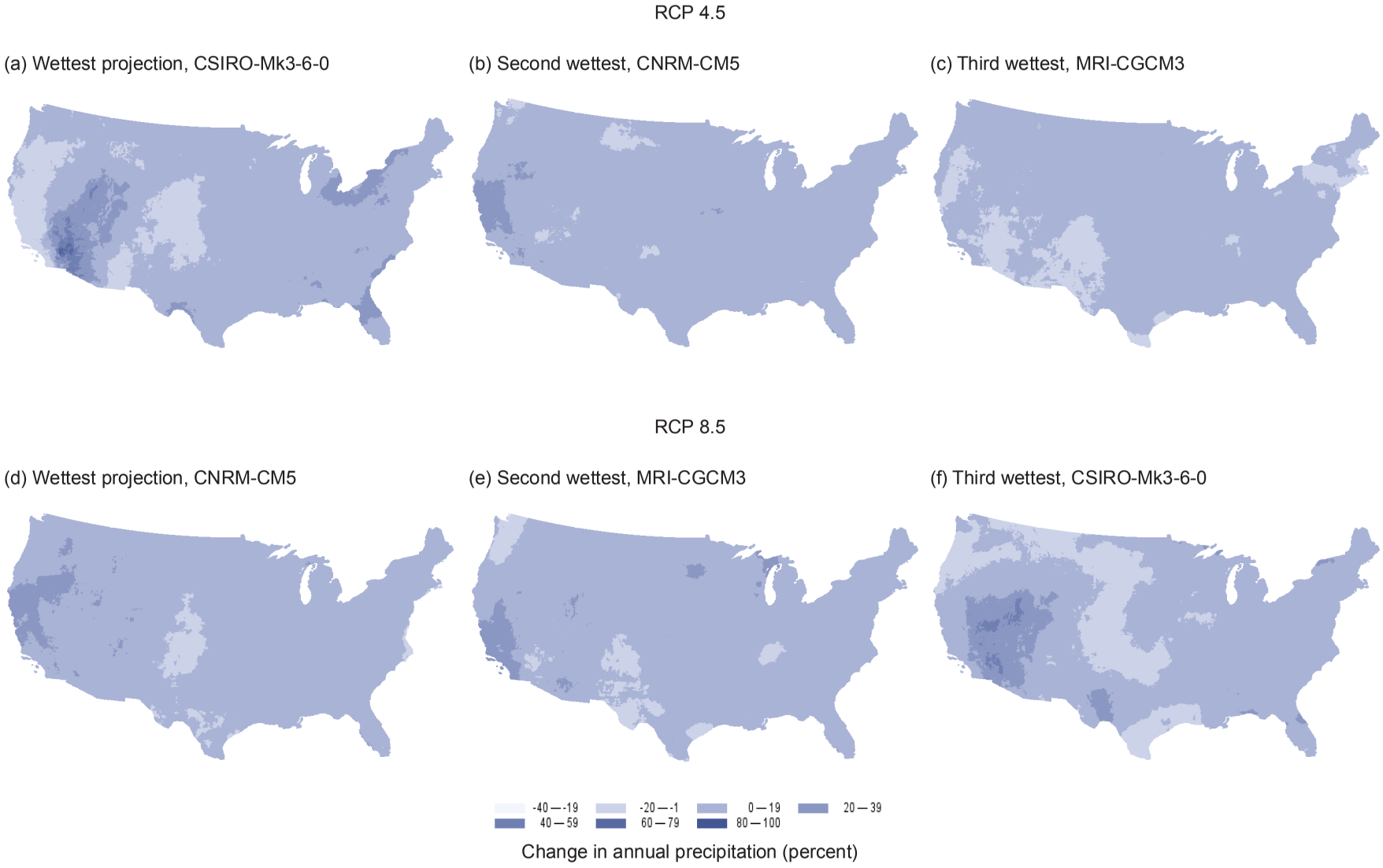

Figure 8—Annual precipitation change (percent) at mid-century (2041–2070) from the historical period (1971–2000) for the three wettest projections under RCP 4.5: CSIRO-Mk3-6-0 (a), CNRM-CM5 (b), and MRI-CGCM3 (c); and under RCP 8.5: CNRM-CM5 (d), MRI-CGCM3 (e), and CSIRO-Mk3-6-0 (f).

Ideally, the rankings of the wettest projection would fall primarily in the 14 through 16 grouping. However, in contrast to the patterns seen in the least warm and hottest projections, all three top-ranked wet models had grid-cell rankings in the wettest (ranks 14–16), moderate (ranks 4–13), and driest categories (ranks 1–3) (fig. 9). Under RCP 4.5, the CSIRO-Mk3-6-0 projections were in the wettest category for grid cells in the eastern United States; but from west-central California through Washington, grid cells were in the driest category. Under RCP 8.5, the CSIRO-Mk3-6-0 projections were the wettest in the southern and southwestern areas, but were the driest of nearly all projections in the northwestern United States. Under both scenarios, the MRI-CGCM3 projections were in the wettest ranking across the central United States but were in the driest category in the northeastern United States and small areas in the West. The projections by the CNRM-CM5 model were in the wettest category through the Midwestern to southern United States and along the West Coast under both scenarios.

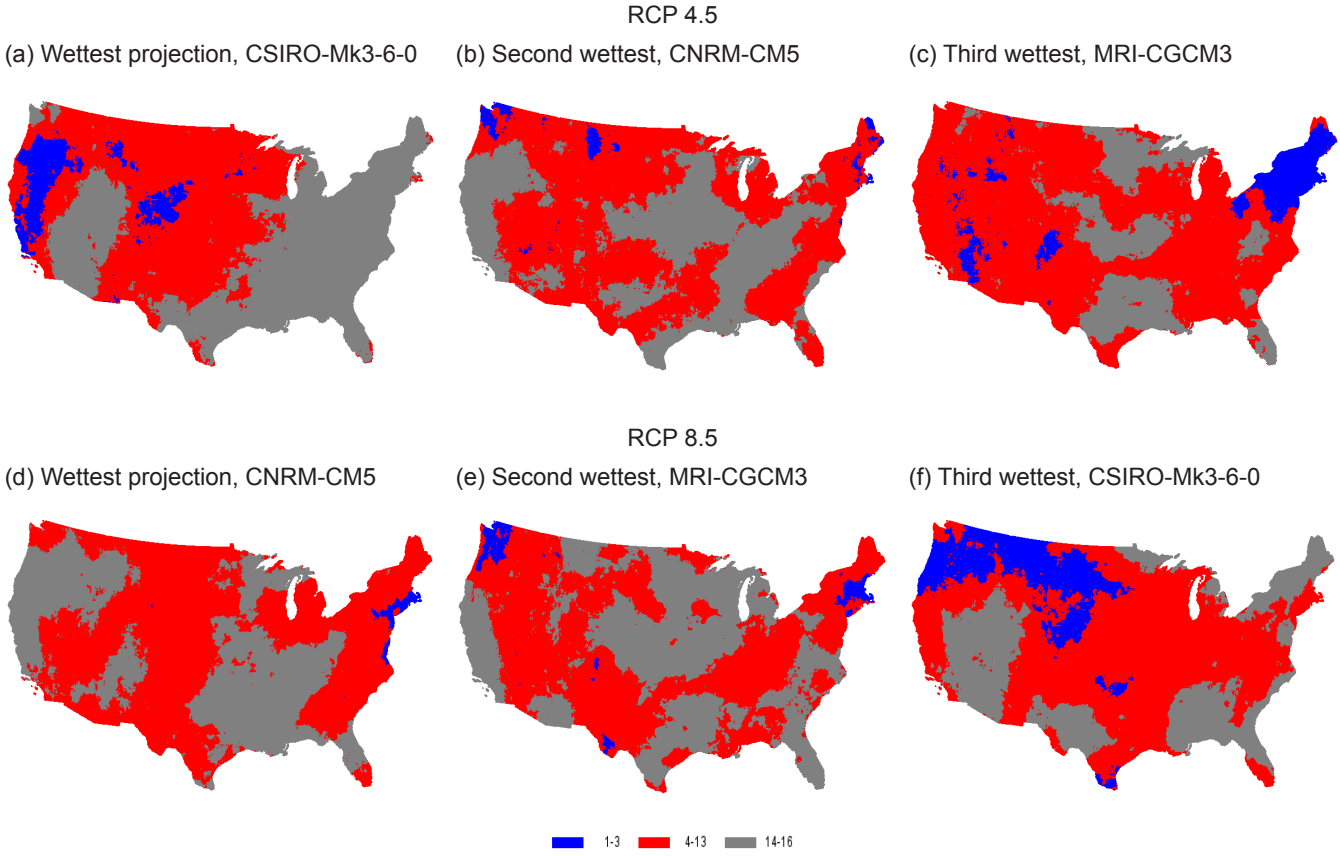

Figure 9—Ranking of grid-cell projected precipitation change at mid-century (2041–2070) from the historical period (1971–2000) for the three wettest projections under RCP 4.5 and RCP 8.5. Rankings are relative to all 16 models and are grouped into categories: ranks 1 through 3 (least change), ranks 4 through 13 (middle change), and ranks 14 through 16 (greatest change). Wettest projections for RCP 4.5: CSIRO-Mk3-6-0 (a), CNRM-CM5 (b), and MRI-CGCM3 (c); for RCP 8.5: CNRM-CM5 (d), MRI-CGCM3 (e), and CSIRO-Mk3-6-0 (f).

We used the frequency distributions of grid-cell rankings to compare the relative contributions of the top-ranked wet models (fig. 10). Under RCP 4.5, the CSIRO-Mk3-6-0 projection had a greater share of grid cells in the driest category than the CNRM-CM5 projection. The distribution across the 16 categories for MRI-CGCM3 under RCP 4.5 and for CSIRO-Mk3-6-0 under RCP 8.5 was nearly uniform (fig. 10). While the CSIRO-Mk3-6-0 model projected the wettest future (rank 16) for nearly 30 percent of the grid cells under RCP 4.5, both CSIRO-Mk3-6-0 and CNRM-CM5 captured 50 percent of the conterminous United States if the top five ranks are considered, a greater area than MRI-CGCM3 (fig. 10a).

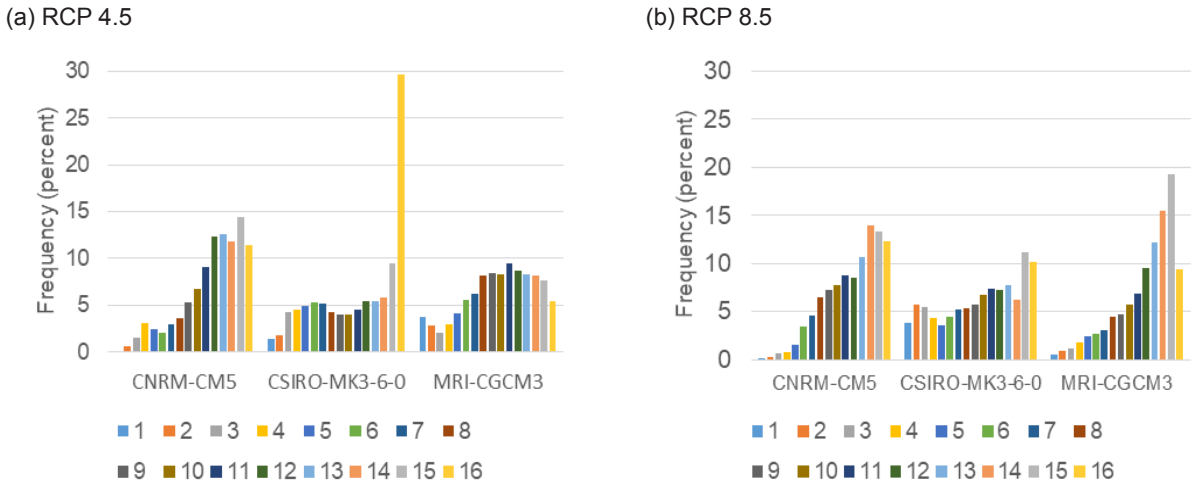

Figure 10—Frequency distribution of grid-cell ranks for the three wettest projections under RCP 4.5 (a) and RCP 8.5 (b): CSIRO-Mk3-6-0 (wettest projection under RCP 4.5), CNRM-CM5 (wettest projection under RCP 8.5), and MRI-CGCM3.

At the conterminous scale, the projection by CNRM-CM5 was the wettest under RCP 8.5 and second under RCP 4.5. At the grid-cell scale, this model projected the wettest changes for a large portion of the conterminous United States under both scenarios. The other models had areas of the Nation where the projections were among the driest of all 16 models. Hence, we selected CNRM-CM5 as the Wet core model for both scenarios.

Middle of the Set of Projections

To find a projection that could represent the middle of the temperature and precipitation change projected by all 16 models, we searched for the projection with change in temperature and precipitation comparable to the 16-model mean change in temperature and precipitation. Distance from the 16-model mean change in temperature and precipitation at the conterminous scale was used to identify a projection that could serve as the middle projection. Determining the middle projection in this manner identified a projection that reflected the mean change—change was still occurring.

The projection that was closest to the 16-model mean change in temperature and precipitation under both scenarios was by the NorESM1-M model (fig. 2, table 5). The temperature change projected by NorESM1-M was within 0.13 °C of the 16-model mean under both scenarios. The precipitation change projected by NorESM1-M was drier than the mean change under RCP 4.5 and wetter under RCP 8.5 (table 5). Though the precipitation projection for inmcm4 under RCP 4.5 was closer to the mean change in precipitation, the temperature change was 1.17 °C, in contrast to the 16-model mean change of 2.34 °C. Other projections were closer to the precipitation change under RCP 8.5, but projections were either cooler or hotter than the mean temperature change.

Table 5—Change in mean temperature and annual precipitation from historical to mid-century at the conterminous U.S. scale for the 16-model ensemble and the NorESM1-M model under the RCP 4.5 and RCP 8.5 scenarios. Median change of the 16-model ensemble is also shown.

Scenario	Model or 16-model ensemble change	Temperature change (°C)	Precipitation change (percent)
RCP 4.5	NorESM1-M mean	2.47	2.81
	16-model mean	2.35	3.54
	16-model median	2.45	3.76
RCP 8.5	NorESM1-M mean	3.23	4.53
	16-model mean	3.10	3.55
	16-model median	3.25	4.59

We used the frequency distribution of grid-cell ranks to explore the NorESM1-M projection in the context of the other 15 models. For the Middle core model, we wanted the distribution to have the fewest grid cells in the wettest and driest categories, as well as in the least warm and hottest ranks. For temperature under each scenario, the NorESM1-M projection had no grid cells in the hottest ranks (14–16) or those with the least change (1–3) (fig. 11a). Under RCP 4.5, grid cells peaked around the rankings of 9 and 10, and under RCP 8.5, as expected, the distribution shifted up into warmer ranks 10 through 12. The distribution of grid-cell rankings for precipitation encompassed all 16 ranks (fig. 11b), and fewer than 2 percent of the grid cells were ranked as the wettest or driest. The proportion of grid cells in each rank for precipitation was less than 10.58 percent, giving the appearance of a somewhat uniform distribution under each scenario (fig. 11b). The NorESM1-M model was selected as the Middle core model projection for both RCP 4.5 and RCP 8.5.

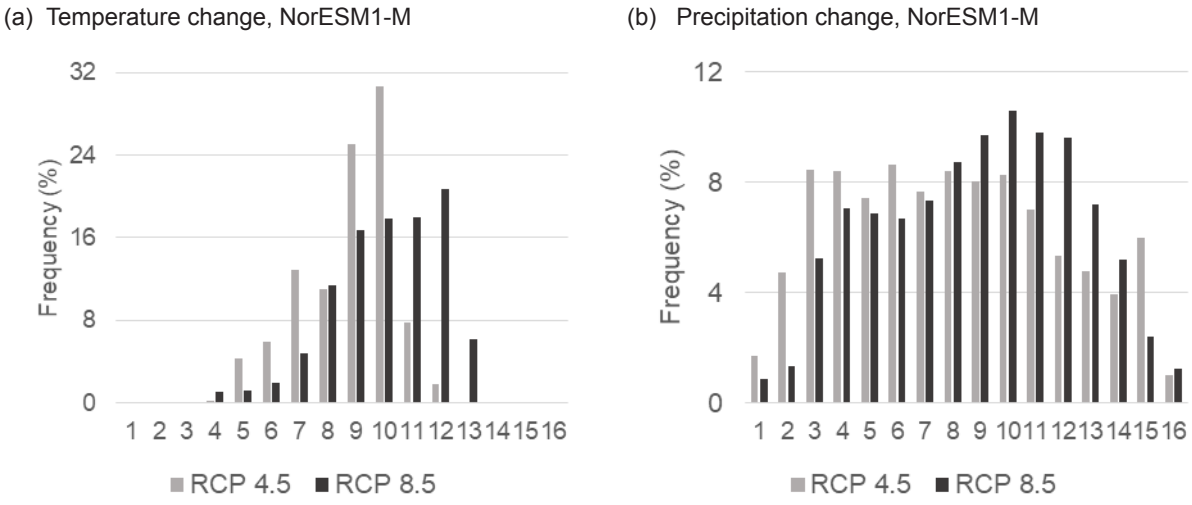

Figure 11—Frequency distribution (percent) of grid-cell ranks from NorESM1-M projection under RCP 4.5 and RCP 8.5 relative to all 15 other models: mean temperature change (°C) at mid-century (2041–2070) (a); and annual precipitation change (percent) by 2041–2070 (b).

Mid-Century Core Models

Climate Change and Spatial Patterns at Mid-Century

The strategy of model selection focused on the range in projected temperature and precipitation change across 16 models, at the conterminous scale. As explained in previous sections, identification of core models and projections involved three criteria: (1) historical model performance, (2) selection of only one model from a modeling institution, and (3) identification, if possible, of one model for projections under RCP 4.5 and RCP 8.5. Based on the preceding analysis, we selected five core models for the 2020 RPA Assessment (table 6, fig. 12). These core models reflected the least warm, hottest, driest, and wettest projections, and a projection that represents the middle of the entire set of projections. We were able to select the same model under RCP 4.5 and under RCP 8.5 for each of the climate ranges.

While these models represented the end of a range for one climate variable, the user should be aware of what the core model projected for the other climate variable. Ideally, models selected to represent the range of one climate variable (such as temperature) would project the ensemble value for the other climate variable (such as precipitation). For example, HadGEM2-ES was selected as the Hot core model. For precipitation, this model projected a 3.84-percent increase in precipitation, close to the mean change (ensemble) in precipitation of 3.54 percent under RCP 4.5. As each projection will be interpreted with respect to a resource condition, understanding the nature of the projection in terms of the other climate variable will be important.

Table 6—Core models for mid-century analysis in the 2020 RPA Assessment.

	Least Warm	Hot	Dry	Wet	Middle
RCP 4.5	MRI-CGCM3	HadGEM2-ES	IPSL-CM5A-MR	CNRM-CM5	NorESM1-M
RCP 8.5	MRI-CGCM3	HadGEM2-ES	IPSL-CM5A-MR	CNRM-CM5	NorESM1-M
Climate modeling institution	Meteorological Research Institute, Japan	Met Office Hadley Centre, United Kingdom	Institut Pierre Simon Laplace, France	National Centre of Meteorological Research and European Centre for Advanced Research and Training, France	Norwegian Climate Center, Norway

(a) RCP 4.5

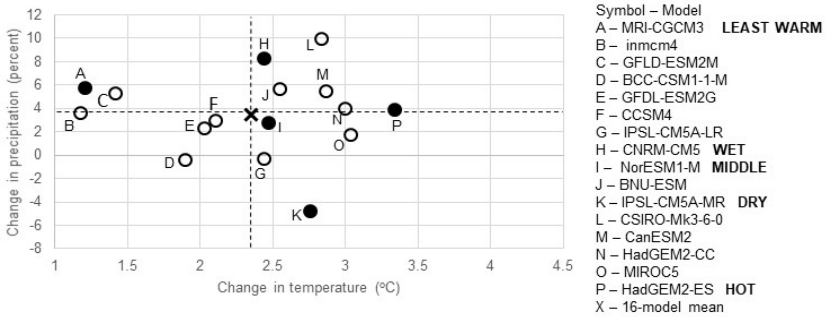

(b) RCP 8.5

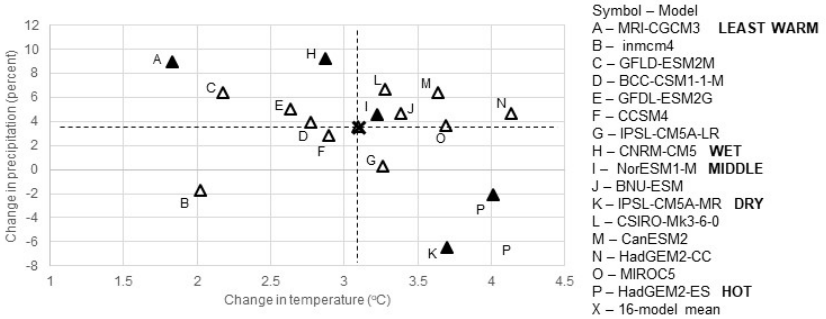

Figure 12—Annual precipitation change (percent) plotted against mean temperature change (°C) at mid-century (2041–2070) from the historical period (1971–2000) under RCP 4.5 (a) and RCP 8.5 (b) for all 16 models at the conterminous U.S. scale. Individual models are denoted by open circles in the RCP 4.5 scenario and open triangles in the RCP 8.5 scenario. The black "X" represents the mean temperature and precipitation change for the 16 models in each scenario. The core model projections are identified as filled circles or triangles and noted Least Warm, Hot, Dry, Wet, and Middle in legend.

The MRI-CGCM3 projection was chosen for the Least Warm core model because it had the smallest change in temperature of the 16 models. Under RCP 4.5, the MRI-CGCM3 model projected a precipitation increase of 5.73 percent at mid-century, as compared to the 16-model ensemble mean projection of 3.54 percent, and the Wet core model (CNRM-CM5) projection of 8.31 percent (compare A, H to X in figure 12a). The MRI-CGCM3 projection is 2.19 percentage points wetter than the ensemble mean but 2.58 percentage points less than the Wet core model projection. Under RCP 8.5, MRI-CGCM3 projected an 8.86-percent increase in precipitation, very close to the Wet core model projection of 9.41 percent, and both greater than the ensemble mean projection of a 3.54-percent increase (compare A, H to X in figure 12b). Under RCP 8.5, the other least warm projection candidates were also wet or very dry (compare A, B, and C to X in figure 12b). Given that the Least Warm core model, MRI-CGCM3, and the Wet core model, CNRM-CM5, projected similar precipitation increases (figs. 8d,e), investigators may want to determine for their areas of interest whether the differences in projected temperature (MRI-CGCM3 were "cooler" than CNRM-CM5) suggest that the MRI-CGCM3 projection is ecologically wetter than the CNRM-CM5 projection under RCP 8.5. Interpretation of the potential implications of this Least Warm core model projection for a natural resource should consider this relatively large coincident increase in precipitation under RCP 8.5.

The HadGEM2-ES model was selected as the Hot core model, the hottest projection of all 16 models. The precipitation projection by the Hot core model (HadGEM2-ES) under RCP 4.5 was very close to the ensemble mean of a 3.54-percent increase (compare P to X in figure 12a). Under RCP 8.5, HadGEM2-ES projected a 2.16-percent decrease in precipitation, as compared to the ensemble mean increase of 3.55 percent (compare P to X in figure 12b). The HadGEM2-ES projection is a warmer projection than the Dry core model (IPSL-CM5A-MR) and is not as dry as the Dry core projection (compare K to P in figure 12b). At the regional scale, this decrease in precipitation projected by HadGEM2-ES was seen across the southern United States (see figure 13b, discussed later). This projection by HadGEM2-ES of decreased precipitation under RCP 8.5 would be important for users to consider when interpreting the potential implications of this Hot core model projection for natural resources.

The model selected as the Dry core model, IPSL-CM5A-MR, projected a mean temperature increase of 2.76 °C under RCP 4.5, as compared to the ensemble mean and median increase of 2.35 °C and 2.45 °C, respectively (compare K to X in figure 12a). Under RCP 8.5, IPSL-CM5A-MR projected a mean temperature increase of 3.70 °C, as compared to the ensemble mean and median increase of 3.10 °C and 3.25 °C, respectively. This dry model was slightly warmer than the mean and median projections under RCP 8.5. The temperature increase was predominantly within the western central United States and was coincident with area of the largest projected precipitation decreases (see figure 16d, discussed later).

The CNRM-CM5 model was selected as the Wet core model for both scenarios. The CNRM-CM5 temperature projection under RCP 4.5 was very close to the ensemble mean temperature increase (compare H to X in figure 12a). Under RCP 8.5, CNRM-CM5 projected a 2.88 °C increase in temperature, as compared to the ensemble mean and median increase of 3.10 °C and 3.25 °C, respectively (fig. 12b).

Other considerations with respect to the selection of these core models include the choice of the temporal periods for comparison. We used the 1971–2000 period to avoid an overlap between the historical modeled data and the projection data. In this dataset, the projections begin in 2005. We chose the future period of 2041–2070 as a 30-year normal that would be the basis for management decisions around 2070. If a different historical or future period were chosen, the rankings of temperature and precipitation change could be different. For the comparison with end-of-century projections with the same historical period, see the *Temporal Influence on Core Model Selection: End of Century* section.

Similarly, if a different climate metric were to be used, such as seasonal temperature or precipitation, or water balance, the rankings of the models by these metrics might be different. Rupp et al. (2013) explored some aspects of seasonality in temperature and precipitation, and the models do vary in their ability to capture seasonal metrics.

We mapped projected changes in temperature and precipitation for each core model. Temperature changes under RCP 4.5 for the Least Warm, Hot, and Middle core models are shown with the corresponding changes in precipitation, along with the 16-model ensemble, in figure 13. Precipitation changes under RCP 4.5 for the Dry, Wet, and Middle core models are shown with the corresponding changes in temperature, along with the 16-model ensemble, in figure 14. Temperature changes under RCP 8.5 for the Least Warm, Hot, and Middle core models are shown with the corresponding changes in precipitation, along with the 16-model ensemble, in figure 15. Precipitation changes under RCP 8.5 for the Dry, Wet, and Middle core models are shown with the corresponding changes in temperature, along with the 16-model ensemble, in figure 16. The ensemble maps for temperature and precipitation under RCP 4.5 are the same as those in figures 13g,h and figures 14g,h for ease of comparison with the individual model maps. Similarly, under RCP 8.5, the ensemble maps for temperature and precipitation are the same figures as those in figures 15g,h and figures 16g,h for ease of comparison with the individual model maps.

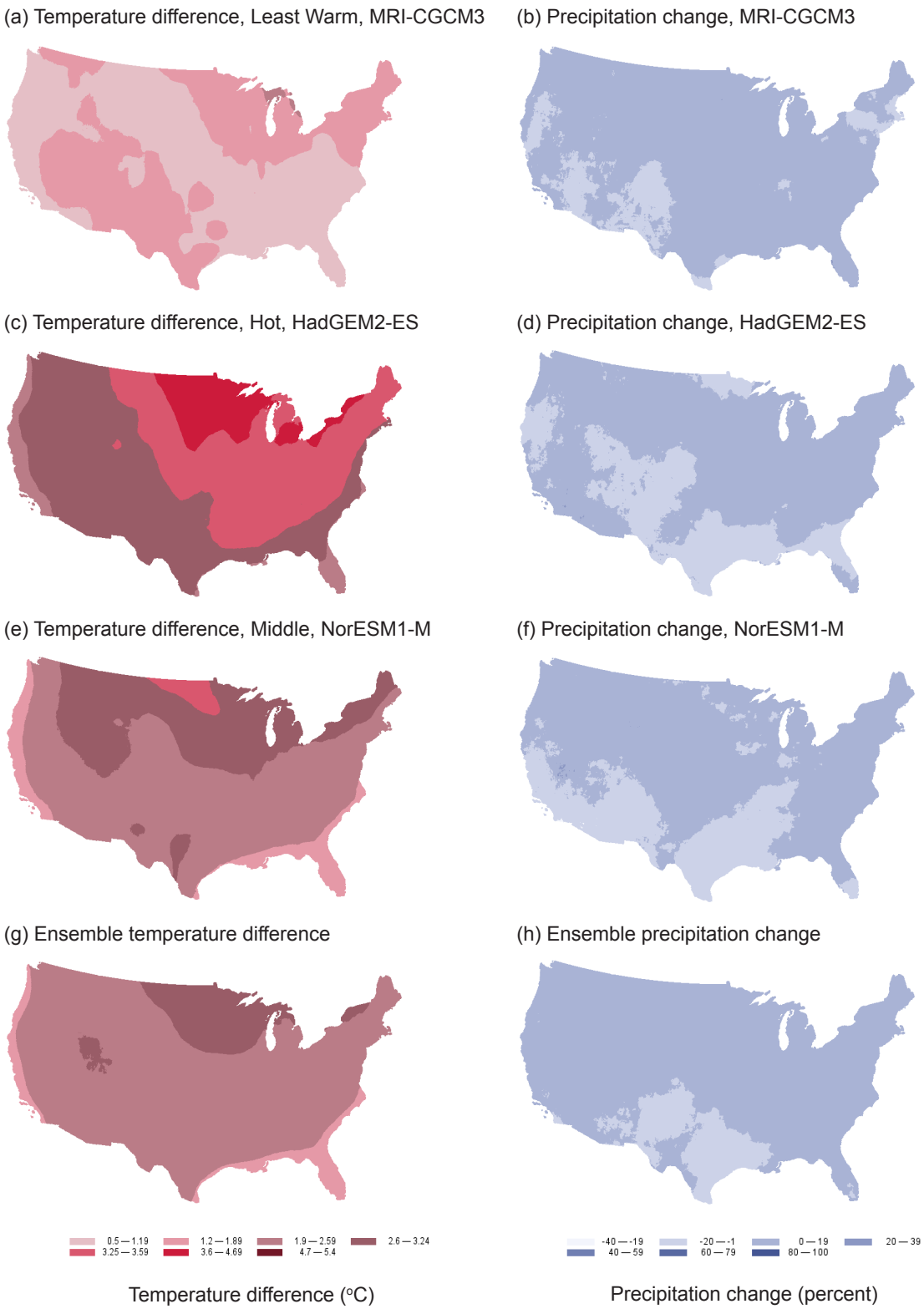

Figure 13—Mean temperature difference (°C) and annual precipitation change (percent) at mid-century (2041–2070) for Least Warm (a,b), Hot (c,d), and Middle (e,f) temperature core models and the 16-model ensemble (g,h) under RCP 4.5.

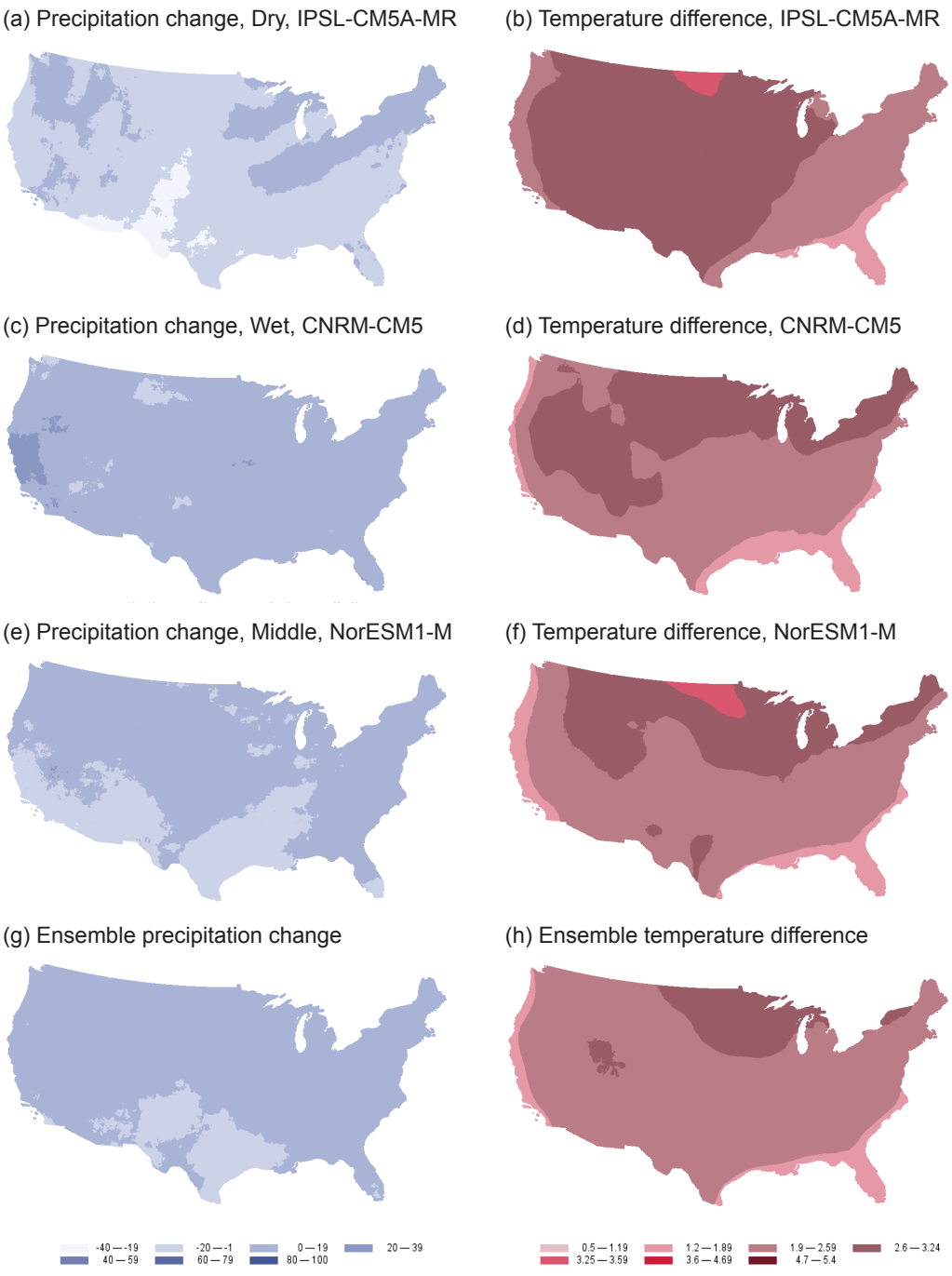

Figure 14—Annual precipitation change (percent) and mean temperature difference (°C) at mid-century (2041–2070) from the historical period (1971–2000) for Dry (a,b), Wet (c,d), and Middle (e,f) precipitation core models, and the 16-model ensemble (g, h) under RCP 4.5.

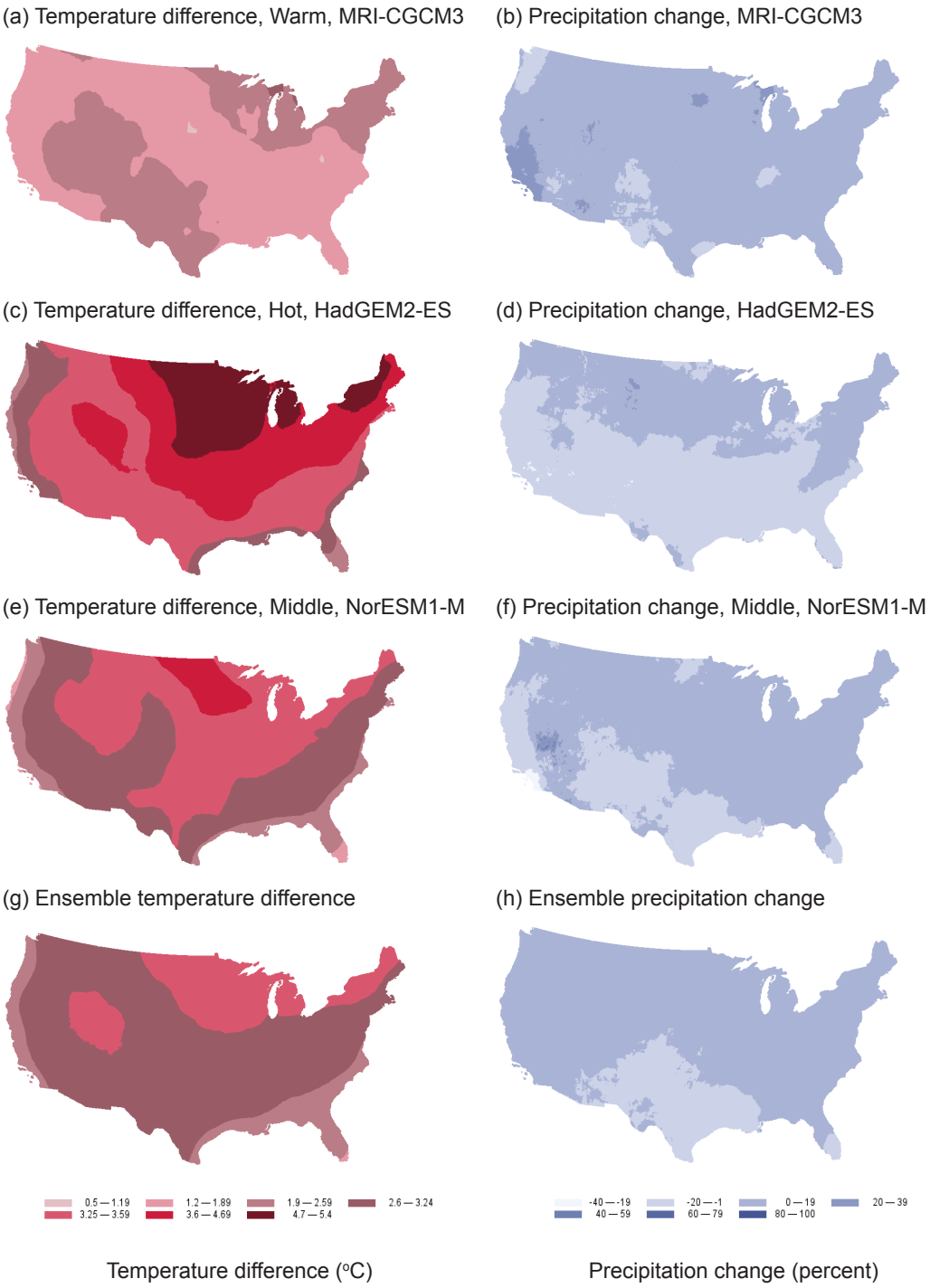

Figure 15—Mean temperature difference (°C) and annual precipitation change (percent) at mid-century (2041–2070) from the historical period (1971–2000) for Least Warm (a,b), Hot (c,d), and Middle (e,f) temperature core models and the 16-model ensemble (g,h) under RCP 8.5.

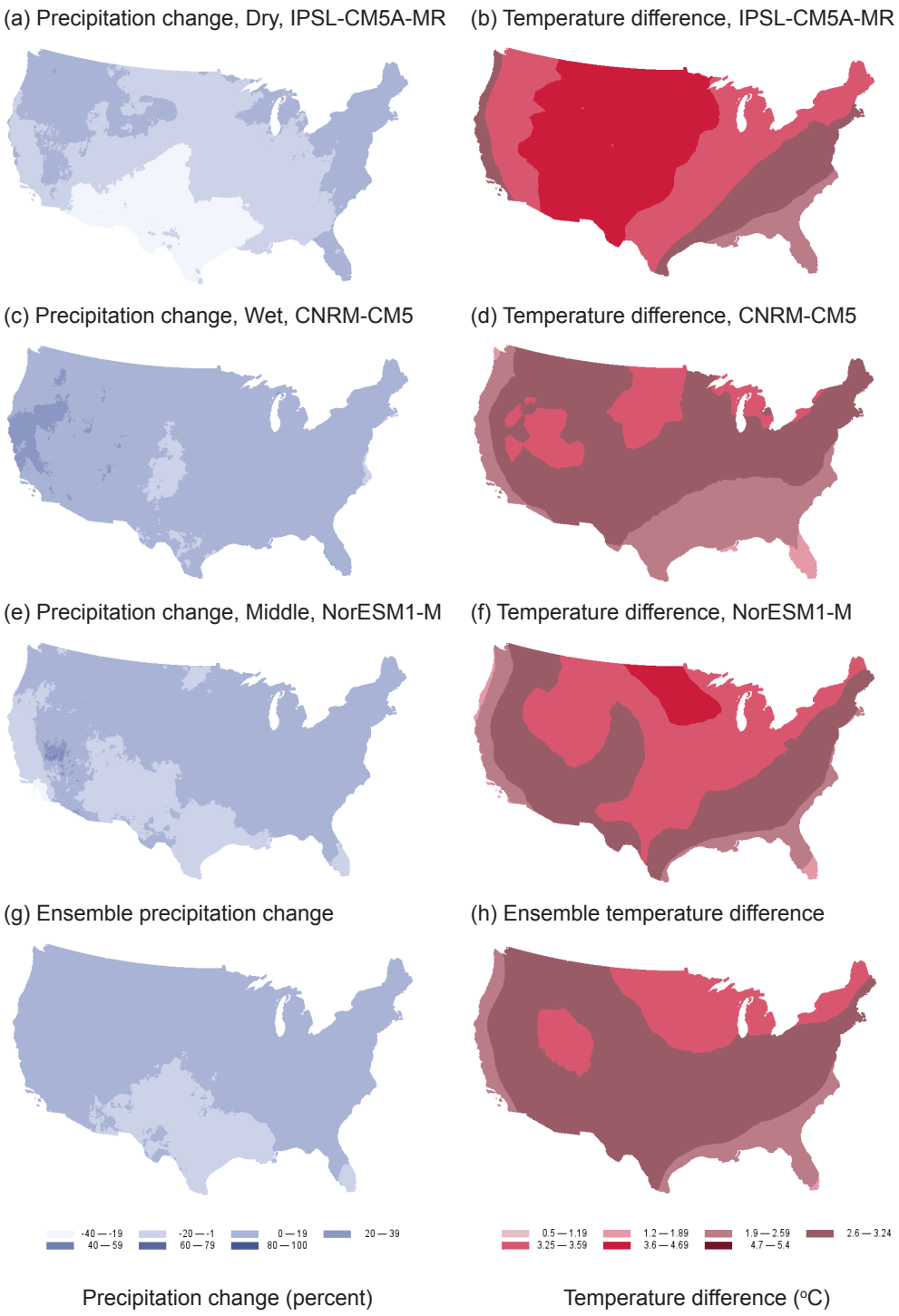

Figure 16—Annual precipitation change (percent) and mean temperature difference (°C) at mid-century (2041–2070) from the historical period (1971–2000) for Dry (a,b), Wet (c,d), and Middle (e,f) precipitation core models, and the 16-model ensemble (g,h) under the RCP 8.5.

Temperature and Precipitation Trends to End of Century in Core Model Projections

Projected mean temperatures continued to increase to end of century, whereas annual precipitation projected by the core models increased in variability to end of century under RCP 4.5 (fig. 17) and RCP 8.5 (fig. 18). Under RCP 4.5, the three core model projections for mean annual temperature spread out through time (fig. 17a). Projections of mean temperature by the Hot core model, HadGEM2-ES, rose to 15 °C by 2050 and approached 17 °C at end of century, well above the middle and least warm projections. The middle projections ranged between the Least Warm and Hot core models, and the Least Warm core model, MRI-CGCM3, projected the lowest end-of-century mean temperatures of around 13 to 14 °C. Under RCP 8.5 and the hottest projection, the conterminous U.S. mean temperature reached 19 °C by the end of the century (fig. 18a). The Least Warm core model (MRI-CGCM3) projection remained cooler than the middle projection by NorESM1-M, particularly in the later 21st century (fig. 18a). Under both RCP 4.5 and RCP 8.5, mean temperatures for the Dry and Wet core models varied around the NorESM1-M projection (figs. 17b, 18b).

Annual precipitation projections were highly variable; figures 17c,d and 18c,d show the 10-year moving average of projected annual precipitation. As expected, the Wet core model, CNRM-CM5, projected increasing amounts of annual precipitation, rising above all the other projections after 2025 under RCP 4.5 and around 2050 under RCP 8.5 (figs. 17d, 18d). Similarly, precipitation projected by the Dry core model, IPSL-CM5A-MR, decreased after 2025 under both scenarios, remaining generally below the projected precipitation of all other core models. The projections by NorESM1-M stayed between these two precipitation extremes (figs. 17c,d; 18c,d), but did increase through time as did most of the 16 model projections. For the temperature core models, annual precipitation projections were highly variable (figs. 17c, 18c). Under RCP 4.5, the MRI-CGCM3 (least warm), HadGEM2-ES (hot), and NorESM1-M (middle precipitation) projections intermingled through time to the end of the century. Under RCP 8.5, the MRI-CGCM3 precipitation projection was a wetter projection than the HadGEM2-ES (hot) projection (fig. 18c), but not as wet as the Wet core model (CNRM-CM5) projection (fig. 18d).

(a) Annual mean temperature projections (°C) by the temperature core models under RCP 4.5

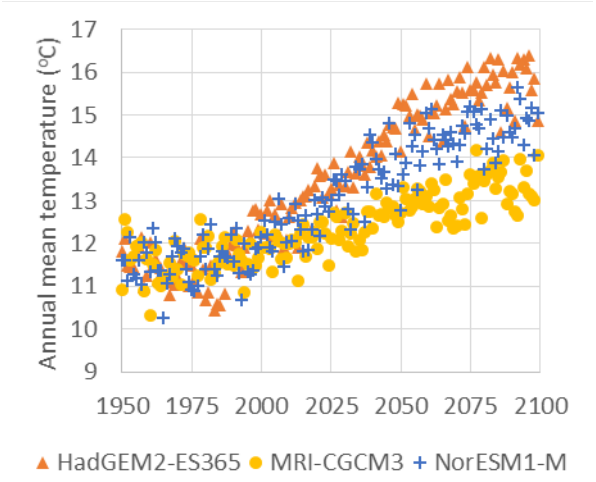

(b) Annual mean temperature projections (°C) by CNRM-CM5, IPSL-CM5A-MR, and NorESM1-M under RCP 4.5

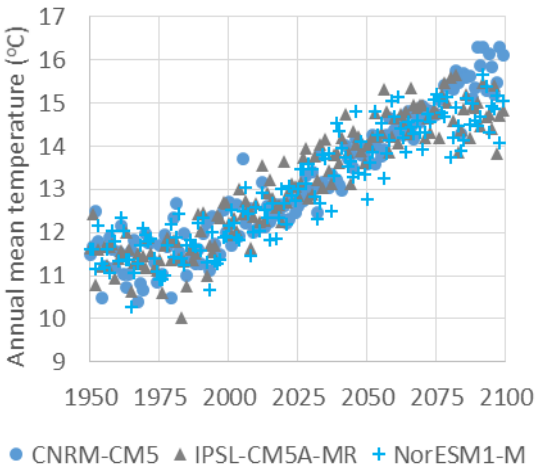

(c) Annual precipitation projections (mm, 10-year moving average) by HadGEM2-ES, MRI-CGCM3, and NorESM1-M under RCP 4.5

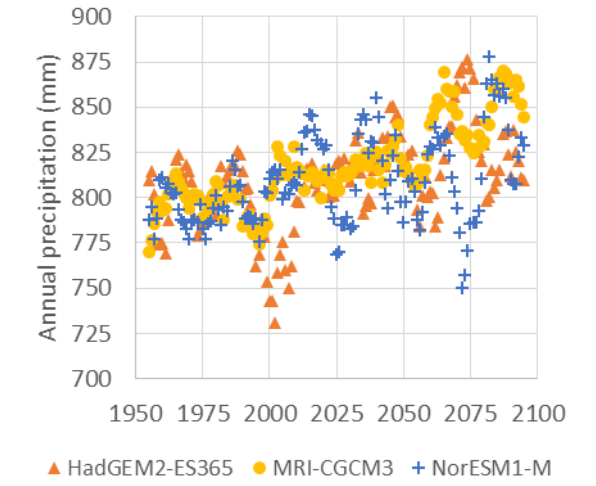

(d) Annual precipitation projections (mm, 10-year moving average) by the precipitation core models under RCP 4.5

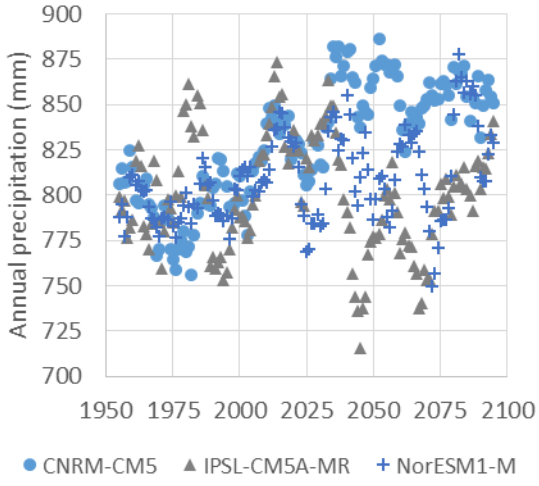

Figure 17—Mean temperature and annual precipitation projections under RCP 4.5 for the conterminous United States. Annual mean temperature projections (°C) by core models for Least Warm (MRI-CGCM3), Hot (HadGEM2-ES), and Middle (NorESM1-M) (a); and by core models for Dry (IPSL-CM5A-MR), Wet (CNRM-CM5), and Middle (NorESM1-M) (b). Annual precipitation projections (mm, 10-year moving average) by core models for Least Warm, Hot, and Middle (c); and Dry, Wet, and Middle (d).

(a) Annual mean temperature projections (°C) by the temperature core models under RCP 8.5

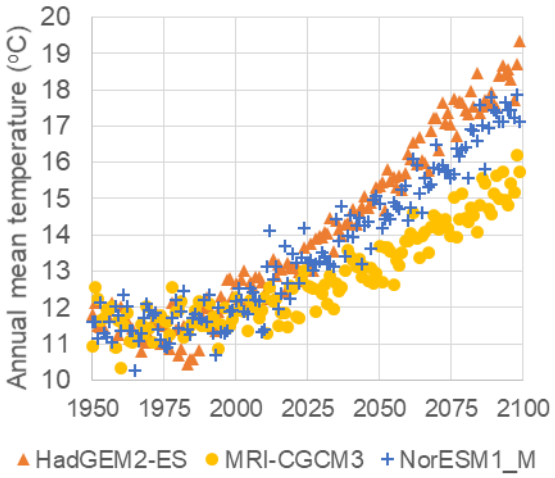

(b) Annual mean temperature projections (°C) by CNRM-CM5, IPSL-CM5A-MR, and NorESM1-M under RCP 8.5

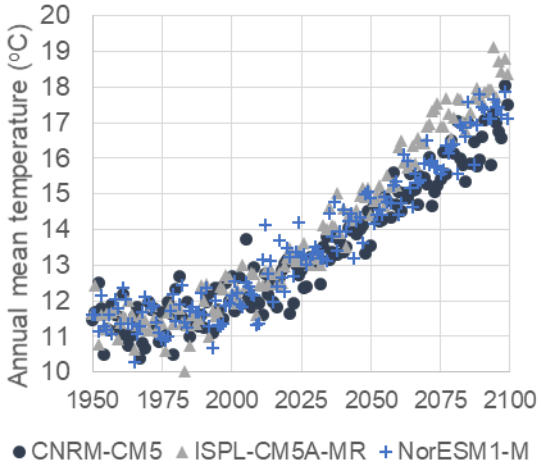

(c) Annual precipitation projections (mm, 10-year moving average) by HadGEM2-ES, MRI-CGCM3, and NorESM1-M under RCP 8.5

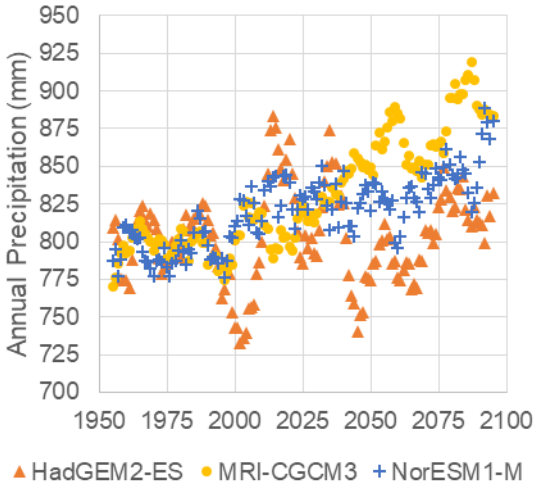

(d) Annual precipitation projections (mm, 10-year moving average) by the precipitation core models under RCP 8.5

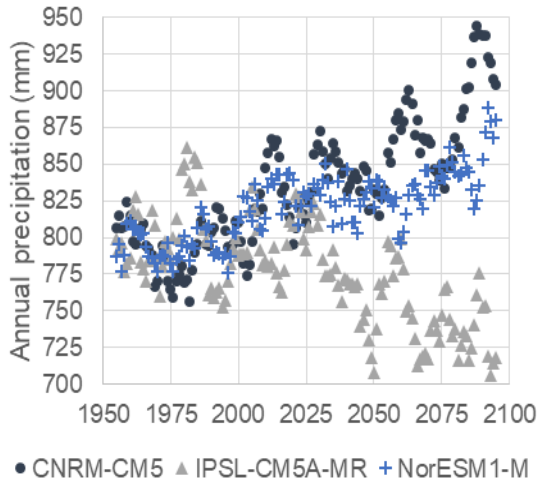

Figure 18—Mean temperature and annual precipitation projections under RCP 8.5 for the conterminous United States. Annual mean temperature projections (°C) by core models for Least Warm (MRI-CGCM3), Hot (HadGEM2-ES), and Middle (NorESM1-M) (a); and for Dry (IPSL-CM5A-MR), Wet (CNRM-CM5), and Middle (NorESM1-M) (b). Annual total precipitation projections (mm, 10-year moving average) by core models for Least Warm, Hot, and Middle (c); and Dry, Wet, and Middle (d).

TEMPORAL INFLUENCE ON CORE MODEL SELECTION: END OF CENTURY

The RPA Assessment focus is the next 50 years; however, many assessments explore future climate projections and potential effects through 2099. The question arose as to whether core models selected based on mid-century projections would be different if the basis for selection were end-of-century (2070–2099) projections.

Selecting Projections that Characterize Climate Change at End of Century

Projected mean temperature change continued to rise from mid-century to end of century under both scenarios (compare figures 2 and 19). At mid-century, projected temperature increases ranged from 1.17 to 4.26 °C across RCP 4.5 and RCP 8.5 (fig. 2). At end of century, projected temperature increases ranged from 1.64 to 6.77 °C across the two scenarios (fig. 19). Projections for precipitation change at mid-century ranged from a decrease of 6.47 percent to an increase of 10.00 percent across both scenarios; at end of century, the range was from a decrease of 9.37 percent to an increase of 12.34 percent. Notably at end of century, only 1 of the 20 models projected a decrease in precipitation under RCP 4.5; in contrast, 4 models projected decreases at mid-century (compare figures 2 and 19). Under RCP 8.5, 3 of the 20 models projected decreased precipitation at mid-century as well as at end of century; however, the models were not the same in both periods (compare figures 2 and 19).

As with the mid-century analysis, temperature and precipitation changes at end of century were used to identify the top three least warm, hottest, driest, and wettest projections (fig. 19). We used the same analysis for model behavior and dropped the poor performers from further consideration: bcc-csm1-1, MIROC-ESM, MIROC-ESM-CHEM, and IPSL-CM5B-LR.

When the top three projections for least warm, hot, dry, and wet under each scenario for end of century were selected, the mid-century core models were among the top-ranked projections for least warm, hot, and wet under both scenarios (compare tables 4 and 7). The mid-century Dry core model was among the three driest projections under RCP 8.5, but was fourth ranked under RCP 4.5.

Table 7—Top three ranked projections in terms of temperature (least warm, hot) and precipitation (dry, wet) at end of century (2070–2099) under scenarios (RCP 4.5 and RCP 8.5) at the conterminous U.S. scale, with poor performers excluded. Temperature and precipitation change was computed relative to the historical period (1971–2000) as shown in figure 19. Core models based on the mid-century analysis (table 4) are in bold.

Scenario	Rank	Least Warm	Hot	Dry	Wet
RCP 4.5	1	**MRI-CGCM3**	**HadGEM2-ES**	bcc-csm1-1-m	CSIRO-Mk3-6-0
	2	GFDL-ESM2M	HadGEM2-CC	inmcm4	**CNRM-CM5**
	3	inmcm4	CNRM-CM5	HadGEM2-CC	MRI-CGCM3
				IPSL-CM5A-MR	
RCP 8.5	1	**MRI-CGCM3**	HadGEM2-CC	**IPSL-CM5A-MR**	**CNRM-CM5**
	2	inmcm4	**HadGEM2-ES**	IPSL-CM5A-LR	MRI-CGCM3
	3	GFDL-ESM2M	IPSL-CM5A-MR	MIROC5	CanESM2

Least Warm

The three top-ranked Least Warm models at end of century were the same models as in the mid-century analysis (tables 4, 7). Under RCP 4.5 and RCP 8.5, differences between the three projections at end of century are less than 0.50 °C (fig. 19), and under both scenarios, MRI-CGCM3 is the model projection with the smallest change in temperature.

MRI-CGCM3 was selected as the Least Warm core model for end of century for both scenarios (see figures A.1–A.4 in Appendix A). This model was also selected as the Least Warm core model at mid-century.

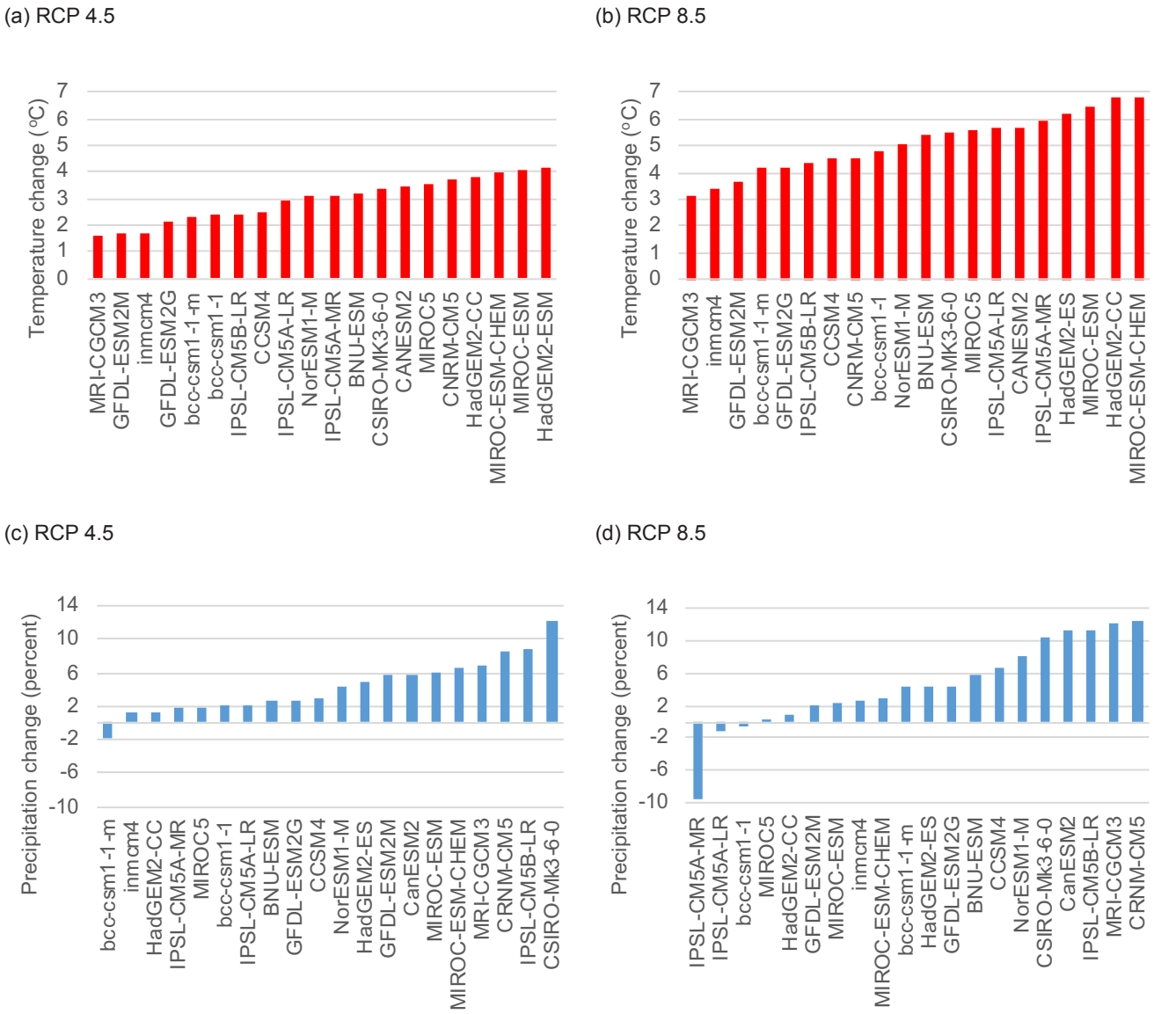

Figure 19—Area-weighted change in mean temperature (°C) and annual precipitation (percent) at end of century (2070–2099) from the historical period (1971–2000) under RCP 4.5 (a,c) and RCP 8.5 (b,d) for all 20 models at the conterminous U.S. scale. Poor performing models retained here for comparison only (MIROC-ESM, MIROC-ESM-CHEM, bcc-csm1-1, IPSL-CM5B-LR).

Hot

The two Hadley model projections, HadGEM2-CC, HadGEM2-ES, were ranked as the hottest or second hottest projections for end of century (table 7), with HadGEM2-ES being the hottest projection under RCP 4.5 and HadGEM2-CC, the hottest under RCP 8.5. Projected temperature change varied little between these two models. At end of century, differences between these projections were less than 0.40 °C under RCP 4.5, with HadGEM2-ES the hottest at 4.12 °C and HadGEM-CC at 3.76 °C (fig. 19). Under RCP 8.5, differences were less than 0.61 °C. The third-ranked model differed between the scenarios, so it failed the criterion of being used for both scenarios. Given that the Hadley models were ranked as the top and second hottest projections under both scenarios, we explore the tradeoffs in selecting one Hadley model. This selection would meet the criteria of using only one model from the same modeling institution and identifying one model for both scenarios.

The spatial patterns of temperature change in both Hadley models were similar, with the expected pattern of greater temperature change under RCP 8.5 (fig. 20). The greatest temperature change occurred in the north-central area of the conterminous United States, radiating out to areas of least change along the coasts and southern United States. These spatial patterns were similar to the mid-century projections, with the expected pattern of greater temperature change at end of century (compare figures 7 and 20).

The overall temperature differences at end of century are small between the two Hadley models under both scenarios. Either projection could be selected as the Hot core model for end of century. Here, one advantage of selecting HadGEM2-ES was that this model was the Hot core model for mid-century. Thus, HadGEM2-ES was also selected as the Hot core model at end of century.

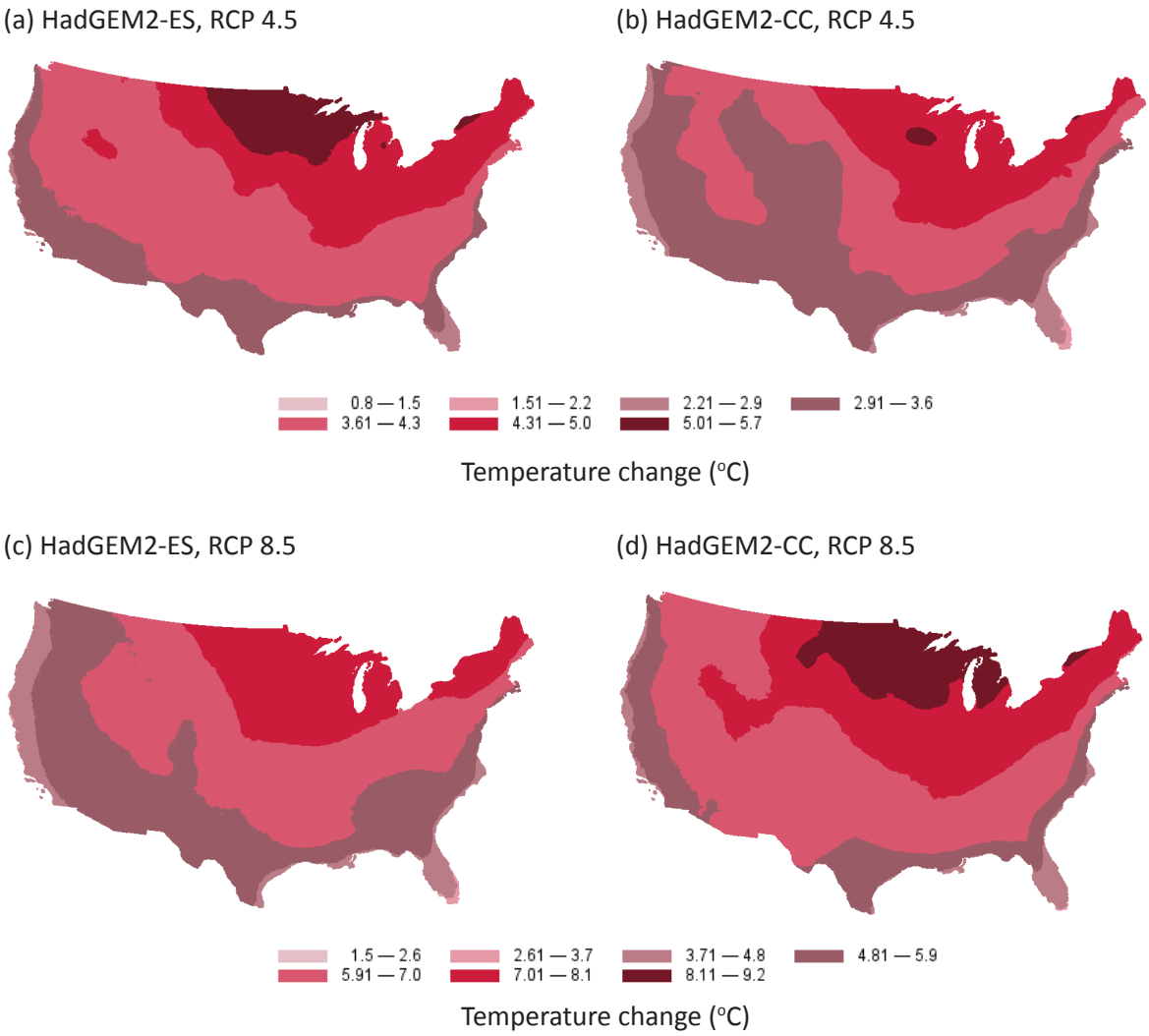

Figure 20—Mean temperature change (°C) for the hottest projections at end of century (2070–2099) relative to the historical period (1971–2000): hottest under RCP 4.5 (a); second hottest under RCP 4.5 (b); second hottest under RCP 8.5 (c); and hottest under RCP 8.5 (d). Color bands differ by scenario with the temperature bands under RCP 8.5 going to 9.2 °C.

Dry

After the poor performers were aside, the three driest projections at end of century differed by scenario. Under RCP 4.5, the three driest projections were, in order of ranking: bcc-csm1-1-m, inmcm4, and HadGEM2-CC (table 7). Only 1 of the 16 models, bcc-csm-1-1-m, projected a decrease (1.95 percent) under RCP 4.5 (fig. 19). The models ranked second (inmcm4) and third (HadGEM2-CC) projected increases of 1.14 percent and 1.16 percent, respectively. The fourth driest model (IPSL-CM5A-MR) projected a 1.81-percent increase. Under RCP 8.5, only 3 of the 16 models projected decreases in precipitation (fig. 19; note that bcc-csm1-1, one of the poor performers, was dropped). The driest projection was by the IPSL-CM5A-MR model, projecting a decrease in annual precipitation of 9.37 percent (fig. 19), and the second driest model (IPSL-CM5A-LR) projected a decrease of 1.10 percent.

The likely candidates for the Dry core model at end of century varied by scenario. Under RCP 4.5, the driest projection was by the bcc-csm1-1-m model, and under RCP 8.5, the driest projection was by the IPSL-CM5A-MR model (fig. 19). An objective was to select, if possible, the same model as the core model for both scenarios. Under RCP 4.5, the IPSL-CM5A-MR model projected an increase of 1.81 percent, whereas the mean projection was 4.14 percent. Under RCP 8.5, bcc-csm1-1-m was the seventh driest projection, projecting an increase of 4.16 percent, very close to the ensemble projection of 4.49 percent. The bcc-csm1-1-m model was not a dry projection under RCP 8.5 at end of century. The IPSL-CM5A-MR model was the Dry core model at mid-century, and we explored the implications of selecting this model as the Dry core model at end of century.

Across the three driest projections under RCP 4.5 and RCP 8.5, the spatial patterns varied at end of century. Generally, the largest projected decreases were in the south-central to southwestern area in the conterminous United States (fig. 21). However, the inmcm4 model projected drier areas along the northern border. For the driest projection under RCP 4.5, bcc-csm1-1-m, precipitation across most of the conterminous United States decreased, with increases seen at the northern and southern boundaries (fig. 21a). For IPSL-CM5A-MR under RCP 4.5, precipitation decreased within a narrower mid-section of the conterminous United States, with decreases extending into the South and Southwest.

Another consideration with respect to the RPA analysis was the impact of using different sets of models in the mid-century analysis and the end-of-century analysis. Adding the bcc-csm1-1-m model to the end-of-century analysis would require adding this projection to mid-century analyses, in order to capture the resource impacts of this projection at the 50-year timeline used in the RPA analysis. At mid-century under RCP 8.5, the bcc-csm1-1-m model projection was very close to the ensemble mean and was a wetter projection than IPSL-CM5A-MR (compare figures 2 and 19).

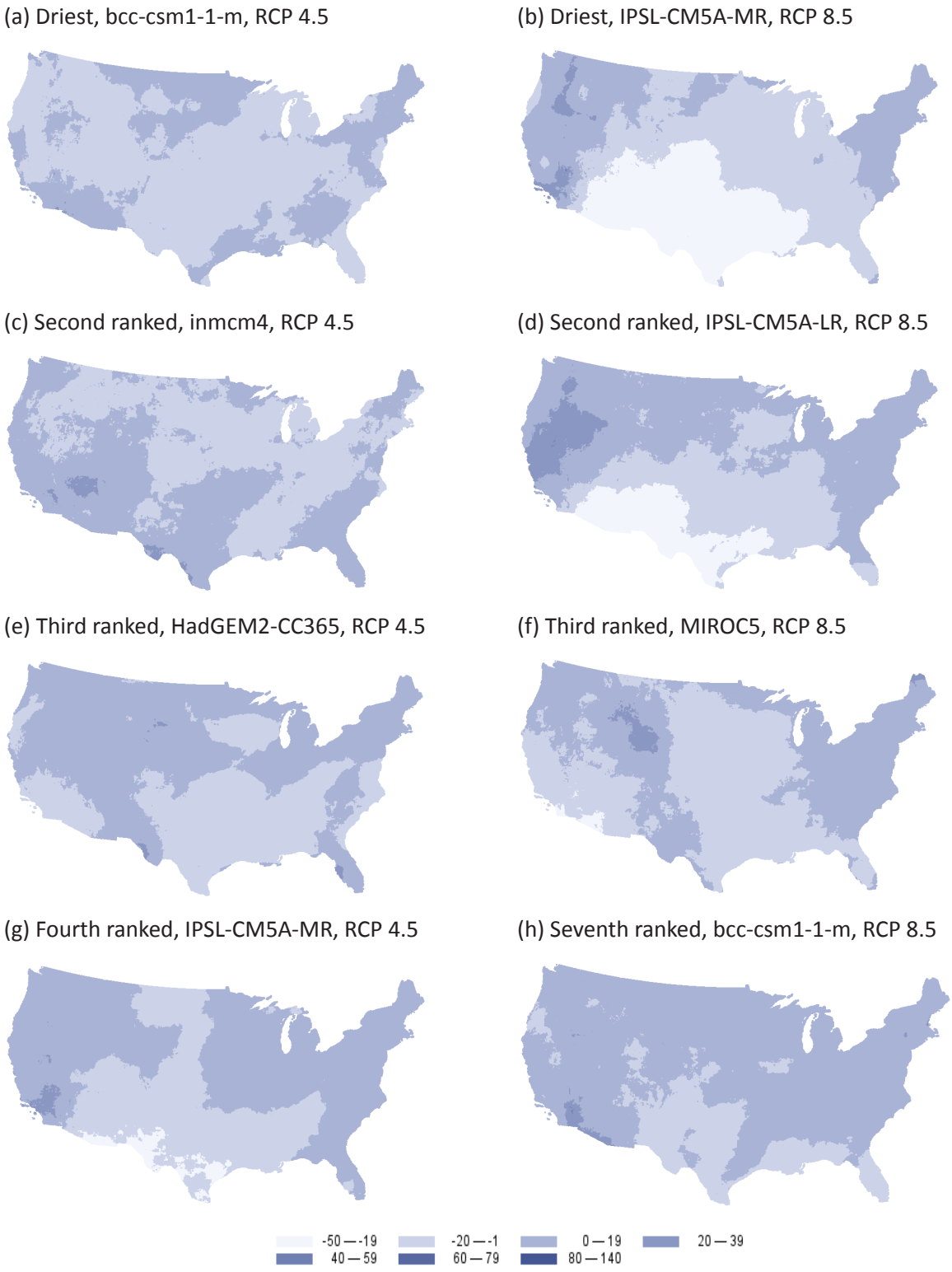

Figure 21—Annual precipitation change (percent) for the driest projections at end of century (2070–2099) relative to the historical period (1971–2000): driest under RCP 4.5 and RCP 8.5 (a,b), second driest (c,d), and third driest (e,f); fourth driest (g); and seventh driest (h). Core model for Dry at mid-century was IPSL-CM5A-MR.

Projections by IPSL-CM5A-MR were the driest projections of all 16 models under both scenarios at mid-century and under RCP 8.5 at end of century. Though the IPSL-CM5A-MR projection under RCP 4.5 for end of century resulted in a 1.81-percent increase, as compared to the 1.95-percent decrease projected by bcc-csm1-1-m, the selection was advantageous in reducing model variation through time. Analysts interested only in end of century may wish to use the bcc-csm1-1-m projection, recognizing that this projection is near the ensemble precipitation mean for mid-century under RCP 8.5. We selected IPSL-CM5A-MR as the Dry core model at end of century under RCP 4.5 and RCP 8.5.

Wet

The three wettest projections under RCP 4.5 at end of century were, in order of ranking (percent increase in precipitation): CSIRO-Mk3-6-0 (12.11 percent), CNRM-CM5 (8.59 percent), and MRI-CGCM3 (6.86 percent) (table 7, fig. 19). Under RCP 8.5, the wettest projection was by model CNRM-CM5 (12.37 percent), followed by MRI-CGCM3 (12.15 percent), and CanESM2 (11.20 percent). Likely candidates for the Wet core model varied by scenario: CSIRO-Mk3-6-0 under RCP 4.5, and CNRM-CM5 under RCP 8.5. The likely candidate under RCP 4.5 (CSIRO-Mk3-6-0) was ranked fourth under RCP 8.5, projecting a 10.33-percent increase, whereas CNRM-CM5 projected a 12.37-percent increase (fig. 19). The likely candidate under RCP 8.5 (CNRM-CM5) was ranked second under RCP 4.5, projecting an 8.58-percent increase, as compared to the 12.11-percent increase by CSIRO-Mk3-6-0 (fig. 19). One objective was to select, if possible, one Wet core model for both scenarios at end of century. Though the MRI-CGCM3 projection was among the three wettest projections, the model was ranked third under RCP 4.5, projecting only a 6.86-percent increase (table 7, fig. 19). Both the CSIRO-Mk3-6-0 and CNRM-CM5 projections were wetter, and we dropped MRI-CGCM3 from further consideration. We explored the tradeoffs between selection of CNRM-CM5, the Wet core model for mid-century, and CSIRO-Mk3-6-0.

The spatial patterns of the projections for the two wettest projections varied by scenario, particularly in areas of increased precipitation (fig. 22). The CSIRO-Mk3-6-0 model under RCP 4.5 projected the largest increase in the Intermountain area and the Northeast. Under RCP 8.5, CNRM-CM5 also projected increases over a larger western area, including the Intermountain region and extending into the Pacific Northwest. All projections under both scenarios had areas where precipitation was projected to decrease.

Though both CSIRO-Mk3-6-0 and CNRM-CM5 were among the three wettest projections at mid-century, the CSIRO-Mk3-6-0 model projected substantial areas in the driest categories (figs. 8, 9). Consequently, the CNRM-CM5 model was selected as the Wet core model at mid-century.

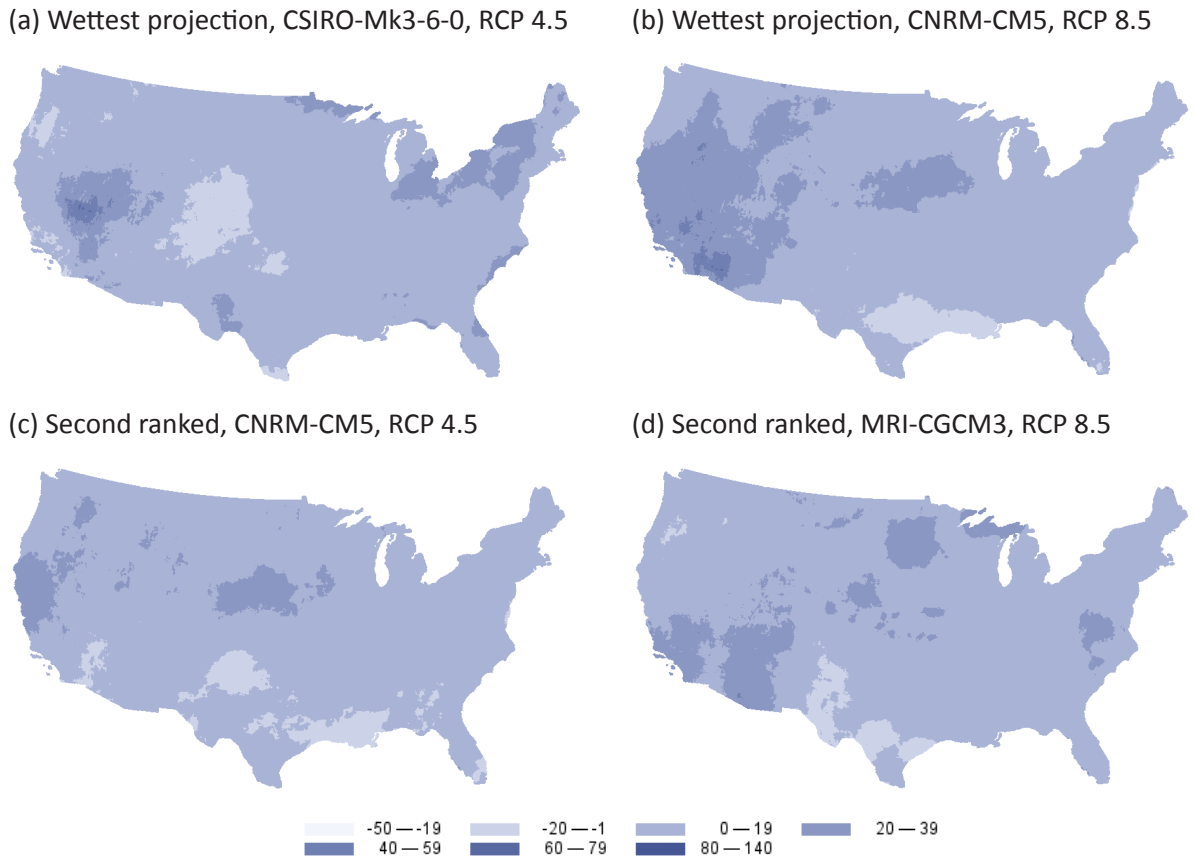

Figure 22—Annual precipitation change (percent) at end of century (2070–2099) relative to the historical period (1971–2000) for the wettest two projections under RCP 4.5 and RCP 8.5 (a,b) and second wettest projections under RCP 4.5 and RCP 8.5 (c,d).

Consideration of CSIRO-Mk3-6-0 as the Wet core model for end of century under both scenarios raised the issue of model consistency across time, similar to the discussion in the *Dry* section. At end of century, the CNRM-CM5 projection under RCP 8.5 was wetter than the CSIRO-Mk3-6-0 projection. Though the CNRM-CM5 projection under RCP 4.5 at end of century was not as wet as the CSIRO-Mk3-6-0 projection, both projections were at least twice the mean projection of all 16 models. Selecting one model at end of century reduced model variation across the two time periods. Hence, we selected the CNRM-CM5 projection as the Wet core model for end of century.

Middle of the Set of Projections

To find a model that could represent the middle of the temperature and precipitation change projected by all 16 models, we compared each model's projected change in temperature and precipitation to the 16-model mean change. Determining the middle projection in this manner identified a projection that reflects the mean change—change was still occurring.

The closest projection to the 16-model mean change in temperature and precipitation under both scenarios was by the model NorESM1-M (table 8). The temperature change projected by NorESM1-M was slightly higher than the 16-model mean and less than the median under both scenarios. Under RCP 4.5, the change in precipitation projected by NorESM1-M was 4.40 percent, as compared to the mean (3.91 percent) and median (2.82 percent). While the IPSL-CM5A-LR model was nearly at the ensemble mean for temperature change, the projected precipitation change was less than half of the ensemble mean (fig. 19). Under RCP 8.5, the NorESM1-M projection was the closest model projection to the 16-model mean for temperature

Table 8—Change in mean temperature and annual precipitation from historical to end of century at the conterminous U.S. scale for the 16-model ensemble and the NorESM1-M model under the RCP 4.5 and RCP 8.5 scenarios. Median change of the 16-model ensemble is also shown.

Scenario	Model or 16-model ensemble change	Temperature change (°C)	Precipitation change (percent)
RCP 4.5	NorESM1-M mean	3.08	4.40
	16-model mean	2.89	3.91
	16-model median	3.11	2.82
RCP 8.5	NorESM1-M mean	5.10	8.17
	16-model mean	4.97	4.64
	16-model median	5.25	4.22

and less than the temperature median; however, the projected change in precipitation was an 8.17-percent increase, a wetter projection than the 16-model mean (4.64 percent) and median (4.22 percent). The next closest projection to the mean temperature change under RCP 8.5 was CNRM-CM5, and here the projected change in precipitation was 12.38 percent (fig. 19). The BNU-ESM projection was a warmer projection than the 16-model mean, and not as wet as the NorESM1-M projection; however, this selection resulted in a drier projection under RCP 4.5 than the ensemble mean. We selected NorESM1-M as the middle of the entire set of projections for end of century.

End-of-Century Core Models

Using the same criteria for core model selection as in mid-century, five models were chosen to represent the least warm, hot, dry, wet, and middle projections at end of century (table 9). We selected the same model under RCP 4.5 as under RCP 8.5 for each of the climate ranges and the same models as at mid-century (table 6). A full set of maps showing the temperature and precipitation change from the historical (1971–2000) to end-of-century (2070–2099) periods can be found in Appendix A.

Table 9—Core models for end-of-century analysis in the 2020 RPA Assessment.

	Least Warm	Hot	Dry	Wet	Middle
RCP 4.5	MRI-CGCM3	HadGEM2-ES	IPSL-CM5A-MR	CNRM-CM5	NorESM1-M
RCP 8.5	MRI-CGCM3	HadGEM2-ES	IPSL-CM5A-MR	CNRM-CM5	NorESM1-M
Climate modeling institution	Meteorological Research Institute, Japan	Met Office Hadley Centre, United Kingdom	Institut Pierre Simon Laplace, France	National Centre of Meteorological Research and European Centre for Advanced Research and Training, France	Norwegian Climate Center, Norway

As expected, projected temperatures under both scenarios and for all models continued to increase from mid-century to end of century. However, the relative increases were greater under RCP 8.5 than RCP 4.5 (compare figures 12 and 23). At mid-century, the ensemble mean projected change in temperature under RCP 4.5 was 2.34 °C and under RCP 8.5, 3.10 °C, a difference of 0.76 °C. At end of century, the 16-model mean temperature change under RCP 4.5 was 2.89 °C and under RCP 8.5, 4.97 °C, a difference of 2.08 °C.

At both time periods, the spread of projections under RCP 4.5 covered the lower range of projections under RCP 8.5 (compare figures 2 and 19). At mid-century, only 5 of the 16 projections under RCP 8.5 exceeded the hottest projection under RCP 4.5, a temperature change of 3.34 °C. In other words, the projected temperature changes from 11 models under RCP 8.5 were within the range of all projections under RCP 4.5 at mid-century. However, at end of century, 13 projections under RCP 8.5 exceeded the hottest projection under RCP 4.5, with only 3 model projections under RCP 8.5 within the range of all RCP 4.5 projections (compare figures 13 and 23). The overlap of projections between the two scenarios decreased at end of century.

While these models represented the end of a range for one climate variable, the user should be aware of what the model projected for the other climate variable. Models selected to represent the range of one climate variable (such as temperature) may not project the mid-range value for the other climate variable (such as precipitation).

The MRI-CGCM3 projection was chosen as the Least Warm core model (fig. 23). With respect to precipitation, the MRI-CGCM3 model projected an increase of 6.86 percent under RCP 4.5, as compared to the ensemble mean of 3.91 percent and the ensemble median of 2.82 percent. Other contenders for the Least Warm core model projected either a similar precipitation increase (GFDL-ESM2M, 5.72 percent) or a below-average increase (inmcm4, 1.14 percent). Under RCP 8.5, MRI-CGCM3 was one of the wettest projections, with a 12.15-percent increase in annual precipitation, as compared to the ensemble mean and median increases of 4.64 percent and 4.22 percent, respectively (fig. 23b). Interpretation of the potential effects of the Least Warm core model projection on a natural resource should take into consideration this relatively wet projection under RCP 8.5.

(a) RCP 4.5

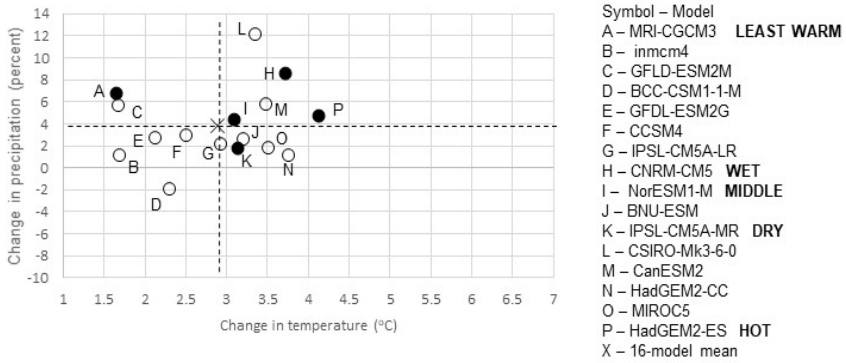

(b) RCP 8.5

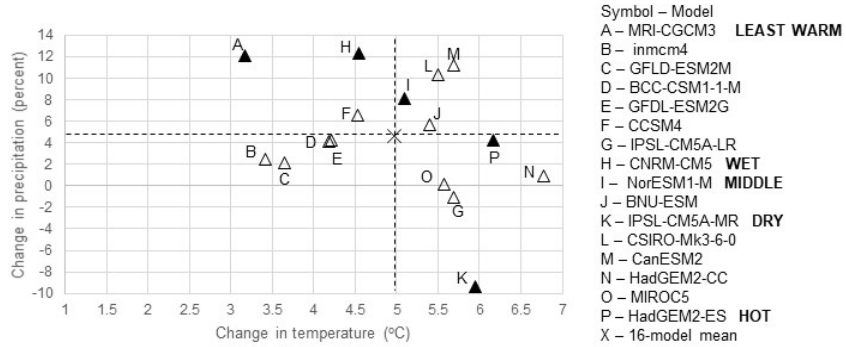

Figure 23—Annual precipitation change (percent) plotted against temperature change (°C) at the conterminous U. S. scale for all 16 models under RCP 4.5 (a) and RCP 8.5 (b) at end of century (2070–2099). Individual models are denoted by open circles in the RCP 4.5 scenario and open triangles in the RCP 8.5 scenario. The black "X" represents the mean temperature and precipitation change for 16 models in each scenario. The core models are identified as filled circles or triangles and noted Least Warm, Hot, Dry, Wet, and Middle in the legend.

The Wet core model at end of century was the CNRM-CM5 model. The temperature projection by this model under RCP 4.5 was 3.71 °C, as compared to the ensemble mean of 2.88 °C and median of 3.11 °C. Under RCP 8.5, the CNRM-CM5 model projection of 4.54 °C is closer to the ensemble mean change of 4.97 °C (compare H to X in figures 23a,b). Interpretation of the Wet core model projection by CNRM-CM5 under RCP 4.5 should take into consideration that this projection was above the mean temperature change under RCP 4.5, but not as hot as the hottest model projection of HadGEM2-ES.

The HadGEM2-ES model was selected as the Hot core model, representing the hottest projection of all 16 models under both scenarios. This model projected nearly the same change in precipitation as the ensemble mean under both scenarios. Under RCP 4.5, HadGEM2-ES projected a 4.81-percent increase, as compared to the ensemble change of 3.91 percent. Under RCP 8.5, the HadGEM2-ES model projected a 4.21-percent increase, as compared to the ensemble mean change of 4.64 percent and the median change of 4.22 percent (fig. 23).

The model selected as the Dry core model, IPSL-CM5A-MR, projected a temperature change of 3.13 °C, as compared to the ensemble mean and median change of 2.88 °C and 3.11 °C, respectively, under RCP 4.5 (fig. 23). Under RCP 8.5, IPSL-CM5A-MR projected a temperature increase of 5.95 °C, as compared to the ensemble mean and median change of 4.97 °C and 5.25 °C, respectively (fig. 23). Under RCP 8.5, the IPSL-CM5A-MR projection was not as hot as the hottest projection; however, it ranks among the three hottest projections (fig. 23).

MODEL AND PROJECTION SELECTION FOR NATIONAL FOREST REGIONS

National forests are undergoing a planning process that is required to explore system drivers and stressors such as climate change (Roske et al. 2019; Timberlake et al. 2018). System drivers include dominant ecological processes, disturbance regimes, and stressors, such as natural succession, wildland fire, invasive species, and climate change, and the ability of terrestrial and aquatic ecosystems on the plan area to adapt to change (USDA FS 2012c). Approaches that have been used to explore the system drivers of climate change vary across national forests from a focused vulnerability assessment at the individual national forest scale (Rice et al. 2012) to regional large-scale synthesis of the literature (Halofsky et al. 2018; Rice et al. 2018; Swanston et al. 2011). Climate change scenarios and projections chosen in these assessments vary in terms of the number and type of scenarios, number of models, and number of projections including the use of ensembles.

The 2020 RPA Assessment will use a consistent set of scenarios to explore the effects of different trajectories of population change, economic growth, and climate change on natural resources. Resources to be studied include forest dynamics, rangelands, forest products, wildlife habitat, outdoor recreation, water resources, and urban forests. Five climate projections under RCP 4.5 and RCP 8.5 were selected to represent climatic ranges—least warm, hot, dry, wet, and middle of the 16 projections (see *Mid-Century Core Models* section). If consistency in models and projections across national forest regions in the conterminous United States is an objective, it is important to understand whether the national core models would be representative of the same climatic range within the national forest regions.

These national core climate projections were selected based on projection results at the conterminous U.S. scale. We explored two questions: (1) If focused on a national forest region, would the method used to select core models at the scale of the conterminous United States identify the same model selected at the national level; and (2) Within a national forest region, were the models selected at the national scale representative of climatic ranges of least warm, hot, dry, and wet at the regional scale? In question 1, we asked whether the national core model surfaced as one of the top three projections in each climatic range. In the second question, we asked whether these five national core models were representative of the least warm-hot spectrum and the dry-wet spectrum within the region under RCP 4.5 and RCP 8.5.

Use of the Selection Process by National Forest System Region

For the 2020 RPA Assessment, two Representative Concentration Pathway (RCP) scenarios were chosen: RCP 4.5 and RCP 8.5. Individual climate model projections were selected to represent the least warm, hot, dry, wet, and middle of the 16 model projections (see *Identification of Core Models* section). Here, we examined whether using the same method, but within individual regions of the National Forest System (NFS), would result in selecting the national core models for regional climate ranges. Eight of the nine national forest regions were analyzed (fig. 24). The MACAv2-METDATA dataset did not include the geographic regions of Alaska, Hawaii and Pacific island territories, U.S. Virgin Islands, and Puerto Rico; consequently, these areas were not analyzed.

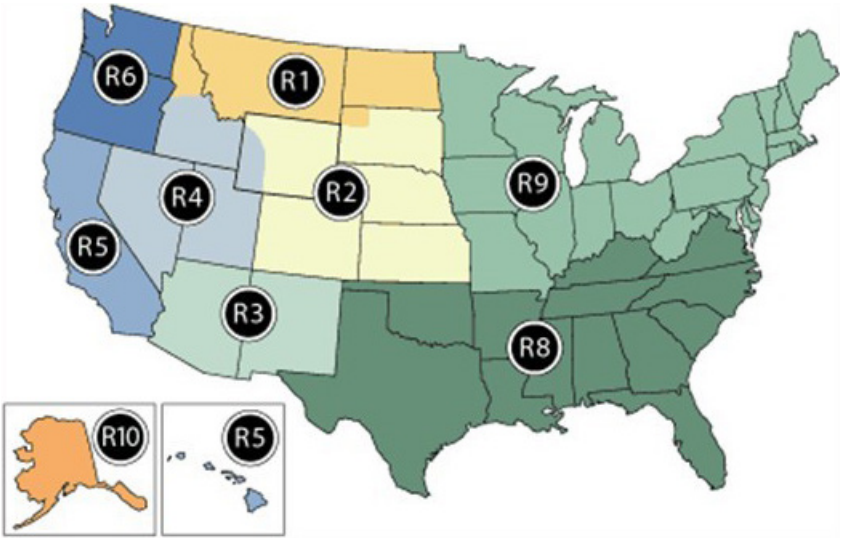

Figure 24—National Forest System regions within the United States.

At the conterminous U.S. scale, we used the model performance analysis by Rupp and others (Rupp 2016a,b; Rupp et al. 2013), which explored how well each model reproduced historical climate (see *Model Performance* section). Our objective was to exclude models that did not capture historical climate well. From the analysis by Rupp and others, four models were consistently poor performers in the Pacific Northwest, Southeast, and Southwest regions. These four models were also dropped from the Midwest and Great Lakes region study by Byun and Hamlet (2018). Thus, for this exploration of national forest regions, we eliminated the identified poor performers: bcc-csm1-1, MIROC-ESM, MIROC-ESM-CHEM, and IPSL-CM5B-LR.

The projected changes in temperature and precipitation were computed using the historical period of 1971–2000 and the mid-century period of 2041–2070. Three models were identified as representative of the two extremes of the

projected changes in temperature or precipitation. These model projections were filtered such that only one projection was selected from a modeling institution, and if possible the same core models were selected for the region under scenarios RCP 4.5 and RCP 8.5.

Least Warm

In all NFS regions, MRI-CGCM3, the national Least Warm core model, was among the three top-ranked projections with the least change in temperature at mid-century under both scenarios (table 10). Regionally, the least warm temperature change ranged from 1.01 to 1.37 °C under RCP 4.5 and from 1.61 to 2.07 °C under RCP 8.5 (Appendix B). If we use the criterion of ranking among the top three projections, the national core model, MRI-CGCM3, would be representative of the least warm spectrum under both scenarios in the eight NFS regions.

We explored the ranking further to determine the differences in the top three projections for least warm. While the MRI-CGCM3 projection for each region was among the top three least warm projections, three other models were also ranked among the top three least warm projections: GFDL-ESM2M, inmcm4, BNU-ESM (table 10). Under RCP 4.5, temperature changes projected by MRI-CGCM3 and the top-ranked model in each region were close, differing by less than 0.22 °C (see Appendix B). For example, in Region 6, the region where MRI-CGCM3 was ranked third (table 10), the projected temperature change across the three top-ranked models was within 0.05 °C, with a projected change in temperature of 1.01 °C for the inmcm4 model, 1.05 °C for the GFDL-ESM2M model, and 1.06 °C for the MRI-CGCM3 model (fig. B.6). Under RCP 8.5, the projection by MRI-CGCM3 was consistently the least warm projection.

Hot

The national Hot core model, HadGEM2-ES, was ranked among the three hottest projections for seven regions under RCP 4.5 and four regions under RCP 8.5 (table 11). Regionally, the hot temperature change ranged from 2.78 to 3.87 °C under RCP 4.5 and from 3.47 to 4.68 °C under RCP 8.5. If we use the criterion of ranking among the top three projections, the national Hot core model would be representative of the hot spectrum for seven regions under RCP 4.5 and four regions under RCP 8.5. The national Hot core model HadGEM2-ES was not among the three hottest projections in Region 3 under RCP 4.5 and in Regions 3, 4, 5, and 6 under RCP 8.5. We explored the projected temperature change for those regions.

Under RCP 4.5, the HadGEM2-ES projection was ranked the fourth hottest projection in Region 3. The hottest projection (CanESM2) projected a temperature change of 3.05 °C, and the fourth-ranked HadGEM2-ES projected a change of 2.89 °C, a difference of 0.16 °C. In Region 3, the national core model projection was within 0.02 °C of the 2.91 °C increase projected by the third-ranked CSIRO-Mk3-6-0. Across all regions, the top

Table 10—Top three ranked least warm projections by mid-century (2041–2070) for each national forest region under RCP 4.5 and RCP 8.5 scenarios. Temperature change was computed relative to the historical period (1971–2000). The Least Warm national core model, MRI-CGCM3, is in bold

Region	RCP 4.5	RCP 8.5
1	GFDL-ESM2M **MRI-CGCM3** inmcm4	**MRI-CGCM3** inmcm4 GFDL-ESM2M
2	**MRI-CGCM3** inmcm4 GFDL-ESM2M	**MRI-CGCM3** GFDL-ESM2M inmcm4
3	inmcm4 **MRI-CGCM3** GFDL-ESM2M	**MRI-CGCM3** inmcm4 GFDL-ESM2M
4	inmcm4 **MRI-CGCM3** GFDL-ESM2M	**MRI-CGCM3** inmcm4 GFDL-ESM2M
5	inmcm4 **MRI-CGCM3** GFDL-ESM2M	**MRI-CGCM3** inmcm4 BNU-ESM
6	inmcm4 GFDL-ESM2M **MRI-CGCM3**	**MRI-CGCM3** inmcm4 GFDL-ESM2M
8	inmcm4 **MRI-CGCM3** GFDL-ESM2M	**MRI-CGCM3** inmcm4 GFDL-ESM2M
9	inmcm4 **MRI-CGCM3** GFDL-ESM2M	**MRI-CGCM3** GFDL-ESM2M inmcm4

three projections under RCP 4.5 differed by less than 0.59 °C (figs. B.1a, B.2a, B.4a, B.5a, B.6a, B.7a, B.8a).

Under RCP 8.5, the national Hot core model, HadGEM2-ES, was ranked fourth in Region 3, fifth in Region 4, and sixth in Regions 5 and 6 (table 11). The difference between the hottest projection and the third hottest projection across all regions ranged from 0.10 to 0.60 °C (Appendix B). In Regions 3 and 4, the differences between the fourth- and fifth-ranked HadGEM2-ES projection and the hottest projection were 0.45 and 0.28 °C, respectively. For Regions 5 and 6, the differences between the sixth-ranked HadGEM2-ES projection and the hottest projection were 0.36 °C and 0.85 °C, respectively. While the Hot core model is a hot model for Region 6, the method identified other model projections that are hotter. Except for Region 6, the differences between the HadGEM2-ES projection when ranked fourth, fifth, or sixth and the top-ranked projection in a region were within the range of differences among the top three models across all eight regions (0.10 to 0.60 °C).

Table 11—Top three ranked hottest projections for each national forest region at mid-century (2041–2070) under RCP 4.5 and RCP 8.5. Temperature change was computed relative to the historical period (1971–2000). The national Hot core model projection is in bold.

Region	RCP 4.5	RCP 8.5
1	**HadGEM2-ES** MIROC5 CanESM2	HadGEM2-CC **HadGEM2-ES** CanESM2
2	**HadGEM2-ES** MIROC5 CSIRO-Mk3-6-0	**HadGEM2-ES** HadGEM2-CC IPSL-CM5A-MR
3	CanESM2 IPSL-CM5A-MR CSIRO-Mk3-6-0 ***4th HadGEM-ES***	IPSL-CM5A-MR CanESM2 HadGEM2-CC ***4th HadGEM-ES***
4	MIROC5 CanESM2 **HadGEM2-ES**	HadGEM2-CC IPSL-CM5A-MR CanESM2 ***5th HadGEM-ES***
5	CSIRO-Mk3-6-0 IPSL-CM5A-MR **HadGEM2-ES**	IPSL-CM5A-MR CanESM2 HadGEM2-CC ***6th HadGEM2-ES***
6	CanESM2 **HadGEM2-ES** CSIRO-Mk3-6-0	HadGEM2-CC CanESM2 IPSL-CM5A-MR ***6th HadGEM2-ES***
8	**HadGEM2-ES** HadGEM2-CC MIROC5	HadGEM2-CC **HadGEM2-ES** IPSL-CM5A-MR
9	**HadGEM2-ES** MIROC5 HadGEM2-CC	**HadGEM2-ES** HadGEM2-CC MIROC5

Dry

The national Dry core model, IPSL-CM5A-MR, was one of the three driest projections under RCP 4.5 for all eight regions and among the top three projections under RCP 8.5 for six regions (table 12). Regionally, the driest projected changes in each region ranged from a decrease of 16.47 percent to an increase of 1.46 percent under RCP 4.5, and from a decrease of 26.12 percent to a decrease of 1.06 percent under RCP 8.5 (Appendix B). In contrast to the projected temperature changes, the projected changes in precipitation varied greatly across the models within each region (Appendix B). In Region 9, all models projected increases in precipitation under RCP 4.5, with the driest projection, by MIROC5, an increase of 1.5 percent and the second driest projection, by IPSL-CM5-MR, an increase of 1.83 percent (fig. B.8). If we use the criterion of ranking among the top three projections, the national core model, IPSL-CM5A-MR, would be representative of the dry spectrum for all eight regions under RCP 4.5 and for six regions (Regions 1, 2, 3, 4, 8, 9) under RCP 8.5. For Regions 5 and 6, the national Dry core model was ranked outside the three driest projections under RCP 8.5. We explored the projected precipitation changes in these regions.

Table 12—Top three ranked driest projections for each national forest region at mid-century (2041–2070) under the RCP 4.5 and RCP 8.5 scenarios. Precipitation change was computed relative to the historical period (1971–2000). The national Dry core model projection is in bold.

Region	RCP 4.5	RCP 8.5
1	**IPSL-CM5A-MR** IPSL-CM5A-LR CCSM4	CCSM4 CSIRO-Mk3-6-0 **IPSL-CM5A-MR**
2	**IPSL-CM5A-MR** bcc-csm1-1-m IPSL-CM5A-LR	**IPSL-CM5A-MR** inmcm4 CCSM4
3	**IPSL-CM5A-MR** IPSL-CM5A-LR NorESM1-M	**IPSL-CM5A-MR** HadGEM2-ES inmcm4
4	**IPSL-CM5A-MR** bcc-csm1-1-m CCSM4	HadGEM2-ES inmcm4 **IPSL-CM5A-MR**
5	**IPSL-CM5A-MR** MIROC5 IPSL-CM5A-LR	MIROC5 HadGEM2-ES NorESM1-M ***4th IPSL-CM5A-MR***
6	IPSL-CM5A-LR HadGEM2-CC **IPSL-CM5A-MR**	IPSL-CM5A-LR CSIRO-Mk3-6-0 inmcm4 ***14th IPSL-CM5A-MR***
8	**IPSL-CM5A-MR** GFDL-ESM2G bcc-csm1-1-m	**IPSL-CM5A-MR** HadGEM2-ES inmcm4
9	MIROC5 **IPSL-CM5A-MR** bcc-csm1-1-m	inmcm4 **IPSL-CM5A-MR** IPSL-CM5A-LR

Under RCP 8.5, the national Dry core model was ranked 4th for Region 5 and 14th for Region 6. In Region 5, IPSL-CM5A-MR projected a precipitation decrease of 3.27 percent, whereas the driest model, MIROC5, projected a precipitation decrease of 10.36 percent. Given that the mean change of all 16 models was a 4.45-percent increase, the IPSL-CM5A-MR projection is a dry projection, and within 0.03 percentage points of the third-ranked projection (fig. B.5b). For Region 6, 14 models projected increased precipitation under RCP 8.5. Only two models projected decreases: IPSL-CM5A-LR and CSIRO-Mk3-6-0. The national Dry core model, IPSL-CM5A-MR, was ranked the 14th driest projection, which translates to the third wettest projection of all 16 models under RCP 8.5 (fig. B.6b). For Region 6 under RCP 8.5, IPSL-CM5A-MR was not representative of the dry spectrum.

Wet

The national Wet core model, CNRM-CM5, was among the three wettest projections for Regions 2, 5, 8, and 9 under RCP 4.5, and for Regions 4, 5, 6, and 8 under RCP 8.5 (table 13). The wettest projected change in each region ranged from an increase of 6.51 to 19.42 percent under RCP 4.5 and from an increase of 8.05 to 27.40 percent under RCP 8.5 (Appendix B). If we use the criterion of ranking among the top three projections, the national core model,

Table 13—Top three ranked wettest projections for each national forest region at mid-century (2041–2070) under the RCP 4.5 and RCP 8.5 scenarios. Precipitation change was computed relative to the historical period (1971–2000). The national Wet core model projection is in bold.

Region	RCP 4.5	RCP 8.5
1	GFDL-ESM2M CanESM2 GFDL-ESM2G ***10th CNRM-CM5***	GFDL-ESM2G CanESM2 MRI-CGCM3 ***4th CNRM-CM5***
2	HadGEM2-CC **CNRM-CM5** MRI-CGCM3	MRI-CGCM3 HadGEM2-CC GFDL-ESM2M ***6th CNRM-CM5***
3	GFDL-ESM2M CanESM2 BNU-ESM ***6th CNRM-CM5***	CanESM2 GFDL-ESM2M CSIRO-Mk3-6-0 ***4th CNRM-CM5***
4	CanESM2 CSIRO-Mk3-6-0 HadGEM2-CC ***6th CNRM-CM5***	CanESM2 CSIRO-Mk3-6-0 **CNRM-CM5**
5	**CNRM-CM5** CanESM2 inmcm4	CanESM2 **CNRM-CM5** MRI-CGCM3
6	GFDL-ESM2G CCSM4 BNU-ESM ***7th CNRM-CM5***	**CNRM-CM5** MIROC5 IPSL-CM5A-MR
8	CSIRO-Mk3-6-0 **CNRM-CM5** MRI-CGCM3	**CNRM-CM5** CSIRO-Mk3-6-0 MRI-CGCM3
9	CSIRO-Mk3-6-0 GFDL-ESM2M **CNRM-CM5**	GFDL-ESM2G MRI-CGCM3 GFDL-ESM2M ***4th CNRM-CM5***

CNRM-CM5, would be representative of the wet spectrum for four regions under RCP 4.5 and four regions under RCP 8.5. For Regions 1, 3, 4, and 6 under RCP 4.5 and Regions 1, 2, 3, and 9 under RCP 8.5, the national Wet core model (CNRM-CM5) was ranked outside the three wettest projections. We explored the differences in the projected precipitation changes for those regions.

Under RCP 4.5 in Regions 1, 3, 4 and 6, CNRM-CM5 was ranked 10th, 6th, 6th, and 7th, respectively (table 13). In Region 1, CNRM-CM5 projected a 4.11-percent increase, less than the ensemble projection of 4.65 percent, whereas the wettest projection, by the GFDL-ESM2M model, was a 14.10-percent increase. In Region 3, CNRM-CM5 projected an increase of 5.61 percent and the top-ranked model, GFDL-ESM2M, projected an increase of 9.53 percent. In this region, 8 of the 16 models projected decreases and 8 projected increases, resulting in a projected mean change in precipitation of 0.47 percent, nearly zero change. In Region 4, CNRM-CM5 projected an increase of 8.93 percent, in contrast to the wettest projection, by CanESM2, of 16.55 percent; the ensemble mean was 6.26 percent. In Region

6, the wettest projection, by GFDL-ESM2G, was a 6.51-percent increase and the seventh-ranked CNRM-CM5 projection was 4.33 percent, slightly above the projected mean change of 3.28 percent. The selection method used at the regional scale for Regions 1, 3, 4, and 6 identified other models where the projection for increased precipitation was greater.

Under RCP 8.5 in Regions 1, 2, 3, and 9, CNRM-CM5 was ranked fourth, sixth, fourth, and fourth, respectively (table 13). In Region 1, the CNRM-CM5 model projected a precipitation increase of 10.04 percent, whereas the wettest projection, by GFDL-ESM2G, was 12.11 percent. In Region 2, CNRM-CM5 projected a 6.13-percent increase in precipitation, in contrast to the 11.81-percent increase by MRI-CGCM3. In Region 3, the wettest projection, by CanESM2, was a 16.18-percent increase, and sixth-ranked CNRM-CM5 projected an 8.22-percent increase. In Region 9, CNRM-CM5, ranked fourth, projected an increase of 8.98 percent, and the wettest projection, by GFDL-ESM2G, was an increase of 10.55 percent. For Regions 1, 3, 4, and 9, the differences between the national Wet core model and the regional wettest model was around 2 percent, and in each region, the CNRM-CM5 projection was always greater than the mean projected regional change in precipitation. For Region 2, the national Wet core model projection was nearly 5 percentage points less than the wettest projection.

Middle of the Set of Projections

The process to select a middle core model nationally involved finding a model where the projected change in temperature and precipitation was near the 16-model mean change in temperature and precipitation. Within each region, the variability of the projected temperature change and the projected precipitation change was large (Appendix B). No single model projection, including the national Middle core projection by NorESM1-M, captured the ensemble mean in each region under RCP 4.5 or RCP 8.5. For most regions, the temperature or the precipitation projection by NorESM1-M was close to the regional mean temperature or precipitation change, but not for both projected changes (Appendix B). In only two regions was the NorESM1-M projection a suitable reflection of the middle of the entire suite of projections: Region 4 and Region 6 (figs. B.4; B.6). Despite differing from the mean projected change in precipitation by 3.22 percentage points for Region 4 under RCP 8.5, the NorESM1-M projection was the closest projection to the ensemble mean.

Use of the National Core Model Projections in Individual National Forest Regions

The five national core model projections under RCP 4.5 and RCP 8.5 will be used in a suite of natural resource analyses at the conterminous U.S. scale. In these analyses, the MRI-CGCM3 projection will be interpreted as the least warm projection, HadGEM2-ES as the hot projection, IPSL-CM5A-MR as the dry projection, CNRM-CM5 as the wet projection, and NorESM1-M as

the projection for the middle of the suite of 16 models. The natural resource analyses using these climate projections will present results from these 5 projections, not from the entire suite of 16 projections. Given that context for the use of these projections, we explored the relative behavior of the set of national core models within a region. For example, was the temperature projection by the national Least Warm core model (MRI-CGCM3) always less than the temperature projection of the national Hot core model (HadGEM2-ES)? We asked a similar question for the precipitation change projections.

Within each region, the projected change in temperature by the Least Warm core model was always less than the projected change by the Hot core model under RCP 4.5 and RCP 8.5 (fig. 25a, Appendix B). For example, in Region 5 under RCP 4.5, the national Least Warm model projected a 1.07 °C increase in temperature, and the national Hot core model projected an increase of 2.59 °C. Relative to MRI-CGCM3, the HadGEM2-ES projection was always a hotter projection in each region under both RCP 4.5 and RCP 8.5.

Across the regions, projected changes in precipitation were highly variable. Yet for each region, the national Wet core model projection, CNRM-CM5, was always wetter than the national Dry core model projection, IPSL-CM5A-MR (fig. 25b, Appendix B). Even for those cases where there was a wetter or a drier regional projection, the wet projection by the national Wet core model, CNRM-CM5, was always wetter than the projections by the national Dry core model. For Region 1 under RCP 4.5, the CNRM-CM5 projection of a 4.11-percent increase contrasted with the decrease in precipitation projected by IPSL-CM5A-MR (-4.11 percent). Projections for Region 6 under RCP 4.5 also showed a contrast; CNRM-CM5 projected a 4.33-percent increase, whereas IPSL-CM5A-MR projected a 0.47-percent increase. Under RCP 8.5, the CNRM-CM5 projection was always wetter than the IPSL-CM5-MR projection. Even in Region 6, the projection by CNRM-CM5 was an 11.08-percent increase in precipitation, as compared to the IPSL-CM5A-MR projection of a 7.80-percent increase. The ensemble mean for Region 6 was a 3.84-percent increase in precipitation. This result will require recognition that the wet and dry projections for Region 6 under RCP 8.5 both project increases in precipitation.

(a) MRI-CGCM3 and HadGEM2-ES projections for each region

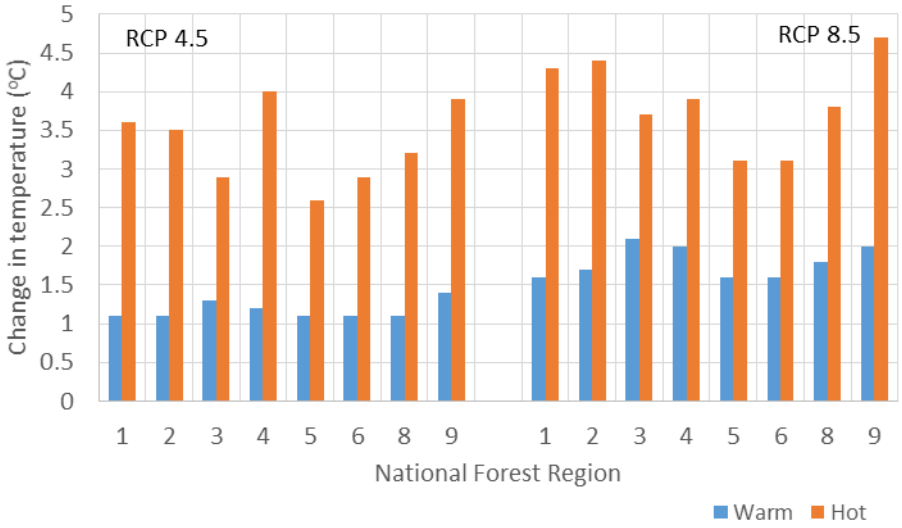

(b) IPSL-CM5A-MR and CNRM-CM5 projections for each region

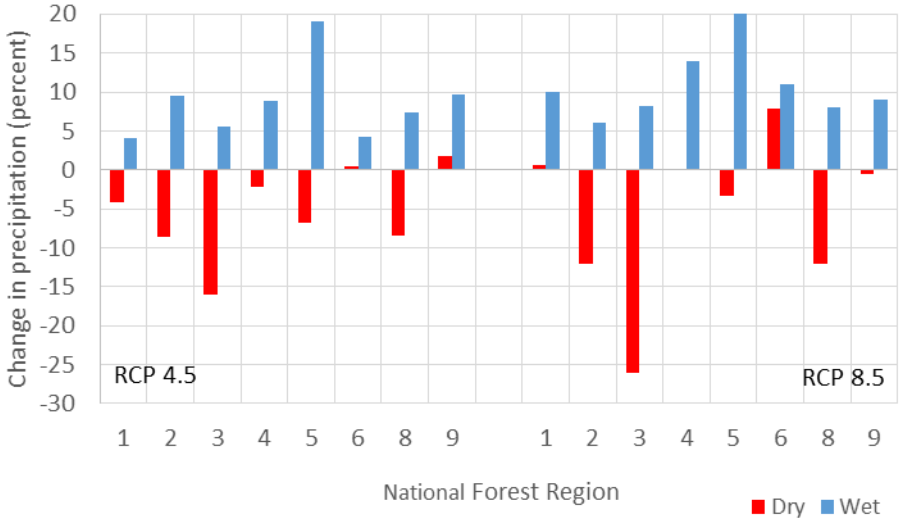

Figure 25—Projected changes in mean temperature and annual precipitation for each national forest region: temperature changes (°C) by the national Least Warm core model (MRI-CGCM3) and national Hot core model (HadGEM2-ES) under RCP 4.5 and RCP 8.5 (a); and precipitation changes (percent) by the national Dry core model (IPSL-CM5A-MR) and the national Wet core model (CNRM-CM5) under RCP 4.5 and RCP 8.5 (b).

Climate Model and Projection Selection in the National Forest Regions

We explored two questions about climate model selection in national forest regions. First, if focused on a national forest region, would the process used at the national level identify the same models as at the conterminous scale; and second, within a national forest region, were the national core models reflective of their respective climatic range within a region? We used the same methodology that we used at the conterminous scale within each region.

Generally, the national core models were identified among the top three regional ranks for temperature and for precipitation, with some exceptions. In using the conterminous methodology at the scale of the region, the national Least Warm core model was consistently in the top three least warm projections in all regions under both scenarios (table 10). The national Hot core model, HadGEM2-ES, was either among the three hottest projections or was within a small difference of the hottest projection (Region 3) in all regions under RCP 4.5. The national Hot core model ranked among the hottest projections for four regions under RCP 8.5 and was within 0.45 °C for three other regions under RCP 8.5, resulting in a relatively straightforward choice for the hot end of the spectrum in most regions (table 11). For Region 6, the HadGEM2-ES was ranked sixth and differed by 0.85 °C from the hottest projection. Other models projected a hotter future.

Projected changes in precipitation varied widely across the regions. The national Dry core model represented the dry spectrum for each region with one exception under RCP 8.5. For all regions under RCP 4.5 and seven of the eight regions under RCP 8.5, the selected national Dry core model, IPSL-CM5A-MR, was among the top three ranks and would be representative of the dry spectrum (table 12). However, for Region 6 under RCP 8.5, the IPSL-CM5A-MR was one of the wettest projections. The availability of moisture in the IPSL-CM5A-MR projections and projected temperature changes above the ensemble mean should be considered in interpreting the results of the natural resource analyses within Region 6 under RCP 8.5. The wettest projections under RCP 4.5 and RCP 8.5 were highly variable. The national Wet core model was among the wettest projections for four regions under RCP 4.5 and four regions under RCP 8.5. In some cases, the models ranked outside of the top three were still wet projections, for example, in Region 1 under RCP 4.5 and Region 9 under RCP 8.5. However, if the geographic focus is solely the region, there were projections that were wetter than the national Wet core model (table 13).

When the behavior of the five core models is the focus, the national Least Warm, Hot, Dry, and Wet core models reflected those spectrums across all regions under both scenarios with one exception. In all regions, the projection of the Hot core model was always a larger change in temperature than projected by the Least Warm model for that region. Similarly, the Wet

core model projected an increase in precipitation greater than the dry model within a region, with one exception. For Region 6, the national Dry core model, IPSL-CM5A-MR, projected a 7.8-percent increase in precipitation under RCP 8.5, the third wettest projection in this region. The national Wet core model, CNRM-CM5, projected an 11.08-percent increase in precipitation. For Region 6 under RCP 8.5, the IPSL-CM5A-MR projection was not representative of the dry spectrum.

National forest regions may not have staff and resources to conduct such a detailed analysis to explore the effects of all 16 climate model projections on the natural resources in their regions. Vano et al. (2018) recommend leveraging the work of others. The RPA resource analyses of climate change will use the national core model projections. The interpretation will be focused on how these five projections under two scenarios influence natural resources. With one exception, the national core models reflect the different extremes of temperature and precipitation. Consistency in scenarios and projections reduces the influence of climate model variation on the interpretation of climate projections. Consistency in scenarios and models aids in the interpretation of the climate and socioeconomic effects on natural resources. The benefits can also be consistency across NFS regions and access to additional analyses in the RPA Assessment.

AVAILABILITY OF RPA CLIMATE DATA

Downscaled Modeled Historical and Projected Data

The historical modeled and projected climate data developed in this report are archived in the Forest Service's Research and Development Data Archive (Joyce et al. 2018). The climate scenarios are the Representative Concentration Pathways (RCPs) 4.5 and 8.5, and the downscaled climate data are the MACAv2-METDATA developed by Abatzoglou and Brown (2012) and Abatzoglou (2013). This downscaled climate dataset covers the conterminous United States at the grid size of approximately 4 km (1/24 degree) on a side. The five projections for each RCP scenario captured a range of future climates at the conterminous scale: Least Warm—MRI-CGCM3; Hot—HadGEM2-ES; Dry—IPSL-CM5A-MR; Wet—CNRM-CM5; Middle—NorESM1-M. The three criteria used to select these projections are described in earlier sections of this publication.

The dataset includes downscaled historical modeled output (1950–2005) and projections (2006–2099) for the RCP 4.5 and RCP 8.5 scenarios for the core set of models. The variables available include monthly mean of daily mean near-surface specific humidity (huss), mean daily mean potential evapotranspiration (pet), mean daily maximum relative humidity (rhmax), mean daily minimum relative humidity (rhmin), monthly mean of daily surface downwelling shortwave radiation (rsds), total monthly precipitation (mm), mean daily maximum air temperature (tasmax), mean daily minimum air temperature (tasmin), and monthly mean of daily mean near-surface wind speed (was). With 2 climate scenarios and 5 models, 10 different climate futures are available.

The MACAv2-METDATA dataset is also used in the Northwest Climate Toolbox (see https://climatetoolbox.org/tool/Future-Time-Series). Users can display historical and projected climate for any location or area in the United States.

Training Data—Historical Observed Gridded Data

A monthly gridded historical (1979–2015) dataset for the conterminous United States, based on the daily MACA observational data (METDATA), is available at the Forest Service's Research and Development Data Archive (Coulson and Joyce 2018). This monthly historical dataset was developed using the daily MACA observational data, also called MACA training data (https://www.northwestknowledge.net/metdata/data/). The MACA training data were used to downscale global climate model projections to the 1/24-degree grid scale. These monthly data are being used in the

modeling analyses for the 2020 RPA Assessment. Data include eight separate files containing mean daily potential evapotranspiration, total monthly precipitation, mean daily minimum and maximum relative humidity, mean daily downward shortwave radiation at surface, mean daily maximum air temperature, mean daily mean air temperature, mean daily minimum air temperature, and mean daily mean wind speed at 10 meters high.

SUMMARY AND CONCLUSIONS

The 2020 RPA Assessment will include climate change as a driver of change affecting natural resources on all forests and rangelands in the United States. This report describes the process used to select the historical and projected climate datasets and summarizes the future climates for the conterminous United States. These climate projections, along with projections for population dynamics, economic growth, and land use change in the United States, constitute the RPA scenarios and will be used in the 2020 RPA Assessment to project future renewable resource conditions 50 years into the future.

Identifying which climate scenarios, which climate models, and how many climate model projections to use to analyze the effects of climate change can be challenging. The number of alternate futures can quickly escalate when climate, social, and economic drivers of change are combined. Two scenarios selected for use in this assessment are the Representative Concentration Pathways (RCPs) 4.5 and 8.5, as these scenarios frame the lower and upper range of projected future greenhouse gas emissions.

The native scale of the global climate models is too coarse for natural resource assessments; thus, finer scale projected climate data were sought using criteria that described the level of detail needed in the assessment. The historical period of 1971 through 2000 was selected for comparison with future climate at mid-century (2041–2070), a typical 50-year outlook that has been a part of the RPA Assessments. Climate variables needed in the analysis included mean monthly maximum temperature (°C), mean monthly minimum temperature (°C), monthly total precipitation (mm), surface downwelling solar radiation (W m^{-2}), potential evapotranspiration (PET, mm), maximum relative humidity (%), wind speed (at 10 m, m s^{-1}), and near-surface specific humidity.

After a review of the available downscaled climate data from the CMIP5 archive, the MACAv2-METDATA developed by Abatzoglou and others at the University of Idaho was selected. This downscaled climate dataset covers the conterminous United States at the grid size of approximately 4 km (1/24 degree) on a side. The dataset includes downscaled projections from 20 models for the RCP 4.5 and RCP 8.5 scenarios. With 2 climate scenarios and 20 models, 40 different climate futures are available.

A climate model selection process was developed that evaluated all 20 climate models under each RCP scenario based on three criteria: (1) historical model performance, (2) selection of only one model from a modeling institution, and (3) if possible, selection of the same model for both

RCP scenarios. The historical performance criteria eliminated 4 of the 20 models. The remaining 16 models under 2 scenarios resulted in a potential set of 32 projections. Based on discussions by the RPA team, the decision was made to use five climate projections under each RCP scenario. Selection of the 5 projections was based on capturing the range of changes in temperature and precipitation within the 16 projections under each scenario (table 14).

These data were developed for researchers and others who are interested in using climate data to model or assess the effects of climate change on natural resources within the conterminous United States. The specific application of these data in the RPA Assessment is in the resource models of forest condition, water supply and use projections, wildlife habitat, recreation analyses, and range forage projection. These data will also be useful input for other applications exploring the impact of climate change on resource management issues in other settings.

Table 14—Core models for mid-century analysis in the 2020 RPA Assessment.

	Least Warm	Hot	Dry	Wet	Middle
RCP 4.5	MRI-CGCM3	HadGEM2-ES	IPSL-CM5A-MR	CNRM-CM5	NorESM1-M
RCP 8.5	MRI-CGCM3	HadGEM2-ES	IPSL-CM5A-MR	CNRM-CM5	NorESM1-M
Climate modeling institution	Meteorological Research Institute, Japan	Met Office Hadley Centre, United Kingdom	Institut Pierre Simon Laplace, France	National Centre of Meteorological Research and European Centre for Advanced Research and Training, France	Norwegian Climate Center, Norway

REFERENCES

Abatzoglou, J.T. 2013. Development of gridded surface meteorological data for ecological applications and modelling. International Journal of Climatology. 33(1): 121–131. doi: 10.1002/joc.3413.

Abatzoglou, J.T.; Brown, T.J. 2012. A comparison of statistical downscaling methods suited for wildfire applications. International Journal of Climatology. 32(5): 772–780. doi: 10.1002/joc.2312.

Bachelet, D.; Ferschweiler, K.; Sheehan, T.; Strittholt, J. 2016. Climate change effects on southern California deserts. Journal of Arid Environments. 127: 17–29.

Byun, K.; Hamlet, A.F. 2018. Projected changes in future climate over the Midwest and Great Lakes region using downscaled CMIP5 ensembles. International Journal of Climatology. 38(Suppl. 1): e531–e553. doi: 10.1002/joc.5388.

Coulson, D.P.; Joyce, L.A. 2018. RPA historical observational data (1979–2015) for the conterminous United States at the 1/24 degree grid scale based on MACA training data (METDATA). Updated February 27, 2018. Fort Collins, CO: U.S. Department of Agriculture, Forest Service, Research Data Archive. https://doi.org/10.2737/RDS-2017-0070 [Accessed September 17, 2019].

Flato, G.; Marotzke, J.; Abiodun, B.; [et al.]. 2013. Evaluation of climate models. In: Climate change 2013: The physical science basis. Contribution of Working Group I to the Fifth Assessment Report of the Intergovernmental Panel on Climate Change. [Stocker, T.F.; Qin, D.; Plattner, G.-K.; [et al.], eds.]. Cambridge, UK and New York: Cambridge University Press: 741–866.

Halofsky, J.E.; Peterson, D.L.; Ho, J.J.; [et al.], eds. 2018. Climate change vulnerability and adaptation in the Intermountain Region. Gen. Tech. Rep. RMRS-GTR-375. Fort Collins, CO: U.S. Department of Agriculture, Forest Service, Rocky Mountain Research Station. Part 1, p. 1–197; Part II, p. 199–513.

Hayhoe, K.; Edmonds, J.; Knopp, R.E.; [et al.]. 2017. Climate models, scenarios and projections. In: Climate science special report: Fourth National Climate Assessment. Vol. I. [Wuebbles, D.J.; Fahe, D.W.; Hibbard, K.A.; [et al.], eds.]. Washington, DC: U.S. Global Change Research Program: 133–160.

Intergovernmental Panel on Climate Change [IPCC]. 2001. Climate change 2001: Synthesis report. A contribution of Workings Groups I, II, and III to the Third Assessment Report of the Intergovernmental Panel on Climate Change. [Watson, R.T.; Core Writing Team, eds.]. Cambridge, UK, and New York: Cambridge University Press. 398 p.

Intergovernmental Panel on Climate Change [IPCC]. 2007. Climate change 2007: The physical science basis. Contribution of Working Group I to the Fourth Assessment Report of the Intergovernmental Panel on Climate Change. [Solomon, S., Qin, D., Manning, M., Chen, Z.; [et al.]]. Cambridge, UK and New York: Cambridge University Press. 996 p.

Intergovernmental Panel on Climate Change [IPCC]. 2011. Workshop report of the Intergovernmental Panel on Climate Change Workshop on impacts of ocean acidification on marine biology and ecosystems. Field, C.B.; Barros, V.; Stocker, T.F.; [et al.]. IPCC Working Group II Technical Support Unit. Stanford, CA: Carnegie Institution. 164 p.

Intergovernmental Panel on Climate Change [IPCC]. 2013a. Annex III: Glossary [Planton, S., ed.]. In: Climate change 2013: The physical science basis. Contribution of Working Group I to the Fifth Assessment Report of the Intergovernmental Panel on Climate Change. [Stocker, T.F.; Qin, D.; Plattner, G.-K.; [et al.], eds.]. Cambridge, UK and New York: Cambridge University Press: 1447–1465.

Intergovernmental Panel on Climate Change [IPCC]. 2013b. Climate change 2013: The physical science basis. Contribution of Working Group I to the Fifth Assessment Report of the Intergovernmental Panel on Climate Change. Stocker, T.F.; Qin, D., Plattner, G.-K.; [et al.], eds. Cambridge, UK and New York: Cambridge University Press. 1585 p.

Intergovernmental Panel on Climate Change [IPCC]. 2014. Annex II: Glossary [Agard, J.; Schipper, E.L.F.; Birkmann, J; [et al.]]. Climate Change 2014: Impacts, adaptation and vulnerability. Part B: Regional aspects. Contribution of Working Group II to the Fifth Assessment Report of the Intergovernmental Panel on Climate Change. Barros, V.R.; Field, C.B.; Dokken M.D.; [et al.]. Cambridge, UK and New York: Cambridge University Press: 1757–1776.

Joyce, L.A.; Birdsey, R., eds. 2000. The impact of climate change on America's forests: A technical document supporting the 2000 USDA Forest Service RPA Assessment. Gen. Tech. Rep. RMRS-GTR-59. Fort Collins, CO: U.S. Department of Agriculture, Forest Service, Rocky Mountain Research Station. 133 p.

Joyce, L.A.; Fosberg, M.A.; Comanor, J.M. 1990. Climate change and America's forests. Gen. Tech. Rep. RM-187. Fort Collins, CO: U.S. Department of Agriculture, Forest Service, Rocky Mountain Forest and Range Experiment Station. 12 p.

Joyce, L.A.; Price, D.T.; Coulson, D.P.; [et al.]. 2014. Projecting climate change in the United States: A technical document supporting the Forest Service RPA 2010 Assessment. Gen. Tech. Rep. RMRS-GTR-320. Fort Collins, CO: U.S. Department of Agriculture, Forest Service, Rocky Mountain Research Station. 85 p.

Joyce, L.A.; Abatzoglou, J.T.; Coulson, D.P. 2018. Climate data for RPA 2020 Assessment: MACAv2 (METDATA) historical modeled (1950–2005) and future (2006–2099) projections for the conterminous United States at the 1/24 degree grid scale. Fort Collins, CO: U.S. Department of Agriculture, Forest Service, Research Data Archive. https://doi.org/10.2737/RDS-2018-0014 [Accessed September 17, 2019].

Knutti, R. 2010. The end of model democracy? An editorial comment. Climatic Change. 102: 395–404. doi: 10.1007/s10584-010-9800-2.

Knutti, R.; Masson, D.; Gettelman, A. 2013. Climate model genealogy: Generation CMIP5 and how we got there. Geophysical Research Letters. 40(6): 1194–1199. doi: 10.1002/grl.50256.

Loehman, R.A.; Bentz, B.J.; DeNitto, G.A.; [et al.]. 2018. Chapter 8: Effects of climate change on ecological disturbance in the Northern Rockies Region. In: Halofsky, J.E.; Peterson, D.L.; Dante-Wood, S.K.; [et al.]; eds. Climate change vulnerability and adaptation in the Northern Rocky Mountains. Gen. Tech. Rep. RMRS-GTR-374. Fort Collins, CO: U.S. Department of Agriculture, Forest Service, Rocky Mountain Research Station. Part 2: 317–352.

Langner, L.L.; Joyce, L.A.; Wear, D.N.; [et al.]. 2020. Future scenarios: A technical document supporting the USDA Forest Service 2020 RPA Assessment. Gen. Tech. Rep. RMRS-GTR-412. Fort Collins, CO: U.S. Department of Agriculture, Forest Service, Rocky Mountain Research Station. 34 p. https://doi.org/10.2737/RMRS-GTR-412

Lute, A.C.; Abatzoglou, J.T.; Hegewisch, K.C. 2015. Projected changes in snowfall extremes and interannual variability of snowfall in the western United States. Water Resources Research. 51(2): 960–972. doi: 10.1002/2014wr016267.

Maurer, E.P.; Wood, A.W.; Adam, J.C.; [et al.]. 2002, A long-term hydrologically-based data set of land surface fluxes and states for the conterminous United States. Journal of Climate. 15(22): 3237–3251. doi: 10.1175/1520-0442(2002)015<3237:althbd>2.0.co;2.

Moss, R.; Babiker, M.; Brinkman, S.; [et al.]. 2008. Towards new scenarios for analysis of emissions, climate change, impacts and response strategies. Technical Summary. Geneva, Switzerland: Intergovernmental Panel on Climate Change. 25 p. https://www.ipcc.ch/site/assets/uploads/2018/05//expert-meeting-report-scenarios-1-1.pdf [Accessed September 3, 2019].

Moss, R.H.; Edmonds, J.A.; Hibbard, K.A.; [et al.]. 2010. The next generation of scenarios for climate change research and assessment. Nature. 463(7289): 747–756. doi: 10.1038/nature08823.

Mote, P.; Brekke, L.; Duffy, P.B.; Maurer, E. 2011. Guidelines for constructing climate scenarios. Eos Transactions American Geophysical Union. 92(31): 257–258. doi: 10.1029/2011eo310001.

Nakićenović, N.; Alcamo, J.; Davis, G.; [et al.]. 2000. Emissions scenarios: A special report of Working Group III of the Intergovernmental Panel on Climate Change. Cambridge, UK and New York: Cambridge University Press. 599 p.

Pierce, D.W.; Cayan, D.R.; Maurer, E.P.; [et al.]. 2015. Improved bias correction techniques for hydrological simulations of climate change. Journal of Hydrometeorology. 16(6): 2421–2442. doi: 10.1175/jhm-d-14-0236.1.

Pierce, D.W.; Cayan, D.R.; Thrasher, B.L. 2014. Statistical downscaling using localized constructed analogs (LOCA). Journal of Hydrometeorology. 15(6): 2558–2585. doi: 10.1175/jhm-d-14-0082.1.

Reeves, M.C.; Bagne, K.E.; Tanaka, J. 2017. Potential climate change impacts on four biophysical indicators of cattle production from western U.S. rangelands. Rangeland Ecology & Management. 70(5): 529–539. doi: 10.1016/j.rama.2017.02.005.

Rice, J.; Tredennick, A.; Joyce, L.A. 2012. Climate change on the Shoshone National Forest, Wyoming: A synthesis of past climate, climate projections, and ecosystem implications. Gen. Tech. Rep. RMRS-GTR-264. Fort Collins, CO: U.S. Department of Agriculture, Forest Service, Rocky Mountain Research Station. 60 p.

Rice, J.R.; Joyce, L.A.; Regan, C.; [et al.]. 2018. Climate change vulnerability assessment of aquatic and terrestrial ecosystems in the U.S. Forest Service Rocky Mountain Region. Gen. Tech. Rep. RMRS-GTR-376. Fort Collins, CO: U.S. Department of Agriculture, Forest Service, Rocky Mountain Research Station. 216 p.

Roske, M.R.; Joyce, L.A.; Nagel, L.M.; [et al.]. 2019. The Rio Grande National Forest Climate Change Plan Revision Workshop: Designing a science-management collaborative process to address 2012 planning rule climate change concerns at the forest plan scale. Res. Note RMRS-RN-84. Fort Collins, CO: U.S. Department of Agriculture, Forest Service, Rocky Mountain Research Station. 17 p.

Rupp, D.E. 2016a. An evaluation of CMIP5 20th century climate for the Southeastern United States as simulated by Coupled Model Intercomparison Project Phase 5 (CMIP5) global climate models. Open-File Report 2016-1047. Reston, VA: U.S. Geological Survey. 32 p. https://doi.org/10.3133/ofr20161047 [Accessed September 17, 2019].

Rupp, D.E. 2016b. Figures from an unpublished report of an evaluation of CMIP 20th century climate for the Southwestern United States as simulated by Coupled Model Intercomparison Project Phase 5 global climate models. Obtained from David Rupp, Oregon State University, 2016.

Rupp, D.E.; Abatzoglou, J.T.; Hegewisch, K.C.; Mote, P.W. 2013. Evaluation of CMIP5 20th century climate simulations for the Pacific Northwest USA. Journal of Geophysical Research: Atmospheres. 118(19): 10884–10906. doi:10.1002/jgrd.50843.

Sanderson, B.M.; Wehner, M.F. 2017. Model weighting strategy. In: Climate science special report: Fourth National Climate Assessment. Vol. I. [Wuebbles, D.J.; Fahey, D.W.; Hibbard, K.A.; [et al.], eds.]. Washington, DC: U.S. Global Change Research Program: 436–443.

Sheehan, T.; Bachelet, D.; Ferschweiler, K. 2019. Fire, CO^2, and climate effects on modeled vegetation and carbon dynamics in western Oregon and Washington. PLoS ONE. 14(1): e0210989. doi: 10.1371/journal.pone.0210989.

Sheffield, J.; Camargo, S.J.; Fu, R.; [et al.]. 2013. North American climate in CMIP5 experiments. Part II: Evaluation of historical simulations of intraseasonal to decadal variability. Journal of Climate. 26(23): 9247–9290. doi: 10.1175/jcli-d-12-00593.1.

Swanston, C.; Janowiak, M.; Iverson, L.; [et al.]. 2011. Ecosystem vulnerability assessment and synthesis: A report from the Climate Change Response Framework project in northern Wisconsin. Gen. Tech. Rep. NRS-82. Newtown Square, PA: U.S. Department of Agriculture, Forest Service, Northern Research Station. 142 p.

Thrasher, B.; Maurer, E.P.; McKellar, C.; Duffy, P.B. 2012. Technical note: Bias correcting climate model simulated daily temperature extremes with quantile mapping. Hydrology and Earth System Science. 16(9): 3309–3314. doi: 0.5194/hess-16-3309-2012.

Thrasher, B.; Xiong, J.; Wang, W.; Melton, F.; Michaelis, A.; Nemani, R. 2013. Downscaled climate projections suitable for resource management. Eos Transactions American Geophysical Union. 94(37): 321–323. doi: 10.1002/2013eo370002.

Timberlake, T.; Joyce, L.A.; Schultz, C.; Lampman, G. 2018. Design of a workshop process to support consideration of natural range of variation and climate change for land management planning under the 2012 Planning Rule. Res. Note RMRS-RN-82. Fort Collins, CO: U.S. Department of Agriculture, Forest Service, Rocky Mountain Research Station. 36 p.

University of Idaho. [n.d.]. Multivariate Adaptive Constructed Analogs (MACA) datasets. Boise, ID: University of Idaho. https://climate.northwestknowledge.net/MACA/index.php [Accessed November 15, 2019].

U.S. Department of Agriculture Forest Service [USDA FS]. 1993. RPA Assessment of the forest and rangeland situation in the United States—1993 Update. Forest Resource Report No. 27. Washington, DC: U.S. Department of Agriculture, Forest Service. 75 p.

U.S. Department of Agriculture, Forest Service [USDA FS]. 2001a. Forest and Rangeland Renewable Resources Planning Act of 1974 [As Amended Through Public Law 106–580, Dec. 31, 2000]. https://www.fs.fed.us/emc/nfma/includes/range74.pdf [Accessed September 17, 2019].

U.S. Department of Agriculture, Forest Service [USDA FS]. 2001b. 2000 RPA Assessment of Forest and Range Lands. FS-687. Washington, DC: U.S. Department of Agriculture Forest Service. 78 p.

U.S. Department of Agriculture, Forest Service [USDA FS]. 2007. Interim update of the 2000 Renewable

Resources Planning Act Assessment. FS 874. Washington, DC: U.S. Department of Agriculture Forest Service. 113 p.

U.S. Department of Agriculture, Forest Service [USDA FS]. 2012a. Future of America's forest and rangelands: Forest Service 2010 Resources Planning Act Assessment. Gen. Tech. Rep. WO-87. Washington, DC: U.S. Department of Agriculture Forest Service. 198 p.

U.S. Department of Agriculture, Forest Service [USDA FS]. 2012b. Future scenarios: A technical document supporting the Forest Service 2010 RPA Assessment. Gen. Tech. Rep. RMRS-GTR-272. Fort Collins, CO: U.S. Department of Agriculture, Forest Service, Rocky Mountain Research Station. 34 p.

U.S. Department of Agriculture, Forest Service [USDA FS]. 2012c. National Forest System land management planning, 36 CFR Part 219.6(3)(b)(3), RIN 0596-AD02. Federal Register. 77: 21260.

U.S. Department of Agriculture, Forest Service [USDA FS]. 2016. Future of America's forest and rangelands: Forest Service. Update to the Forest Service 2010 Resources Planning Act Assessment Gen. Tech. Rep. WO-94. Washington, DC: U.S. Department of Agriculture Forest Service. 250 p.

U.S. Department of Agriculture, Forest Service [USDA FS]. [n.d.]. National Forest System climate change maps. U.S. Department of Agriculture, Forest Service, Rocky Mountain Research Station, Air, Water, and Aquatic Environments Program. https://www.fs.fed.us/rm/boise/AWAE/projects/national-forest-climate-change-maps.html [Accessed December 20, 2019].

U.S. Environmental Protection Agency [USEPA]. 2016. Climate resilience evaluation and awareness tool version 3.0 methodology guide. 43 p. https://www.epa.gov/sites/production/files/2016-05/documents/creat_3_0_methodology_guide_may_2016.pdf [Accessed September 17, 2019].

U.S. Global Change Research Program [USGCRP]. 2017: Climate science special report: Fourth National Climate Assessment. Vol. I. [Wuebbles, D.J.; Fahey, D.W.; Hibbard, K.A.; [et al.], eds.]. Washington, DC: U.S. Global Change Research Program. 470 p.

Vano, J.A.; Arnold, J.R.; Nijssen, B.; [et al.]. 2018. DOs and DON'Ts for using climate change information for water resource planning and management: Guidelines for study design. Climate Services. 12: 1–13. doi: 10.1016/j.cliser.2018.07.002.

Wear, D.N.; Prestemon, J.P. 2019. Spatiotemporal downscaling of global population and income scenarios for the United States. PLOS ONE. 14(7): e0219242. doi: 10.1371/journal.pone.0219242.

Yazzie, K.; Chang, H. 2017. Watershed response to climate change and fire-burns in the Upper Umatilla River Basin, USA. Climate. 5(1): 7. doi:10.3390/cli5010007.

APPENDIX A

Maps of Projected Changes in Temperature and Precipitation at End of Century

This appendix presents maps showing the projected changes in temperature and precipitation at end of century for the RPA core models (figs. A.1–A.4). Temperature change is computed as the difference between the mean temperature at 2070–2099 and the mean temperature of the historical period (1971–2000). Precipitation change is computed as the percent difference in mean precipitation between those two periods.

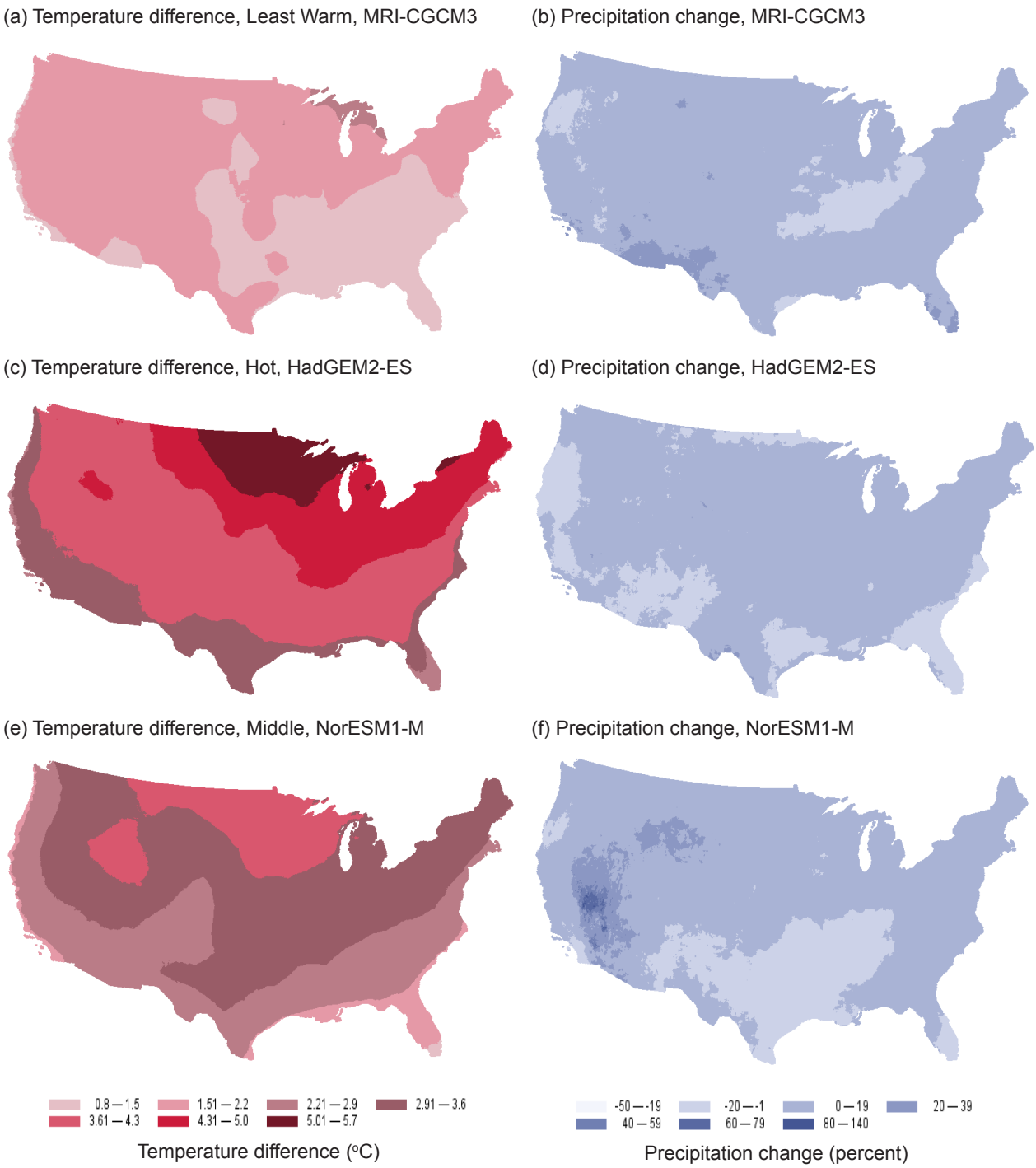

Figure A1—Mean temperature difference (°C) and annual precipitation change (percent) at end of century (2070–2099) from the historical period (1971–2000) for temperature core models under RCP 4.5: Least Warm (a,b), Hot (c,d), and Middle (e,f).

Figure A2—Annual precipitation change (percent) and mean temperature difference (°C) at end of century (2070–2099) from the historical period (1971–2000) for precipitation core models under RCP 4.5: Dry (a,b), Wet (c,d), and Middle (e,f).

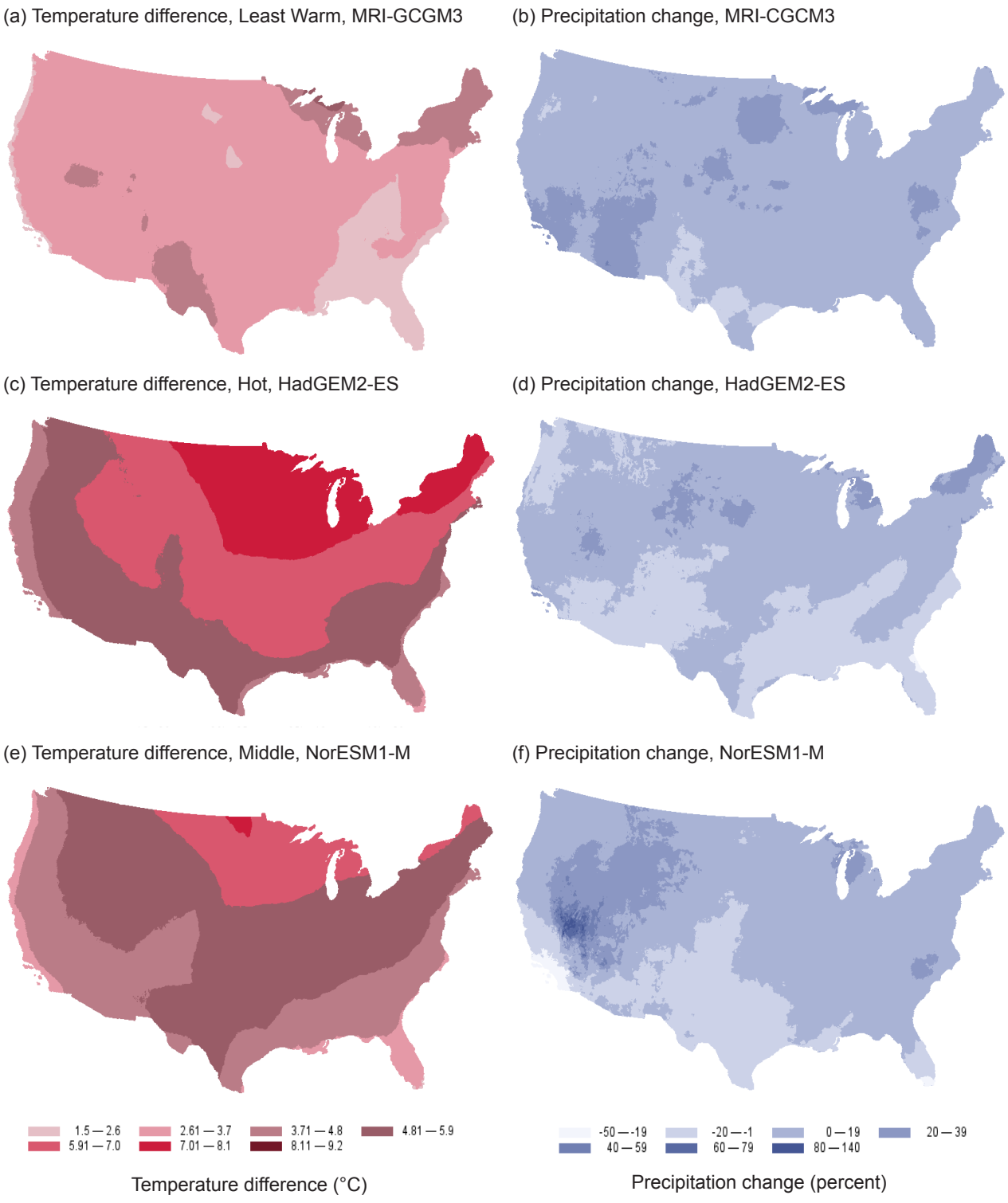

Figure A3—Mean temperature difference (°C) and annual precipitation change (percent) at end of century (2070–2099) from the historical period (1971–2000) for temperature core models under RCP 8.5: Least Warm (a,b), Hot (c,d), Middle (e,f).

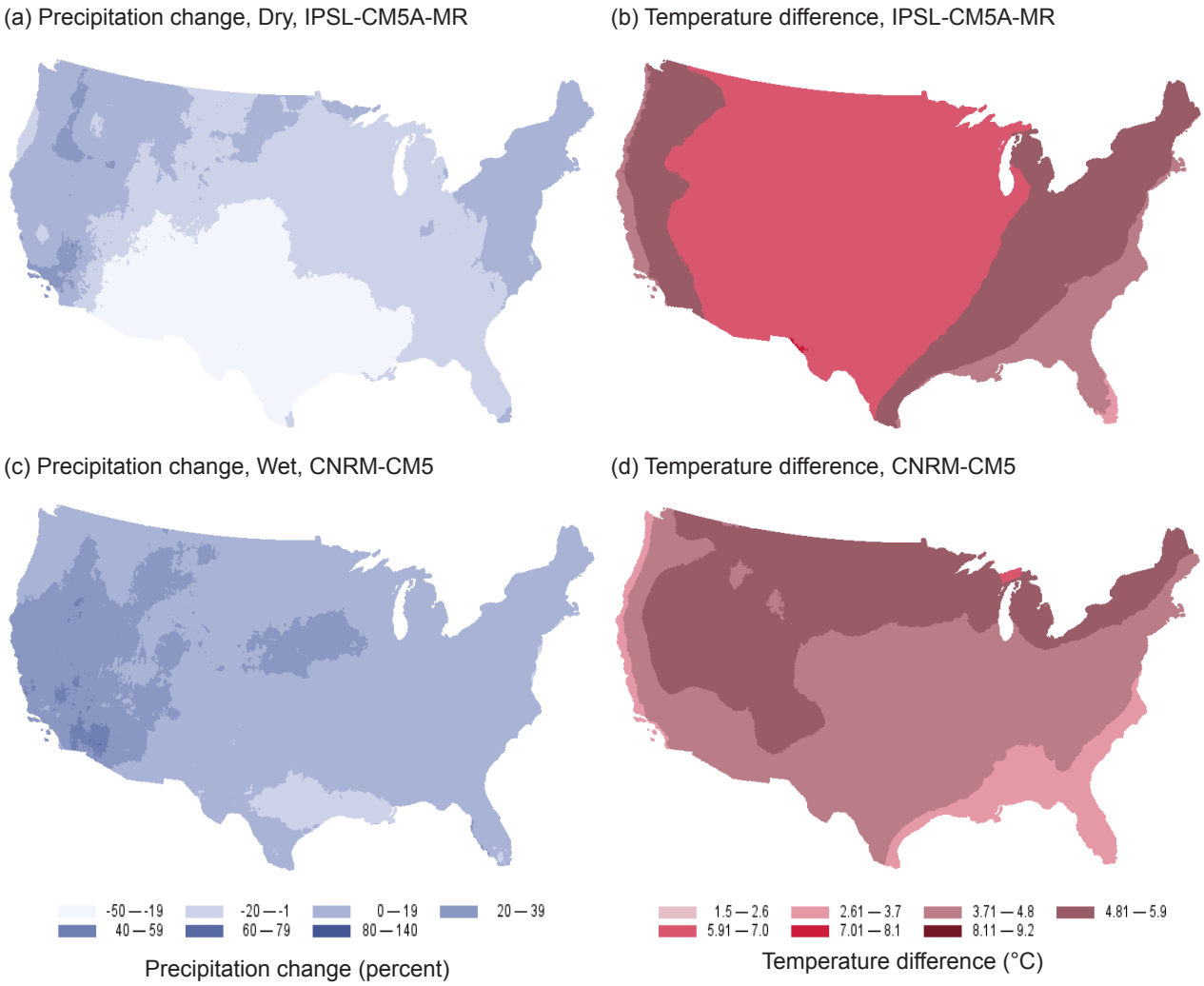

Figure A4—Annual precipitation change (percent) and mean temperature difference (°C) at end of century (2070–2099) from the historical period (1971–2000) for precipitation core models: Dry (a,b), Wet (c,d) under RCP 8.5.

APPENDIX B

Graphs of Projected Changes in Temperature and Precipitation at End of Century by Region

This appendix shows the bivariate plots for projected changes in temperature and precipitation at end of century by National Forest System region (figs. B.1–B.8). Temperature change is computed as the difference between the mean temperature at 2070–2099 and the mean temperature of the historical period (1971–2000). Precipitation change is computed as the percent difference in mean precipitation between those two periods.

(a) RCP 4.5

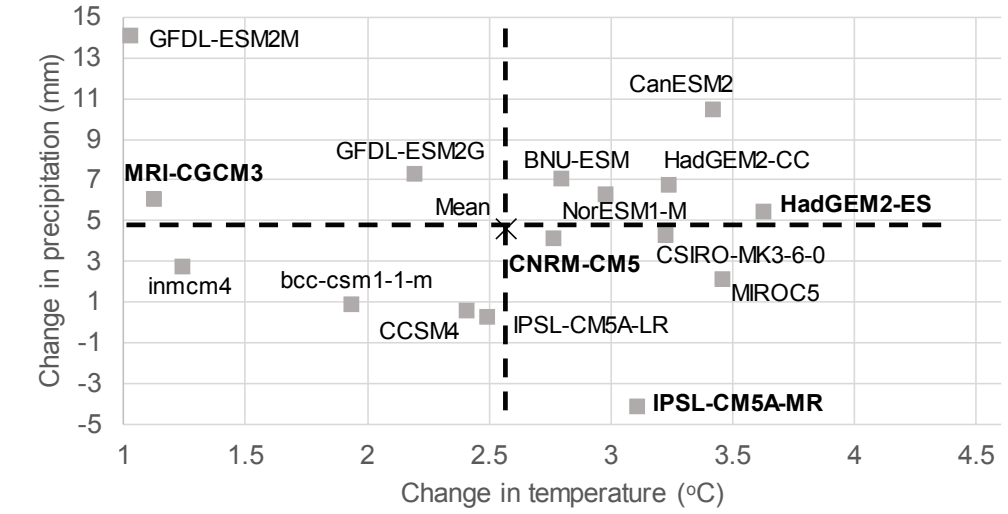

(b) RCP 8.5

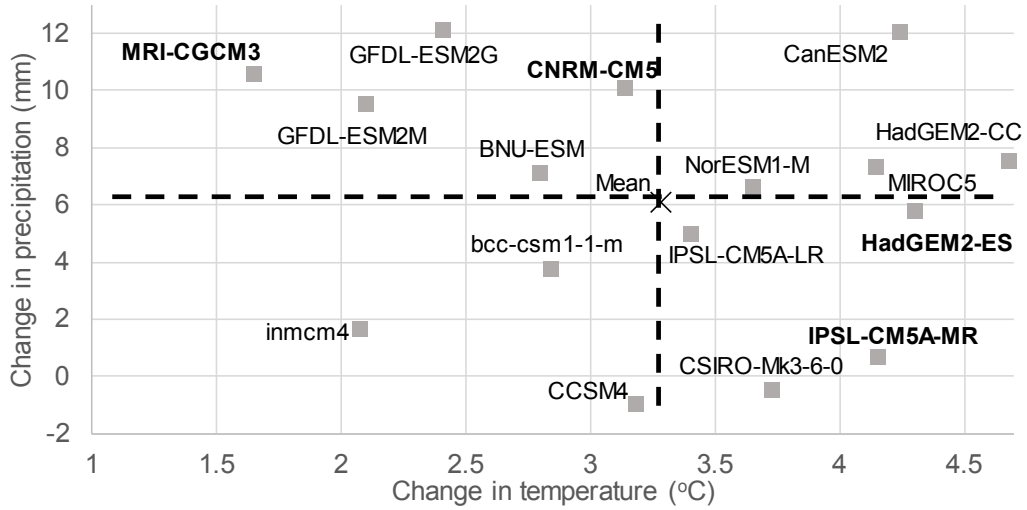

Figure B1—Projected changes in mean temperature (°C) and annual precipitation (percent) at mid-century (2041–2070) from the historical period (1971–2000) in Region 1 under RCP 4.5 (a) and RCP 8.5 (b). Model names in bold are the national core models for mid-century: Least Warm—MRI-CGCM3; Hot—HadGEM2-ES; Dry—IPSL-CM5A-MR; Wet—CNRM-CM5.

(a) RCP 4.5

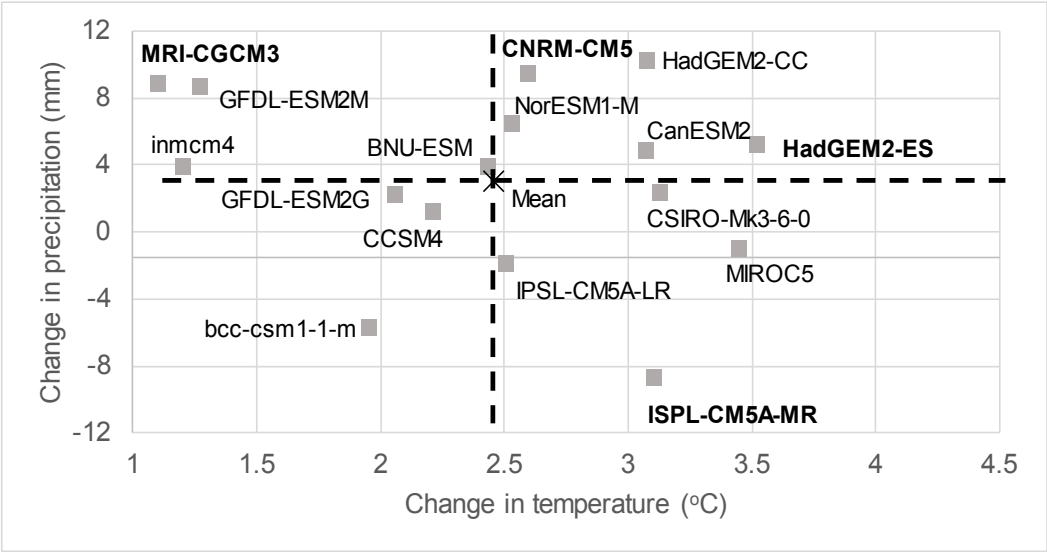

(b) RCP 8.5

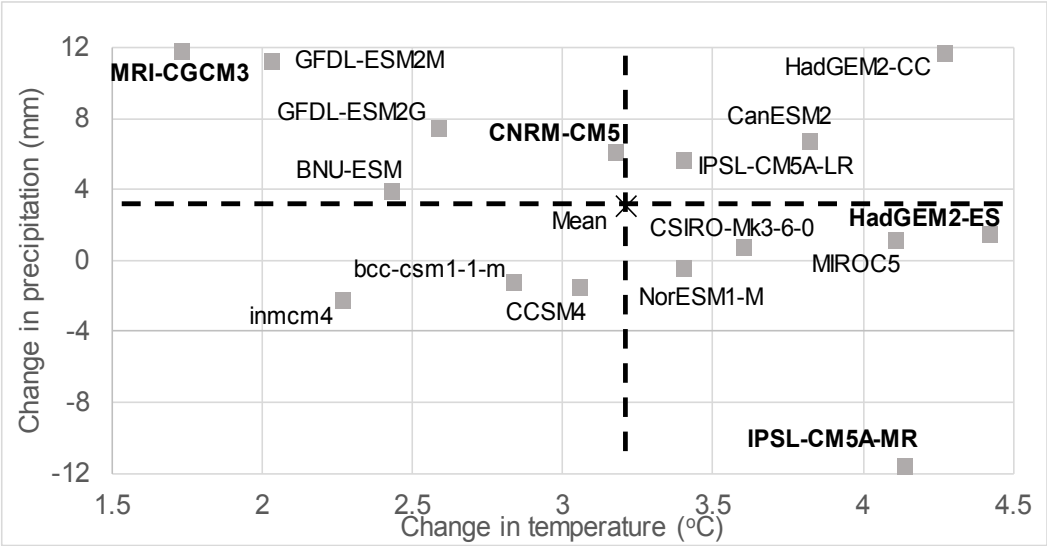

Figure B2—Projected changes in mean temperature (°C) and annual precipitation (percent) at mid-century (2041–2070) from the historical period (1971–2000) in Region 2 under RCP 4.5 (a) and RCP 8.5 (b). Model names in bold are the national core models for mid-century: Least Warm—MRI-CGCM3; Hot—HadGEM2-ES; Dry—IPSL-CM5A-MR; Wet—CNRM-CM5.

(a) RCP 4.5

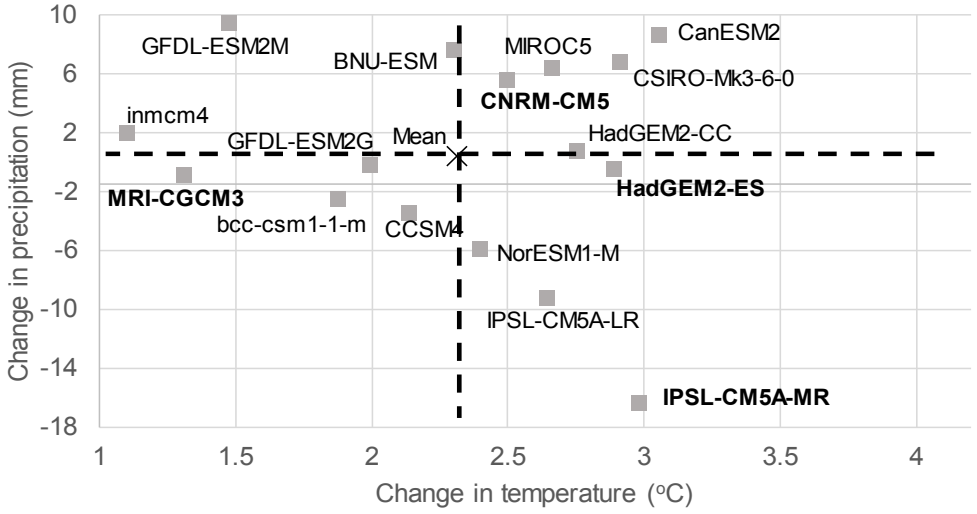

(b) RCP 8.5

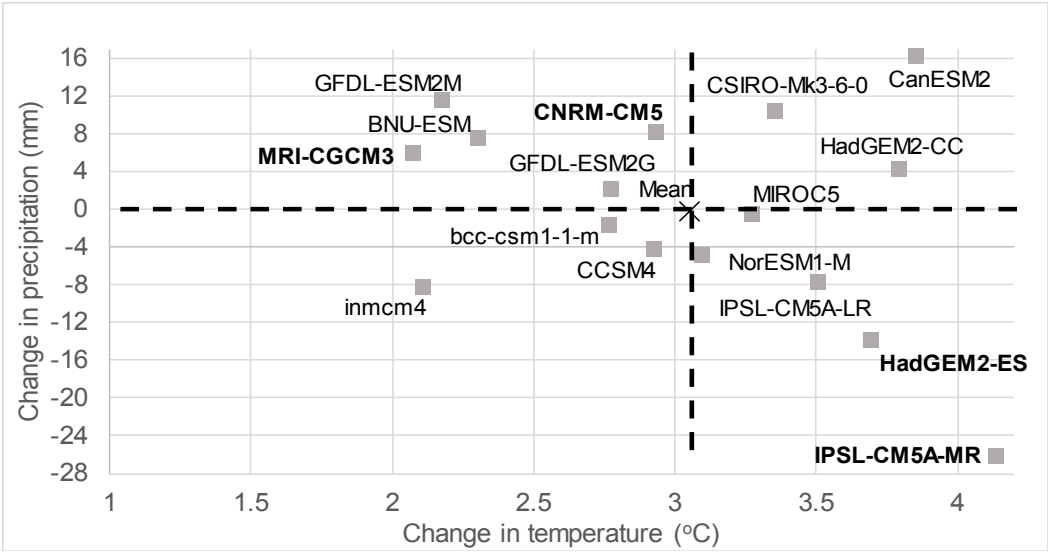

Figure B3—Projected changes in mean temperature (°C) and annual precipitation (percent) at mid-century (2041–2070) from the historical period (1971–2000) in Region 3 under RCP 4.5 (a) and RCP 8.5 (b). Model names in bold are the national core models for mid-century: Least Warm—MRI-CGCM3; Hot—HadGEM2-ES; Dry—IPSL-CM5A-MR; Wet—CNRM-CM5.

(a) RCP 4.5

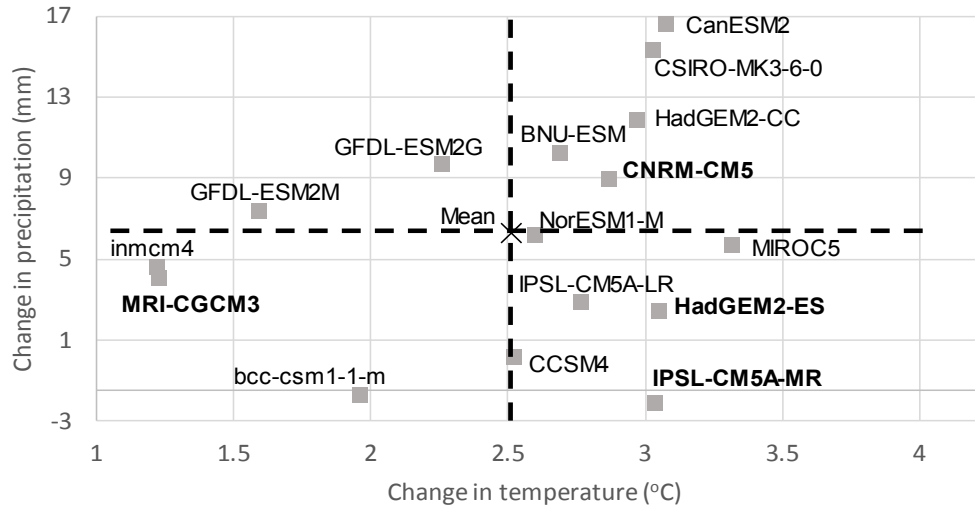

(b) RCP 8.5

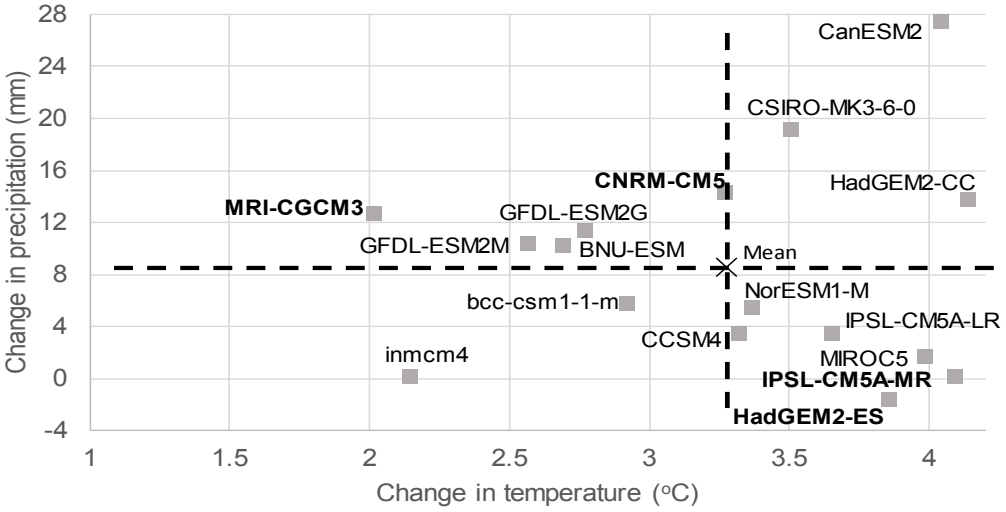

Figure B4—Projected changes in mean temperature (°C) and annual precipitation (percent) at mid-century (2041–2070) from the historical period (1971–2000) in Region 4 under RCP 4.5 (a) and RCP 8.5 (b). Model names in bold are the national core models for mid-century: Least Warm—MRI-CGCM3; Hot—HadGEM2-ES; Dry—IPSL-CM5A-MR; Wet—CNRM-CM5.

(a) RCP 4.5

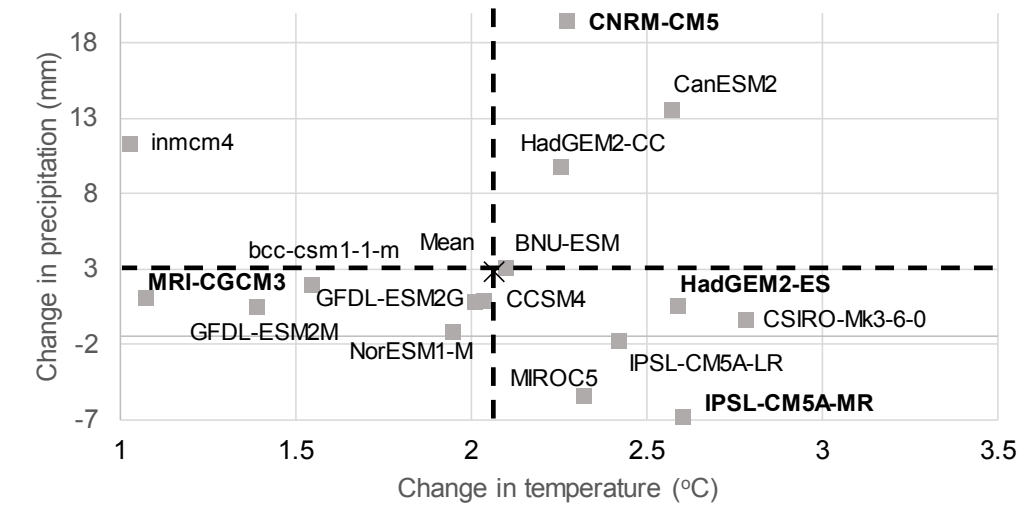

(b) RCP 8.5

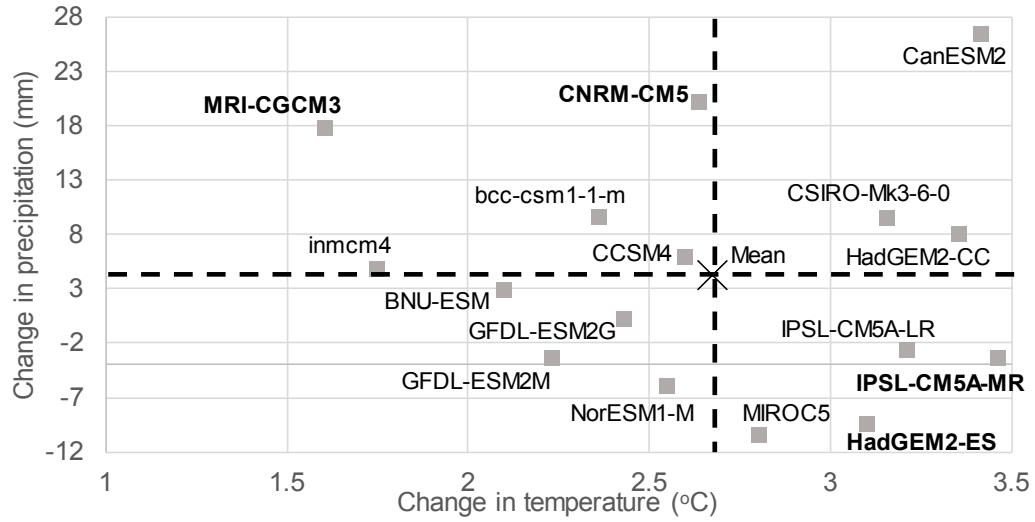

Figure B5—Projected changes in mean temperature (°C) and annual precipitation (percent) at mid-century (2041–2070) from the historical period (1971–2000) in Region 5 under RCP 4.5 (a) and RCP 8.5 (b). Model names in bold are the national core models for mid-century: Least Warm—MRI-CGCM3; Hot—HadGEM2-ES; Dry—IPSL-CM5A-MR; Wet—CNRM-CM5.

(a) RCP 4.5

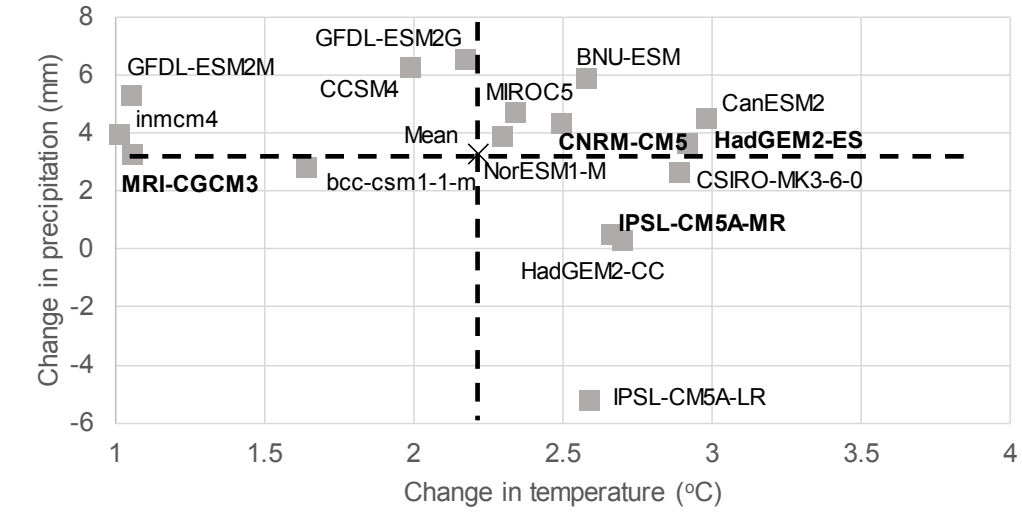

(b) RCP 8.5

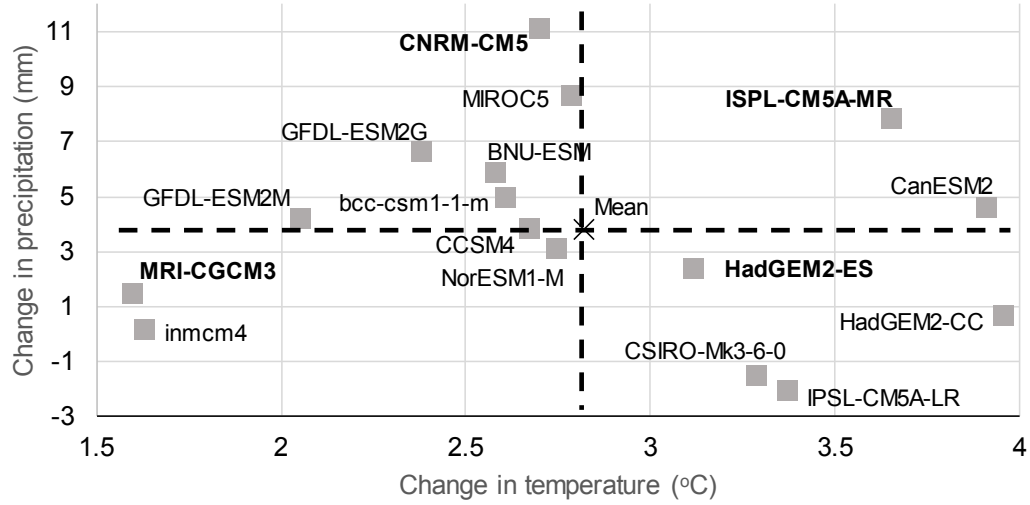

Figure B6—Projected changes in mean temperature (°C) and annual precipitation (percent) at mid-century (2041–2070) from the historical period (1971–2000) in Region 6 under RCP 4.5 (a) and RCP 8.5 (b). Model names in bold are the national core models for mid-century: Least Warm—MRI-CGCM3; Hot—HadGEM2-ES; Dry—IPSL-CM5A-MR; Wet—CNRM-CM5.

(a) RCP 4.5

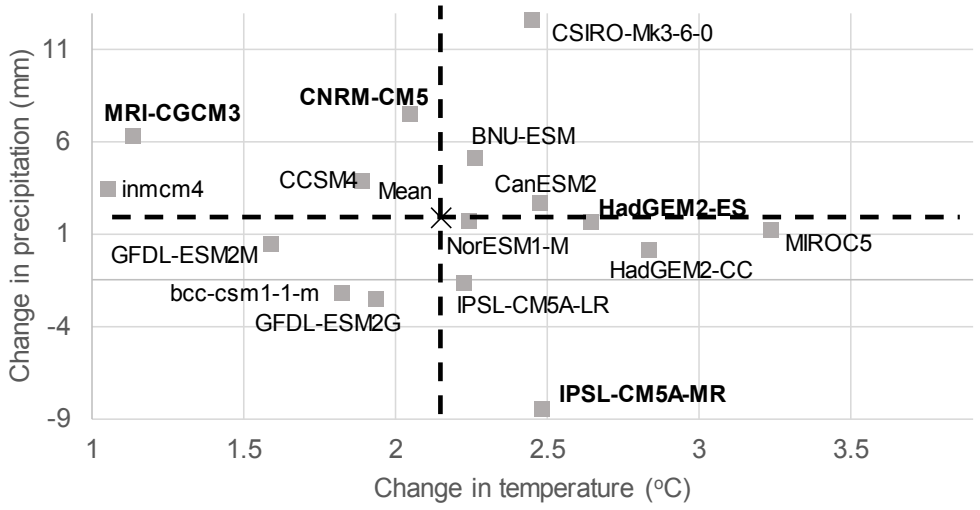

(b) RCP 8.5

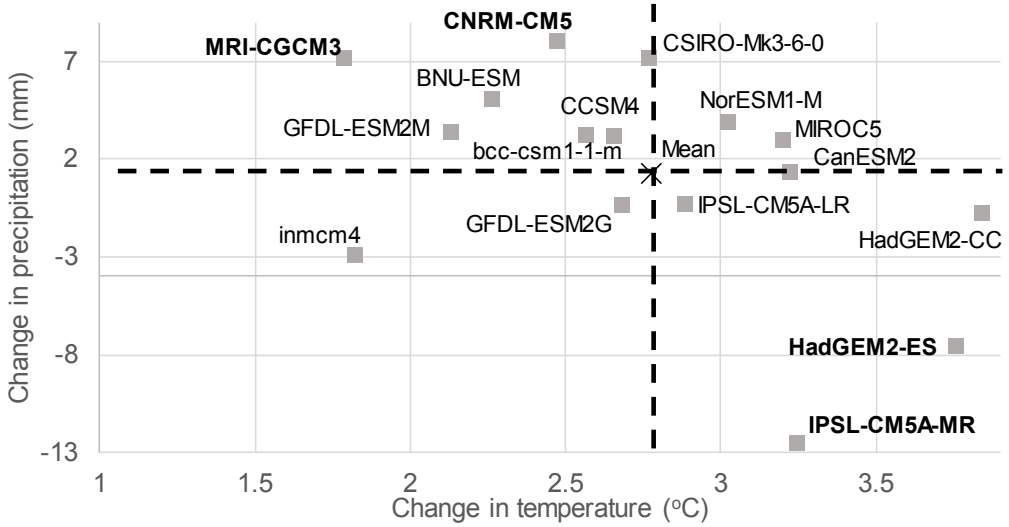

Figure B7—Projected changes in mean temperature (°C) and annual precipitation (percent) at mid-century (2041–2070) from the historical period (1971–2000) in Region 8 under RCP 4.5 (a) and RCP 8.5 (b). Model names in bold are the national core models for mid-century at the conterminous scale: Hot—HadGEM2-ES; Least Warm—MRI-CGCM3; Wet—CNRM-CM5; Dry—IPSL-CM5A-MR.

(a) RCP 4.5

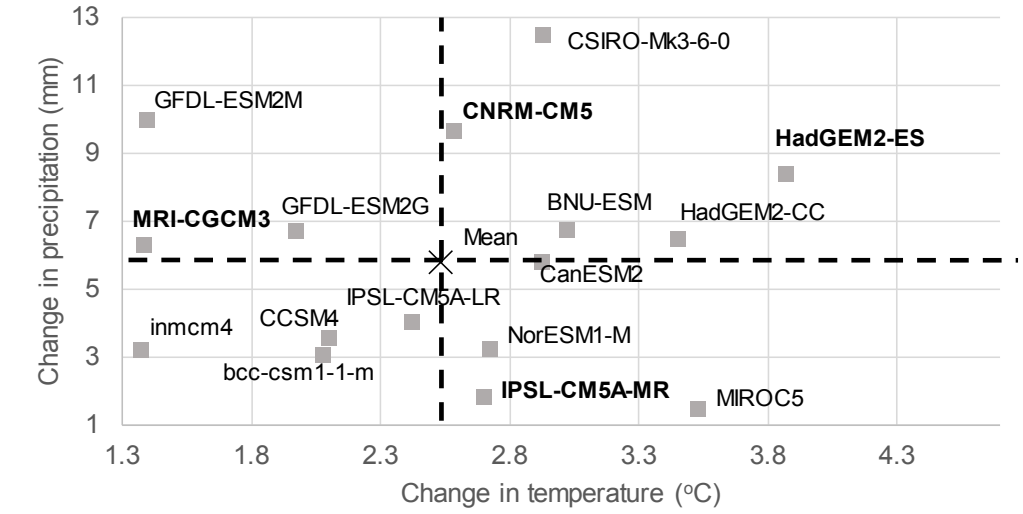

(b) RCP 8.5

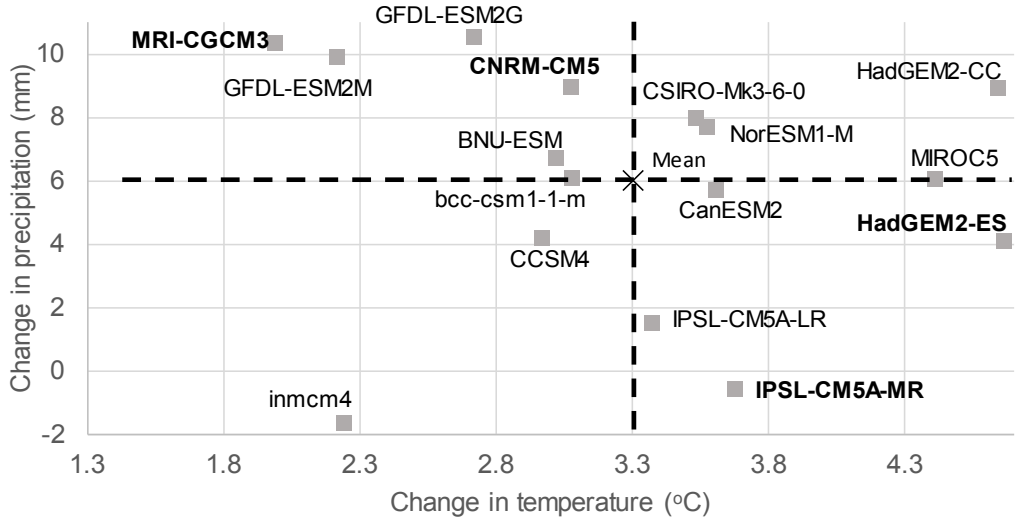

Figure B8—Projected changes in mean temperature (°C) and annual precipitation (percent) at mid-century (2041–2070) from the historical period (1971–2000) in Region 9 under RCP 4.5 (a) and RCP 8.5 (b). Model names in bold are the national core models for mid-century: Least Warm—MRI-CGCM3; Hot—HadGEM2-ES; Dry—IPSL-CM5A-MR; Wet— CNRM-CM5.

To learn more about RMRS publications or search our online titles:
RMRS web site at: https://www.fs.fed.us/rmrs/rmrs-publishing-services